DESIGN CONSIDERATIONS AND PERFORMANCE STUDY OF NONTRACKING SOLAR CONCENTRATORS

A Thesis
Submitted in partial fulfilment of the
requirements for the degree of
DOCTOR OF PHILOSOPHY
In
PHYSICS

By
MURLIDHAR

BIRLA INSTITUTE OF TECHNOLOGY AND SCIENCE
PILANI (RAJASTHAN)
JANUARY 1981

TO MY UNCLE

(LATE) Shri D. C. ARORA

BIRLA INSTITUTE OF TECHNOLOGY AND SCIENCE

PILANI, RAJASTHAN

CERTIFICATE

This is to certify that the thesis entitled 'DESIGN CONSIDERATIONS AND PERFORMANCE STUDY OF NON-TRACKING SOLAR CONCENTRATORS' and submitted by Murli Dhar, ID No. 74S85002 for award of Ph.D. degree of the Institute, embodies original work done by him under my supervision.

Signature in full of the Supervisor ____________

Name in Capital block letters S. KUMAR

Designation Assistant Professor of Physics, Research and Consultancy Division.

Date: Jan.31,1981.

ACKNOWLEDGEMENTS

It gives me a great pleasure to place on record my deep sense of gratitude towards Dr. S. Kumar, Assistant Professor of Physics, B.I.T.S., Pilani(Rajasthan) for encouraging and guiding me to pursue this work.

I am very much grateful to Dr. V.K. Tewary and Dr.(Mrs.) A. Gupta for their keen interest and all possible help during the course of this work.

I wish to express my heartful thanks to Dr. J.S. Verma, Dr. P. Singh, Dr. G.P. Srivastava, Dr. S.K. Jain Dr.S.K.Sharma, Dr. G.S. Shastry, Dr. H.M. Ghule, Mr. S.C. Mittal, Dr. P.K. Jain, Dr.(Mrs.) Uma Jain, Dr. V.S.Kulhar, Dr.(Miss) Amita Agarwala, Dr. P.R.Marwadi, Dr. R. Mehrotra, Dr. R.P. Khare, Dr. Lalit Kumar, Dr. P.C. Jain, Dr.(Mrs.) S.Srivastava, Dr. G.R. Rao, Dr. Chandra Shekhar, Dr. N.K. Joshi, Dr. M.C. Gupta, Dr. A.K. Jain, Dr. S.K. Jain, Dr.Rohtas Chandra, Dr. A.K. Thukral, Dr. G.S.Tyagi, Dr. N.K. Swami, Dr. R.P.S. Jakhar, Mr. S.K. Sharma, Mr. M.K. Madan,Mr. M.K. Joshi, Mr. B.G. Nagvi, Mr. S.B. Bhise, Mr. D.G. Shewade and other friends who made my stay at Pilani a lively and memorable experience in various fields of life.

I thank to Mr. Banwari Lal, Mr. S.L. Sharma, Mr. A.K. Tewathia, Mr. B.P. Singh and Ravi of the Information Processing Centre of B.I.T.S. for help in computational work and also the staff of B.I.T.S. Workshop for fabricating the Concentrators.

Thanks are due to Mr. S.K. Sinha for excellent typing of the manuscript and Mr. B.D. Sukheeja for neat drawing work.

I wish to express my deep sense of gratitude towards my parents, uncle and brothers for their stoical forbearance and continued encouragement.

I have no words to express my thanks to my wife Shashi Bala Arora whose inspirations encouraged me throughout the period of the work.

I am thankful to the Director, B.I.T.S., The Dean Research and Consultancy Division, The Dean A.R.C. Division, The Dean Faculty Division III and The Group Leader Physics Group for providing necessary facilities during the course of this work. I am thankful to B.I.T.S. and the University Grants Commission for providing financial assistance.

Murlidhar

(Murlidhar)

C O N T E N T S

CHAPTER-1

I N T R O D U C T I O N

CHAPTER-1

INTRODUCTION

1.1 World Energy Crisis and Resulting Increased Research Activity in Solar Energy Area

The energy needs of mankind are presently supplied mainly by three sources; fossil fuels, nuclear energy and hydel energy. The rapid depletion of natural fossil fuels and rising cost of petroleum have significantly affected the world economy during the last 10 years. Serious chemical and pollution problems have been posed by the emission during fossil fuel combustion and by radioactive waste from nuclear power plants. Like the fossil fuels, the reserve of fissionable materials is also not unlimited. This has focussed world wide attention to the search for alternative sources of energy which should be available in abundance and which do not pose serious environmental problems. Solar energy appears to have the greatest potential from the fact that incident solar energy is 20,000 times more than the world requirements[1] and hence even if a small fraction of this energy can be harnessed, it will greatly reduce the pressure on conventional sources of energy. The realization of this possibility has led to major worldwide research and development programmes in solar energy during the past few years.

1.2 Scope For Solar Energy In India

In our country 80% of the population lives in villages and most of the villages are not electrified. The energy requirement in a typical village is very low (of the order of 20 Kw). The cost of conventional electrification depends upon the distance of village from main grid lines. It has been estimated that the cost of conventional electrification in the range of 20 KW is of the order of Rs. 20,000- 30,000 per kilometer. Thus a 20 KW load electrification at a distance of 10 kilometer will cost around Rs.3,00,000. This does not include the cost of generating plant and main transmission network. It should also be remembered that fuel cost for conventional system is from .05 to .10 Rs/KWH at present and will continue to increase in future. Therefore conventional electrification is not a viable alternative for large scale rural electrification.

The major load of rural electric system in India is agricultural pumpset. Almost 5 million pumps are being utilised now for lifting ground water, these run on electricity or diesel. In next 10-15 years, the additional utilization of ground water would require several million more pump to be installed. The nature of this load is such that it is seasonal and is often required for a few hours only per day due to limited availability of water itself. This leads to low load factors and is a very undesirable load characteristics for conventional rural electrification. The solar electricity will be available for 6 to 8 hours a day and for 200 to 300 days in a year depending upon location. This can definitely meet most of the irrigation requirements. In monsoon solar electricity is not available and is not required for irrigation. In case of failure of rains, chances are that clouds will not be there and solar electricity will be available for irrigation. In winter and summer, irrigation requirement is there and solar energy is available. Solar energy stored in the form of chemical energy by charging battries can be used for providing light in the houses at night. Thus for a village with population less than 5000 persons and situated at a distance of ten kilometers or more from main transmission line, solar electrification will be a viable alternative compared to conventional electrification.

In some parts of our country, particularly in Rajasthan and Gujrat States so many villages do not have even the most elementary water supply. These depend upon the underground water which is saline and contaminated with constituents causing health hazards. In the absence of any other source of good quality water villagers are drinking saline and contaminated water. In these places, the abundantly available solar energy can be used to desalt the saline water by solar distillation.

Thus most of the energy requirements of the villages in our country can be fulfilled by making use of solar energy.

1.3 Present Problems in Utilizing Solar Energy

The basic processes which are involved in using solar energy are well known. The actual use of solar energy is extremely limited so far. This is due to the high initial cost of the solar devices. Since the solar radiation is dilute, a large collector area is required for any meaningful power output. Further, as solar radiation is intermittent, an energy storage system is also required for a continuous operation of the device. All these factors make the initial investment of solar device high compared to the conventional power system. Thus the problem in the use of solar energy do not really call for any fundamental gaps in the research to be bridged. What is required is that appropriate technology and manufacturing methods should be devised which make the use of solar energy economically viable.

1.4 Brief Review of Various Methods for Harnessing Solar Energy

Various methods are used to convert solar energy into useful form. A brief discussion of these methods is given below:

(i) Photovoltaic conversion

The photovoltaic effect is the process by which the E.M.F. (photovoltage) is produced at the junction of two dissimilar materials by the incident photon flux. The junction can be a metal-semiconductor or a p-n junction. From a p-n junction device no steady current will flow in the external circuit when it is in the darkness. This is due to the fact that the contact potential difference between p- and n-region of semiconductor and metallic leads cancel out the internal potential barrier between the p- and n-regions of the device. When a photon of energy $h\nu$ enters the p-region, it is absorbed by an electron in the valance band. If $h\nu$ is greater than the energy gap E_g of the p-region, the electron will be able to migrate to the n-region. Similarly, if $h\nu$ is greater than E_g in the n-region, the photon will be absorbed by a hole which will migrate to the p-region. This process will result in a net positive charge in the p-region and a net negative charge in the n-region which will create an electric field and effectively lower the initial potential barrier between n-and p-regions. Now at the circuit terminals of the device one can get a measurable voltage which is called as photovoltage. This phenomenon is called the p-n photovoltaic conversion. If the external circuit connecting the p- and n-region is closed, the electrical current will flow through the external load, the electric energy is obtained from the absorbed photons.

(ii) Thermal conversion

When a body is exposed to the Sun, it absorbs radiation and is raised to an excited state (with electrons at high energy levels and lattice vibrations proceeding vigorously) i.e., its temperature has increased. The way in which it gains and loses energy is quite complicated. For understanding the behaviour we simplify the problem by assuming that the body does not lose heat by convection and conduction.

Let I be the intensity of solar radiation and α be the absorption coefficient of the body. If the body is exposed to sun, its temperature will rise until it reaches a temperature, called the equilibrium temperature $T^{o}K$. At this temperature, the rate of emission of radiation will be equal to the rate of absorption. So we have

$$\alpha I = e\,\sigma(T^4 - T_a^4) \qquad (1.1)$$

Where e is the emissivity of the body and σ is the Stephen's Boltzman constant. Now from Eqn.(1.1) we get,

$$T^4 = T_a^4 + \frac{\alpha I}{e\,\sigma} \qquad (1.2)$$

The rise in temperature of the body can be used as a source of heat to the working fluid and hence the solar energy will be converted into useful heat energy.

(iii) Wind energy conversion

The wind blows because the temperatures of the air at various locations on the earth are different. If an area is heated by solar radiations, the air that comes in contact with it is also heated, cooler heavier air from the sorroundings rush-es under the warm lighter air. This movement of air along the surface of the earth is called wind. If the sun does not heat the air, there would be no temperature difference and therefore no movement (wind). So any project to harness the wind is a project to harness indirectly the energy of the sun i.e, Solar Energy. The use of wind energy is not a new concept, as the ancient seamen depend on the wind to power their ships and windmills were used to pump water and grind grain.

(iv) Ocean thermal gradient conversion

Due to the incoming solar radiations, the upper layers of the sea are much warmer than those deep down. The warm water is evaporated rapidly at a low temperature under vacuum. The evaporated water, now a vapor, passes through a turbine that is connected to an electric generator. The pressure of the vaper rotates the generator, which in turn produces the electricity, then the vapor enters a condenser where it is cooledby the deep water and changed to liquid.

The conversion of heat energy (in sea water) into electricity can be attempted only along tropical coasts where the surface temperature of the water is about 82^{o}F; where the temperature difference is sharp near shore and where storms are not frequent. These conditions must be met near to those places where the power is to be used. There are very few such places on the surface of the earth. A violent storm might destroy the entire installation.

(v) Photogalvanic conversion

In this process when light impinges on the electrode, electrons are emitted. These drive the cell from which power can be drawn. For semiconductor electrodes, holes can be activated to be available as acceptors of electrons at the anode.

The photogalvanic conversion is less developed than photovoltaic one. In this conversion, it is not required to have the pure single crystals in the collectors as in photovoltaic conversion and hence this is cheaper compared to the latter. However, the efficiency of conversion is ~0.04% which is very low compared to photovoltaic conversion efficiency (~10%).

(vi) Photosynthesis

Solar energy is used when the plants grow. These plants can be burnt directly to work a heat engine. Similarly algae could be force grown, collected and decomposed by heat to form hydrocarbons. The photosynthetic conversion is less attractive since the average efficiency of solar energy conversion this way is very small i.e., about 1%.

1.5 <u>Solar Energy Programme in India</u>

Realising the importance of the utilization of solar energy in view of the increasing cost of the fossil fuels (as mentioned earlier in Sec. 1.1) the Department of Science and Technology (DST) Government of India has established a department of new energy sources which looks after all the research, development and utilization of alternate energy sources. The national solar energy programme which has been formulated consists of (i) development of solar thermal energy hardware and systems, (ii) development of direct energy conversion devices like photovoltaic solar cells and (iii) establishment of solar energy data collection observatories, data processing and information transfer to solar research scientists.

The energy requirements of typical indian village are of the order of 20 KWs which is very less compared to the requirement of urban sectors. Therefore the research and development projects have been divided into two categories.

(a) For rural sector

(i) Irrigation pump of 2.5 horse power.

(ii) Solar convective dryers (for grains and commercial crops) of one ton capacity.

(iii) Distillation plants for conversion of brackish water into portable water.

(iv) Solar refrigeration devices for food preservation in rural areas.

(v) Electric supply through solar cells for domestic lighting, radio and television sets.

(vi) Minielectric stations and prime movers delivering about 10 KW to 20 KW of power for rural settlement of remote areas.

(b) For urban sectors

(i) Solar water heater of about 150 litres for domestic water heating.

(ii) Large scale water heating systems for installations in hotels, hospitals, factories etc.

(iii) Dryer for tea, milk and paper industry.

(iv) Desalination plants for supply of water to coastal industries.

(v) Refrigeration and cold storage facilities of 1-5 tons capacity working on vapor absorption cycles.

Since the electricity can be used most convinently for most of the energy requirements, the major importance has been given on the utilization of solar energy through direct conversion into electricity. The Central Electronics Limited, a public sector undertaking of the DST, has been entrusted with the overall responsibility of research, development and production of economically viable photovoltaic system in cooperation with national laboratories and institutes of higher learning. The programme consists of the following:

(1) To conduct research on various types of low cost solar cells.

(2) To identify the most promising type solar cell suitable for conversion of solar energy into electricity.

(3) Setting up of plant for production of low cost photo-voltaic energy systems.

The main solar energy research activities in India are going on in the following laboratories/Institutions.

S.No.	Institute/Lab.	Solar Devices*
1.	Annamalai University	CONCOL(N), PUMP, STILL, DRYER, HEATCOOL.
2.	Bharat Heavy Electricals Ltd., Delhi	PUMP.
3.	Bharat Heavy Electricals Ltd., Hyderabad	CONCOL (N)
4.	B.I.T.S., Pilani	CELL,CONCOL(N,T), PUMP,STILL, DRYER, HEATCOOL, WATHEAT.
5.	Central Arid Zone Research Institute, Jodhpur	CONCOL(N), STILL, DRYER, COOKER, HEATCOOL, WATHEAT.
6.	Central Building Research Institute, Roorkee	WATHEAT, HEATCOOL.
7.	C.E.E.R.I., Pilani	CELL.
8.	Central Electronics Ltd., Sahibabad.	CELL.

9.	Central Mechanical Engg. Research Institute, Durgapur.	PUMP, DRYER.
10.	Central Salt and Marine Chemicals Research Institute, Bhavnagar.	STILL, COOKER, PUMP.
11.	Hindustan Brown Bovery, Baroda	PUMP, WATHEAT.
12.	Indian Association For Cultivation of Science, Calcutta.	STILL, COOKER.
13.	Indian Institute of Science, Bangalore.	FRELENS, WIMILL.
14.	I.I.T., Bombay.	CELL, CONCOL(N,T), DRYER.
15.	I.I.T., Delhi.	CELL, CONCOL(N), PUMP, STILL, WATHEAT, HEAT COOL, COOKER.
16.	I.I.T., Kanpur	CELL, PUMP, DRYER, HEAT COOL.
17.	I.I.T., Kharagpur.	STILL, HEAT COOL.
18.	I.I.T., Madras.	CELL, CONCOL(N), HEAT COOL.
19.	Jawahar Lal Nehru Agri. Engg. University, Jabalpur	DRYER, HEATCOOL.
20.	Jyoti Ltd., Baroda.	WATHEAT, HEAT COOL, CONCOL(N,T).
21.	Jadavpur University, Calcutta.	CELL.

22.	National Physical Lab., Delhi.	CELL, COOKER.
23.	Punjab Agriculture University, Ludhiana	CONCOL(N), COOKER, HEATCOOL.
24.	Solid State Physics Laboratory, Delhi.	CELL.
25.	Tata Energy Research Institute, Pondicherry	SOLPOND, HEATCOOL.
26.	University of Roorkee, Roorkee.	WATHEAT, HEAT COOL.

* Abbreviations

CELL	Solar Cell
CONCOL(N),(T)	Solar concentrators and Collectors (Nontracking), (Tracking)
COOKER	Solar Cooker
DRYER	Solar Dryer
FRELENS	Fresnel's Lens
HEATCOOL	Heating and Cooling (Including Refrigeration) and Air Conditioning.
PUMP	Solar Pump
SOLPOND	Solar Pond
STILL	Solar Still
WATHEAT	Solar Water Heater
WINMILL	Wind Mills

1.6 Solar Geometry

A place on the surface of earth is identified by its latitude and longitude. We need not bother about the longitude since only latitude variation is reflected in the apparent motion of the sun.

Sun light falls normally, at the equator on equinox days (March 21 and Sept. 23), at the tropic of cancer on summer solstice day (June 21) and at the tropic of capricorn on winter solstice day (Dec. 22) at noon time. The time refers always to the local time and not to the standard time.

To an adequate approximation, the apparent motion of the sun as viewed from a fixed point on the earth describes the cone[2] as shown in Fig. 1.1(a). In the figure the X-axis is in north-south direction, the Y-axis is in east-west direction and Z-axis is in the vertical direction. The cone axis is in the X,Z plane, inclined at an angle λ, which is the latitude (of the fixed point). The cone opening angle β is the angle between the earth's axis of rotation and the earth-sun direction. Since the earth axis in inclined at an angle of approximately 23.5° with respect to the normal to the plane of the ecliptic, the angle β varies from 66.5° to 113.5° during the year. On the equinox days, when $\beta = 90^{\circ}$, the apparent path of the sun is a great circle and the sun

[illegible] APPARENT MOTION OF THE SUN AS VIEWED
FROM A FIXED POINT ON THE EARTH

[illegible] OF THE APPARENT MOTION OF
[illegible] N-S VERTICAL PLANE

does not 'rise or fall' in the vertical. However on solstice days ($\beta = 90^{\circ} \pm 23.5^{\circ}$) the sun rises and falls in the vertical, which can be observed if a pencil hanged horizontally, with its length in the east-west direction, is pointed towards the sun at noon, a horizontal line image would be formed which on equinox days will move along its own length and on any other day a sideway translation of the image occurs in the morning and evening.

The projection of the apparent motion of the sun on N-S vertical plane is shown in Fig. 1.1(b). The observer is at O and P is its zenith point. The line OR represents the plane of the ecliptic at the equinoxes. The angle ROP is the latitude of the observer. WW' and SS' represent the plane of ecliptic at the winter and summer solstice days, respectively. If we draw a line OC from O at any given time and month on Fig. 1.1(b) e.g. at 8 a.m. on the winter solstice, then the angle BOC is called the EWV altitude[3] of the sun at that time. The EWV altitude is the altitude as generally defined projected on a vertical N-S plane. It can be shown that

$$\text{EWV altitude} = \tan^{-1} (\tan \text{altitude} \times \sec \text{Azimuth})$$

The change in the EWV altitude with time is called the EWV altitude swing and it is the swing which must be accommodated by any cylindrical mirror system mounted in east-west direction.

If this swing, measured from equinox (By measuring V from equinox instead of from the ground we eliminate the

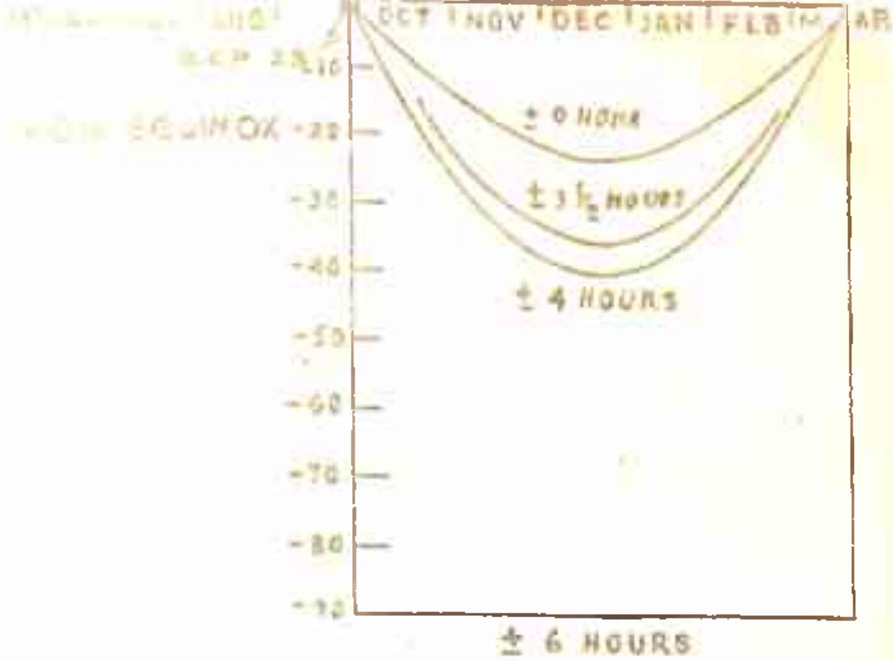

FIG. 1.2 VARIATION OF EWV ALTITUDE WITH DAYS FROM EQUINOX

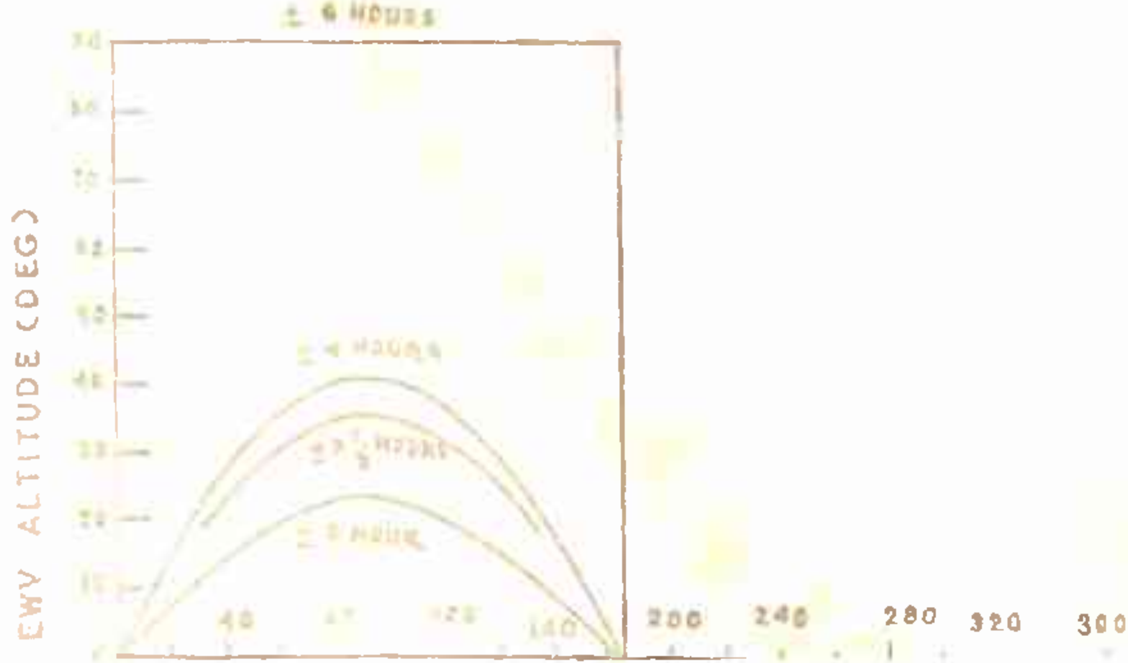
EWV ALTITUDE (DEG)
200
240
280
320

need to know the lattitude) position, is called V and it can be shown, to a first approximation,[3]

$$\tan V = \frac{\tan\left(23.5^{\circ} \sin \frac{2n\pi}{365}\right)}{\cos(15^{\circ} t)} \qquad (1.3)$$

where n is the number of days from the equinox

t is the time in hours, measured from solar noon and

$\pm 23.5^{\circ}$ is the swing of the noon altitude of the sun during the year.

The values of V with respect to the number of days from the equinox for various values of $t = \pm 6, \pm 4, \pm 3\frac{1}{2}$ and ± 0 are plotted in Fig. 1.2.

It is clear from the Fig. 1.2 that if we want to accept all the solar radiation from 8 a.m. to 4 p.m. the total swing of V will be $\pm 41^{\circ}$ or 82° for whole the year while the swing of $\pm 36^{\circ}$ is sufficient to accept the solar radiation for $\pm 3\frac{1}{2}$ hours on the solstice month.

The mirrors with an acceptance angle of the order of 72° or 82° will not have concentration power greater than one[3], hence the mirror fixed during the whole year can not provide any useful concentration.

The situation however can be improved if we make the periodic adjustment in the tilt of the mirror, since an acceptance angle of 17°(Fig. 1.2) will collect sun shine for ± 4 hours on the solstices (even longer on other days), while only 12° is required to collect sunshine for $\pm 3\frac{1}{2}$ hours on the solstices. The concentration power of mirror having acceptance angle of 17° is 2.4 and for acceptance angle of 12° is 3.8. Thus stationary mirror can yields a useful concentration power if we make the periodic adjustment in the tilt of the mirror.

1.7 Role of Concentrators In Utilizing Solar Energy

Solar concentrators are the collection devices which increase the flux density at the receiver surface as compared to the flux density existing on the concentrator entrance aperture. Two types of concentrators are used to concentrate the solar radiations.

(a) Tracking concentratore

In tracking concentrators one has to use a tracking mechanism either by using electronic sensor or by using clockwork mechanism to track the motion of the sun. One such mechanism of the latter type has been developed recently by Gupta[4].

(b) Nontracking concentrators.

In this type of concentrators no diurnal tracking is required but the tilt of the concentrator is adjusted after certain period i.e., once a week.

The concentrators are mainly used for thermal and photovoltaic conversion of solar energy:

(i) Thermal conversion

Solar radiations can be converted into useful mechanical or electrical energy by the thermodynamic process, making use of the temperature higher than ambient. The upper limit to the conversion efficiency in all the thermodynamic process is the Carnot efficiency given by

$$N = 1 - \frac{T_a}{T_H} \qquad (1.4)$$

In general, it is very difficult to change T_a which is the ambient temperature and hence it is clear that higher the value of T_H, the system efficiency will be higher. The maximum temperature which can be obtained without concentrator is only 80°C. The higher temperature can be obtained using concentrators. So that for higher conversion efficiency we require concentrator.

The heat balance equation for a surface collecting solar energy can be written as

Incident Energy = Energy Absorbed + Energy Reflected or Transmitted

or $$IC = \alpha IC + (1-\alpha) IC \qquad (1.5)$$

where I is the solar flux in watts/m^2,

C is the concentration factor which may be greater than or equal to unity and

α is the absorption coefficient of the surface.

Most of the practical solar energy absorbers have high(> 0.7) value of α and negligible transmission, so that it is advantageous to study the energy absorbed in more details. Hence our equation can be written as

Energy Absorbed = Energy Exotracted + Energy Lost by(Radiation+ convection + conduction)

or

$$\alpha IC = \alpha ICP + \epsilon\sigma(T_S^4 - T_a^4) + h(T_S - T_a) + \frac{K}{l}(T_S - T_a)\ \mathrm{W/m^2} \qquad (1.6)$$

where P is the fraction of the absorbed energy extracted,

ε is the emissivity of the surface,

σ is the Stephen-Boltzman constt $=5.67\times10^{-8}$ $\mathrm{Wm^{-2}\ {}^oK^{-4}}$,

T_S is the surface temperature in ^oK,

T_a is the ambient temperature in ^oK.

h is the convection loss coefficient=5 Watts m^{-2} $^oC^{-1}$ and

K is the conductivity of the surface.

Now consider the situation when solar flux I is 1×10^3 Watts m^{-2} and C = 1. The emissivity ε = 1 and α = 0.7

∴ Energy absorbed = αI = 0.7×10^3 Watts/m^2

Let T_a = 20°C and T_S = 80°C we have

Energy lost by radiation = $1\times5.67\times10^{-8}(353^4-293^4)$ Watts/m^2

= 0.46×10^3 Watts/m^2

Energy lost by convection= 5x60 Watts/m^2

= 0.3×10^3 Watts/m^2

Thus we see that at 80°C the sum of losses due to radiation and convection is greater than the energy absorbed, even we have not included the loss due to conduction. Obviously if we want to extract solar energy at temperature in excess of 80°C we have to use optical magnification C (i.e., we have to use concentrators) as is clear from Eq. 1.6.

(ii) Photovoltaic conversion

The cost of solar photovoltaic power generation system can be reduced by increasing the solar cell power output using concentrated sun light on the photovoltaic modules. In this approach the expensive solar cells are replaced by an inexpensive solar concentrator. The concentrated photovoltaic system consists, (i) solar cells, designed to operate efficiently even under concentrated light and (ii) the concentrator of suitable size i.e., the size of the concentrator should not be too small or not too large, since in case of the smaller size the cost of the concentrator may be more than the saving in solar cells and in case of the larger size, handling of the concentrator will be difficult.

Now consider the concentrator with following specifications, as a typical example to illustrate the above point:

(i) Size of the exit aperture = 4 cm

(ii) Length of the concentrator = 200 cm

(iii) Half acceptance angle = 6^0

(iv) Concentration ratio (Geometrical) = 10

The actual concentration ratio will be less than 10. Here we have designed a Winston compound parabolic concentrator (Sec. 2.2) with geometrical concentration ratio equal to 10. The actual concentration ratio observed comes to 6. The solar cells of 4 cm diameter are available(the cost of one solar cell is Rs. 100). So the 50 solar cells can be arranged along the exit aperture of the above mentioned concentrator. Assuming that the solar cells are always illuminated as uniform as possible and power output from solar cells is directly proportional to the concentration ratio. Then the power output from 50 solar cells placed at the exit aperture of the concentrator will be equal to the power output from 300 solar cells, placed in the direct light i.e., placed at the entrance aperture. Hence the cost reduction will be

= [(300 - 50) x cost per solar cell - cost of the concentrator] Rs.

= (250 x 100 - 5000) Rs.

= 20,000 Rs.

where 5000 Rs. is the cost of the above mentioned concentrator.

Thus the cost of solar photovoltaic power system can be reduced greatly by using the concentrators.

1.8 Desirability Of Nontracking Concentrators

In the light of energy crisis the immediate need for a cheaper source of energy in the indian village is felt. In order to make the use of solar energy economically viable one has to use the concentrators (As mentioned earlier in Sec. 1.7).

Even the tracking concentrators have very high concentration ratio compared to nontracking concentrators, but the tracking concentrators will not be appropriate for Indian villages because of their high cost, requirement of sophisticated tracking system and experts to look after these devices. There is clearly a strong case for use of nontracking concentrator in villages as their cost is very less compared to tracking concentrators and are easier in handling. A nontracking concentrator with a concentration ratio between four to ten will be adequate for using in a mini photovoltaic power unit which can fulfil the lighting and some other requirements of villages and also in many solar energy devices.

1.9 Nontracking Concentrators : A Review

The pioneer work in the field of nontracking concentrator was done by Tabor[3] in 1958 when he showed that the maximum concentration ratio which can be obtained (achieved) with nontracking concentrators is of the order of three for an operating period of 8 hours or so. Tabor also showed that the concentration ratio could be increased to about 4 using second stage concentration. Because of rather discouraging nature of Tabor's conclusions there was no significant research activity in this area for more than a decade. The next break through in the field of nontracking concentrators came when Winston[2] in 1974 invented a new design called Winston's compound parabolic concentrator (CPC), which achieves maximum posible concentration allowed by phase rule[5]. Winston's CPC differs from conventional optical focussing devices such as parabolic mirror and Fresnel lenses that it acts as a radiation funnel and does not produce an image of the Sun i.e., it is a nonimaging device. Later on in 1975 Winton and Hinterberger[6] described the principle for calculating the surface of the nontracking concentrators for various types of absorber of arbitrary cross-sections e.g. flat plate, oval tube, circular tube and fin type. However, the surface of nontracking concentrator for cylindrical absorber(i.e., absorber having circular cross-section) has been calculated more explicitly by Rabl[7] . To improve its performance various modifications[8] have been done in this design. Some more models[9-14] of nontracking concentrators have also been developed by various investigators. A few of these models[12-14] will be describedlatter in other chapters. Now we will review the work done on nontracking concentrators in some more detail.

Tabor[3] considered the cylindrical parabolic nontracking concentrator, the cross-section of which is shown in Fig. 1.3. APB is the aperture of the concentrator. The rays after reflection from the concentrator concentrate between I and I' where the absorber is tobe kept. The optical concentration ratio of this design is given by

CROSS-SECTION OF TABOR'S
PARABOLIC CONCENTRATOR

$$P = \operatorname{cosec} 2\delta - 1 \qquad (1.7)$$

where 2δ is the total swing of the incident beam. As mentioned earlier in Sec. 1.6 that if we want to collect all the solar radiations from 8 a.m. to 4 p.m. throughout the year, the total swing will be $\pm 41^\circ$ i.e., 82°. Now it is clear from the Eq. 1.7 that for $2\delta = 41^\circ$, the value of P will be less than one and hence a concentrator (fixed during the whole year) with an acceptance angle of the order of 82° can not give any useful concentration ratio. If we make the periodic adjustment in the tilt of the concentrator, then an acceptance angle of 17° will be required to collect the solar radiation for $\pm$ 4 hours on the solstice (even longer on the other day), while an acceptance angle of 12° will collect the solar radiations for $\pm 3\frac{1}{2}$ hours on the solstice. For a concentrator with an acceptance angle of 15° the optical concentration ratio P is equal to 2.86 i.e., nearly three. It has been shown by Tabor that using an auxiliary side mirror for second stage concentration, the maximum concentration ratio which can be achieved with nontracking concentrator is about four.

Winston's[2] CPC is a two-dimensional cylindrical concentrator, which achieves maximum concentration with minimum tracking requirements. The cross-section of the concentrator is shown in Fig. 1.4. P_R is a parabola with its focus at P' and P'_R is a parabola having focus at P. These parabolas

FIG. [illegible] TRANSVERSE CROSS-SECTION OF WINSTON'S CPC have been extended upto the points at which tangents to the surfaces become parallel to the optic axis. The rays passing through the entrance aperture R R' making angles $\leq \phi$ with the optic axis will pass through the exit aperture P P' after one or more reflections. The absorber is kept at the exit aperture. The concentration ratio of this design is given by

$$C = \frac{D}{d} = \frac{1}{\sin \phi} \qquad (1.8)$$

where D and d are the size of entrance and exit aperture respectively; ϕ is the half-acceptance angle. Thus for an acceptance angle of 12° the concentrator ratio will be of the order of ten (for an average of 8 hours operative time). For a given value of d and ϕ , the height of Winston's CPC is given by

$$H = \frac{d}{2} \left(1 + 1/\sin \phi \right) \cot \phi \qquad (1.9)$$

With increasing concentration ratio C, the reflector area A_R of a CPC grows like 1 + aC with a $\approx$1. Therefore for higher concentration ratios it requires large reflector area for a given entrance aperture A_e. For example, for a concentration ratio of ten, the value of$(A_R/A_e) \approx 11$ while a simple focussing parabola has the value $(A_R/A_e) \approx 1.2$. The problem is not so serious, since a large portion of the top of Winston's CPC can be truncated[15] without any appreciable loss in performance. Therefore from operational as well as economic view points the truncation of CPC is important. In the following Table 1.1, we have given the concentration ratio, height to aperture and reflector area to aperture area ratios for the full and truncated Winston's CPC.

TABLE-1.1

Concentration ratio, height to aperture and reflector area to aperture area ratios for the full and truncated Winston's CPC

Half acceptance angle	Concentration ratio	Height/ Aperture	Reflector area/ Aperture area
	3.65	1.04	2.2
$\sin^{-1}(1/5)=11.5^{\circ}$	4.90	2.25	4.62
	5.00	2.94	6.00
	7.28	1.86	3.86
	9.08	3.03	6.17
$\sin^{-1}(1/10)=5.7^{\circ}$	9.80	4.17	8.44
	10.00	5.47	11.05

It is clear from the Table 1.1 that for an half-acceptance angle = 5.7°, a full CPC achieves a concentration ratio of 10.0; it requires a total of 11.05 meter^2 of reflector area for each meter^2 of aperture area and its height is 5.47 times the aperture width. If this CPC is truncated to a reflector/aperture areas ratios of 6.17, its concentration ratio drops to 9.08. Thus at a loss of 9.2% in concentration, the decrease in reflector/aperture ratio is 44% i.e., the large amount of reflecting material can be saved with very little loss in concentration ratio. At the same time decrease in height to aperture ratio is half time. Due to the reduction in height the handling of the concentrator becomes easier .

Even if the radiations incident on a CPC of half acceptance angle ϕ are distributed uniformly over all angles $|\phi_{in}| < \phi$ the radiations reaching the absorber are totally diffuse i.e., these ranges over all angles ϕ_{out} from $-\pi/2$ to $+\pi/2$. However, the values of $|\phi_{out}|$ near $\pi/2$ are undesirable because most absorber materials shows poor absorptivity at large angle of incidence. If the radiations at the absorber are restricted to angles $|\phi_{out}| < \phi_1$, the highest possible concentration of Winston's[16] CPC will be

$$C' = \frac{\sin \phi_1}{\sin \phi} \tag{1.10}$$

Thus we can have high optical efficiency due to improved absorptivity, bought at the cost of the slight reduction in concentration; For example, with $\phi_1 = 70^\circ$ the concentration is only about 10% smaller than Eq. (1.8).

For a given acceptance angle the compound parabolic concentrator provides a concentration equal to the limit given by Eq. (1.8). A CPC is not suitable however, for high concentration applications because of large surface area[15,17] requirements (as mentioned earlier) and transmission loss. Instead, it has been suggested by Rabl[18] that the use of the CPC as a second stage concentrator with conventional imaging concentrators may be more advantageous and practical to obtain higher concentrations.

Radiations reaching the focal plane of almost all the conventional imaging concentrators such as a lens or a simple parabolic mirror has an angular spread which is less than $\pi/2$. Hence, it can be concentrated further by using a CPC of matched acceptance angle[18,16]. In general, the entrance aperture of the second stage is kept equal to the region of nonzero intensity over the focal plane of the concentrator, but sometimes it may be more desirable to make it equal to the size of central solar image. A somewhat higher and uniform concentration over the final receiver is obtained in the latter case but a fraction of radiation reflected by the primary concentrator is actually lost.

Now we will describe the geometry of two-step[9] and three-step[10] compound wedge concentrators (CWC) developed by Mannan and Bannerot. The transverse cross-section of two-step CWC is shown in Fig. 1.5(a). The inclinations α_1

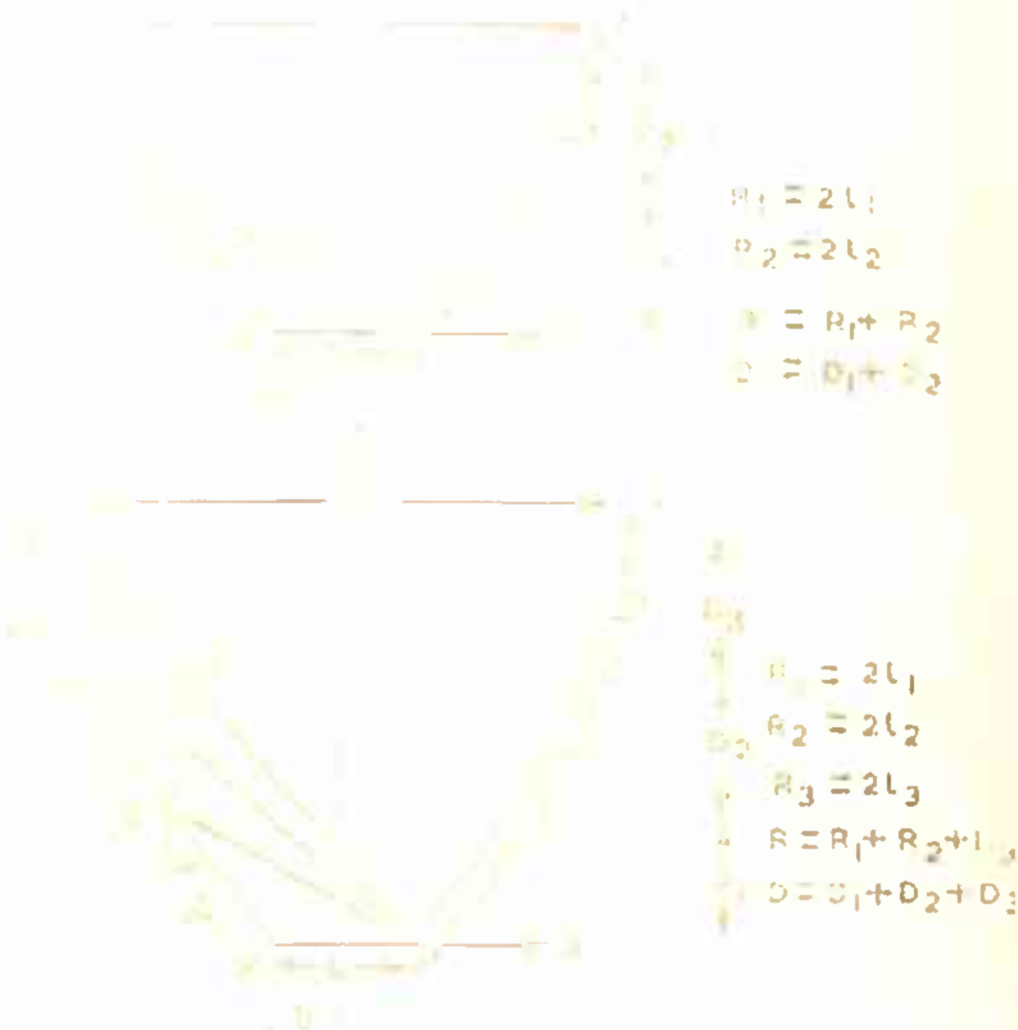

FIG. 1.5 TRANSVERSE CROSS-SECTIONS OF COMPOUND WEDGE STATIONARY CONCENTRATORS

(a) TWO STEP CONFIGURATION

(b) THREE STEP CONFIGURATION

and α_2 of sides P Q and Q R respectively have been chosen in such a way that the ray making an angle δ with the vertical, after reflection from points Q and R reaches to the point P'. The angle δ is called the half-acceptance angle of the concentrator. The sides P' Q' and Q' R' are the mirror images of P Q and Q R respectively about Z-axis. The concentration ratio of the concentrator is given by[9]

$$C = \frac{A}{B} = \frac{2 \cos \alpha_1 \sin(2\alpha_1 - \alpha_2 + \delta) \sin(2\alpha_2 + \delta)}{\sin(\alpha_1 + \delta) \sin(\alpha_2 + \delta)} - 1 \qquad (1.11)$$

The maximum concentration ratio obtainable for a given δ with two-step CPC can be found by solving the following two equations simultaneously.

$$\left(\frac{\partial C}{\partial \alpha_1} \right)_{\alpha_2, \delta} = 0 \qquad (1.12)$$

and

$$\left(\frac{\partial C}{\partial \alpha_2} \right)_{\alpha_1, \delta} = 0 \qquad (1.13)$$

which implies that α_1 and α_2 must satisfy the following pair of transcedental Eqs.

$$\sin(\alpha_2 + \delta) \sin(2\alpha_1 - 3\alpha_2) = \sin \alpha_2 \sin(2\alpha_1 + \delta - \alpha_2) \qquad (1.14)$$

and

$$\sin(\alpha_1 + \delta) \cos(3\alpha_1 - \alpha_2 + \delta) = \cos \alpha_1 \sin(\alpha_1 - \alpha_2) \qquad (1.15)$$

These two equations can be used to generate a series of graphs to illustrate the geometrical characterstics of the two-step CWC. For each value of α_1 there is a α_2 which maximises the concentration ratio. The maximum concentration ratio of two-step CWC for $\delta = 9^{\circ}$ is 2.68 at $\alpha_1 = 21^{\circ}$ and $\alpha_2 = 8^{\circ}$.

The transverse cross-section of the three-step CWC is shown in Fig. 1.5(b). The inclinations α_1, α_2 and α_3 of the side walls P Q, Q R and R S from the vertical have been chosen in such a way that the extreme rays after reflection from Q, R and S will reach to the point P'. The concentration ratio of this concentrator is given by[10]

$$C = \frac{2 \cos \alpha_1 \sin(2\alpha_1 - \alpha_2 + \delta) \sin(2\alpha_2 - \alpha_3 + \delta) \sin(2\alpha_3 + \delta)}{\sin(\alpha_1 + \delta) \sin(\alpha_2 + \delta) \sin(\alpha_3 + \delta)} - 1 \tag{1.16}$$

The maximum concentration ratio of three-step CWC is obtained in the same way as is done for the two-step CWC. This comes out to be 3.19 for $\delta = 9^{\circ}$ at $\alpha_1 = 25.25^{\circ}$, $\alpha_2 = 13.5^{\circ}$ and $\alpha_3 = 5.5$, as compared to the value 2.68 of the maximum concentration ratio for the two-step CWC. It can be shown that the three-step model is more economical than the two-step model in the sense that it requires less reflecting material in order to obtain the same concentration ratio.

The Fig. 1.6 shows the vertical cross-section of the 'nontracking' solar concentrator developed by Sing.al

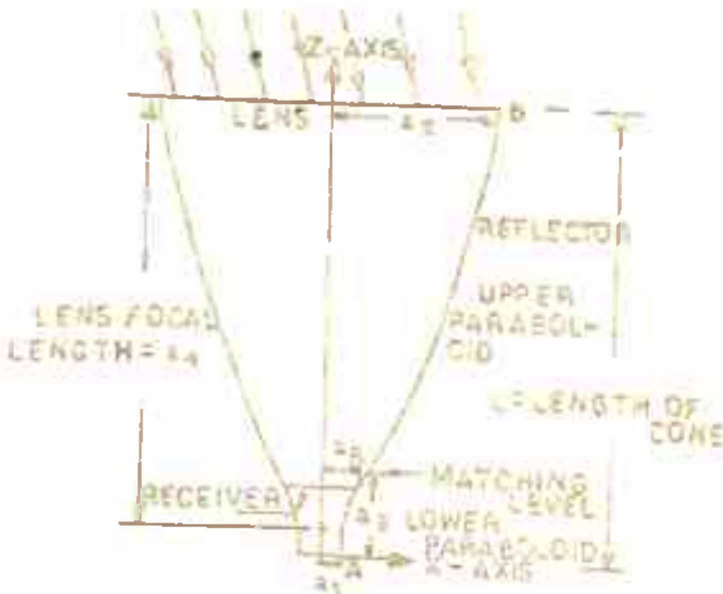

FIG. 1.6 VERTICAL CROSS-SECTION OF SOLAR CONCENTRATOR
(DESIGNED BY SINGAL AND SHIL)

and Shil[11]. The concentrator is obtained by rotating AB (which is a combination of two parabolas) about Z-axis. Thus the entrance and exit apertures are the circles of diameters $2a_2$ and $2a_1$ respectively. A converging lens of diameter $2a_2$ and focal length a_4 is fitted at the entrance aperture. The concentration ratio of the concentrator is given by

$$C = (a_2/a_8)^2 \qquad (1.17)$$

The advantage of this design compared to tracking concentrator is that it does not require continuous tracking and can give the concentration ratio of the order of hundred. However, it requires periodic adjustment of its orientation after about one hour in the east-west direction during its operating period. In other words, this concentrator is not nontracking in the usual sense of the word since it requires adjustments for the diurnal motion of the sun and hence is in between the nontracking and tracking types of concentrators.

1.10 Plan Of Presentation

We have fabricated a number of models of nontracking concentrators using different reflecting materials to study the effect of reflecting material on the various parameters e.g. concentration ratio, thermal efficiency and intensity profile. Out of the models fabricated three are Winston CPC

-to study its experimental performance, one is modified Winston CPC-- to calculate the effect of second stage concentration on the thermal efficiency and three models are of uniform cylindrical concentrators-- to obtain uniform lateral intensity profile at the exit aperture of the concentrator.

In chapter 2 we have studied the experimental performance of Winston's CPC using different reflecting materials. The different reflecting materials used by us are; plain aluminium, granular anodised aluminium and mirror strips. The effect of reflecting material on the efficiency of extraction and on the lateral intensity profile (at the exit aperture) has been discussed in Sec. 2.3. It has been observed that uniformity of illumination increases using granular anodised aluminium sheets.

The concentration ratio of Winston's CPC can be increased by introducing second stage concentration. We have achieved the geometrical concentration ratio in the range of 20 to 30 by combining the focussing properties of a pair of circles/ellipses and that of Winston's CPC. In chapter 3, we have discussed the four configuration of this type (i.e. modified Winton's CPC). One of these models has been fabricated here. In Sec. 3.5 the efficiency of solar energy extraction of this model has been calculated and efficiency is compared to that of Winston's CPC.

The lateral intensity profile at the exit aperture of Winston's CPC is nonuniform. Nonuniformity of illumination reduces the effiency of solar cell. Therefore to obtain uniform illumination we have designed a nontracking concentrator, called uniform cylindrical concentrator. In chapter 4 we have discussed the mathematical formulation of this design. The lateral intensity profile (theoretically) of uniform cylindrical concentrator and that of Winston's CPC are given in Sec. 4.4. The experiments performed to test the uniformity of illumination of the models fabricated are discussed in Sec. 4.6.

R E F E R E N C E S

1. Hal Hellman, Energy In The World of Future. M.Evans and Co., New York, pp, 105(1973).

2. R. Winston, Principles Of Solar Concentrator Of A Novel Design, Solar Energy 16 (2), 89-95 (1974).

3. H. Tabor, Stationary Mirror Systems For Solar Collectors, Solar Energy 2 (3-4), 27-33 (1958).

4. K.C. Gupta, R. K. Mirakhur And A.P. Sathe, A Simple Solar Tracking System, SUN I, 2, Proc. International Solar Energy Society Congress, Jan. 1978, New Delhi, pp. 1336-40.

5. R. Winston, Light Collection Within The FrameWork Of Geometrical Optics, Journal Of Optical Society Of America 60 , 245-47 (1970).

6. R. Winston And H. Hinterberger, Principles Of Cylindrical Concentrators For Solar Energy, Solar Energy 17 (4), 255-58 (1975).

7. A. Rabl, Solar Concentrators With Maximal Concentration For Cylindrical Absorbers, Applied Optics 15 (7),1871-73 (1976).

8. R. Winston, Ideal Flux Concentrators With Reflectors Gaps, Applied Optics 17 (11), 1668-69 (1978).

9. K.D. Mannan And R.B. Bannerot, Optimal Geometries For One And Two Faced Symmetric Side-Wall Booster Mirrors, Solar Energy 21 (5), 385-91 (1978).

10. K.D. Mannan, Performance Of Optimal Geometry Three Step Compound Wedge Stationary Concentrator, SUN I,2, Proc. International Solar Energy Society Congress, January, 1978, New Delhi, pp. 1218-22.

11. C.M. Singal And S.K. Shil, Nontracking Solar Concentration For Solar Cell, Proc. National Solar Energy Convention 1976, Calcutta, pp. 58-61.

12. A. Gupta, S. Kumar And V.K. Tewary, Design Of A Nontracking Concentrator Which Will Distribute Sunlight In A Uniform Manner Over A Flat Receiving Surface, Proc. National Solar Energy Convention 1976, Calcutta, pp. 66-67.

13. A Gupta And S. Kumar, Design Of Nontracking Concentrator Capable Of Avoiding Shadow On The Obserber Plate, Proc. National Solar Energy Convention 1978, Bhavnagar, pp. 127-30.

14. Murlidhar, A. Gupta And V.K. Tewary, A Nontracking Heat Concentrator Capable Of Giving Concentration Factor Of The Order Of 20, Proc. National Solar Energy Convention 1976, Calcutta, pp. 62-63.

15. A Rabl, Optical And Thermal Properties of Compound Parabolic Concentrators, Solar Energy 18 (6), 497-511 (1976).

16. A. Rabl And R. Winston, IDeal Collectors For Finite Sources And Restricted Exit Angles, Applied Optics 15 (11), 2880-83 (1976).

17. D.P. Grimmer, A Comparision Of CPC And SPC Concentrating Solar Collectors, Solar Energy 22 (1), 21-25 (1979).

18. A. Rabl, Comparision Of Solar Concentrators, Solar Energy 18 (2), 93-111 (1976).

19. M. Collares-Pereira, A. Rabl and R. Winston, Lens-Mirror Combinations With Maximal Concentration, Applied Optics 16 (10), 2677-83 (1977).

CHAPTER-2

PERFORMANCE STUDY OF WINSTON'S COMPOUND PARABOLIC CONCENTRATORS

CHAPTER-2.

PERFORMANCE STUDY OF WINSTON'S COMPOUND PARABOLIC CONCENTRATORS

2.1 Introduction

To study the performance of a concentrator one may conduct experiments on the response of the concentrators in the following two ways:

(i) Optical performance: In the optical performance study photo-voltaic devices e.g., solar cells, photodiodes etc. are used for measuring the response of the concentrator to the visible part of the spectrum. With the help of these devices we can calculate how much optical radiation is concentrated at the absorber. This information is useful for using the concentrator to fabricate power units using photodevices.

(ii) Thermal performance: In the thermal performance study we are mainly interested in investigating how much energy (in the form of heat) concentrator can transfer from solar radiation to the useful gain of the working fluid which may be a liquid, vapor or gas.

In the earlier discussion on nontracking concentrators (Sec. 1.9) it is mentioned that a breakthrough in this area has been achieved by Winston's[1] compound parabolic concentrator. Various investigators[2-6] have studied its experimental performance which we shall discuss latter at the end of this chapter. In order to study the effect of different reflecting surfaces on the performance of the concentrators in general and as regards the extent of uniformity of illumination in particular, we have fabricated three models of Winston's CPC. The different reflecting surfaces used in the models fabricated by us are: plain aluminium, granular anodised aluminium and mirror strips. The specifications and methods of fabrication of these models are given in Sec. 2.2. In Sec. 2.3 we have calculated the concentration ratio and efficiency of solar energy extraction for first two of these models. In this section we also describe the lateral intensity profile at the exit aperture measured for two of these models. The discussion and conclusions of the experiments performed are given in Sec. 2.4.

2.2 Specifications of the Models Fabricated

The specifications of these models fabricated are given in Table 2.1.

Table-2.1

Model No.	Specifications D (cm)	d (cm)	H (cm)	l (cm)	ϕ (Deg.)	Geometrical concentration ratio	Material used
W1	20.0	2.8	81.0	50.0	8.0	7.1	Aluminium shee
W2	20.0	2.0	109.4	200.0	5.7	10.0	Mirror strips
W3	20.0	4.0	58.8	150.0	11.5	5.0	Granularly anodised al. sheets.

Notation used (See. Fig. 1.4)

D - Size of the entrance aperture

d - Size of the exit aperture

H - Height of the concentrator

l - Length of the concentrator [not shown in Fig.(1.4)]

ø - Half-acceptance angle

These models have been fabricated by using two methods which we have described below:

First Method

In this method, first of all two wooden pieces of 2 cm thickness are made having the shape P R R' P'(Fig. 1.4), which is the cross-section of the concentrator, to be fabricated. On one side of these wooden pieces (called end walls) aluminium sheet used as reflecting material is nailed. The end walls are errected on the wooden frame of the absorber at a distance equal to the length of the concentrator. The two reflecting surfaces of proper dimension, made out of the aluminium sheet of above thickness are fixed on the sides of the concentrator so as to fit exactly with the curved boundaries P R and P' R' of the end walls. At the outer side of these reflecting surfaces the plywood of 3 mm thickness and of same size are nailed. To keep the concentrator into vertical position four legs are attached on the end walls as shown in Fig. 2.1. On one end wall a plywood piece of 15 x 20 cm^2 is nailed perpendicular to it. A line, called the central line

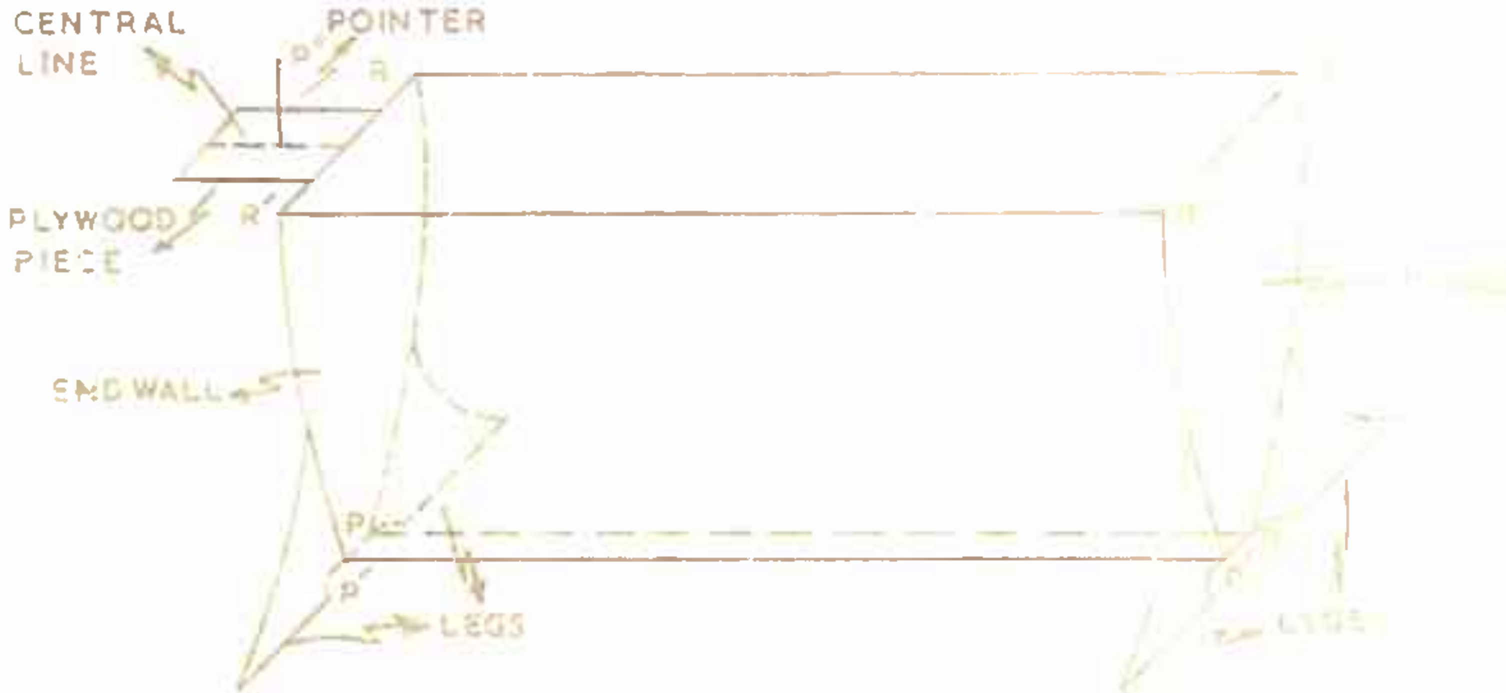

FIG. 2.1 THREE - DIMENSIONAL VIEW OF A TYPICAL WINSTON'S CPC
FABRICATED AT BITS

is marked on this plywood piece exactly at the centre of the RR' (Fig. 1.4). Thus, this line will be perpendicular to the optic axis of the concentrator. A pointer P'' is fixed at the middle point of this line. A provision is made so that the concentrator can be used for both purposes i.e., for thermal and photovoltaic conversion. This is achieved by cutting a semicircular portion of diameter PP' (Fig. 2.2) from both the end walls. The model W1 is fabricated by this method.

Second Method

Let P R R' P' (Fig. 2.3) be the cross-section of the concentrator which is going to be fabricated. In this method first the ribs[7] of the shape P R Q S (Fig. 2.3) are made from the 2 cm thick wood. The R Q is taken 2.5 cm and hence PS is equal to 1/2 (D-d) + R Q. These ribs are assembled to form the two rib assemblies of the type shown in Fig. 2.4. The length of the rib assembly is equal to the length of the concentrator and the number of ribs in the rib assembly depends upon the length of the concentrator. In the fabrication of these concentrators we have taken the distance between two ribs equal to 30 cm. On the inner side of these rib assemblies the plywood of 3 mm thickness of proper dimension is nailed, after that the aluminium sheet (1.5 mm thickness) of same size is nailed on the plywood. These rib assemblies are fixed on a plane wooden piece, seperated at the bottom by a distance equal to the exit aperture of the concentrator. The ends are

FIG. 2.2 SHAPE OF THE END WALL

FIG. 2.3 TRANSVERSE CROSS—SECTION OF THE CONCENTRATOR SHOWING THE SHAPE OF THE RIB ON RIGHT SIDE

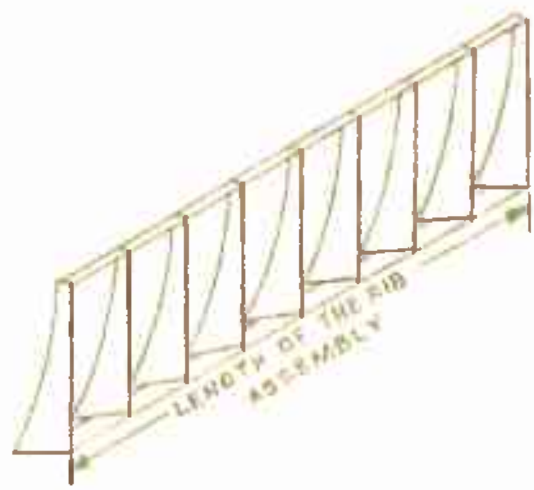

FIG. 2.4 RIB ASSEMBLY

closed by two wooden pieces (called end walls) of proper dimensions having aluminium sheet on inner side. On one end wall a plywood piece of 15 x 20 cm^2 is nailed perpendicular to the end wall. A line, called the central line is marked on this plywood piece exactly at the centre of RR' (Fig. 2.3). Thus, this line will be perpendicular to the optic axis of the concentrator. A pointer is fixed at the middle point of this line. The same provision, described earlier in the first method is made so that the concentrator can be used for both thermal and photo-voltaic applications. The models W2 and W3 are fabricated by this method. In case of model W2 mirror strips of proper dimensions are fixed on the plywood by favicol, instead of aluminium sheets.

2.3 Experiments Performed and Results

Three following types of experiments have been performed on these models: (a) Measurements of concentration ratio using solar cells, (b) Thermal efficiency of the concentrator and (c) Intensity profile at the exit aperture. The experimental set up is same in all the cases i.e., in all the experiments the concentrator is placed in such a way that its length is along the east-west direction. Then the concentrator is tilted from the vertical so that the solar rays are parallel to the optic axis (See Fig. 1.4), of the concentrator. This is achieved by tilting the concentrator from the vertical until the shadow of the pointer P'' falls on the central line (Fig. 2.1). The time at which the concentrator is tilted from the vertical depends upon the operative time of the concentrator. If the operative time of the concentrator is 8 hours i.e., ± 4 hours from the local noon, then the concentrator is tilted from the vertical roughly two and half hours prior to the local noon. After that the concentrator remain fixed during the whole operative time. The tilt of the concentrator from the vertical has to be changed only after a week (Sec. 1.6). The experiments performed are described below:

(a) Concentration ratio using solar cell

For moderate values of concentration ratio, the short circuit current I_{sc} of the solar cell is directly proportional to the intensity. So, in order to calculate the concentration ratio of a concentrator, it is required to measure the short circuit current of solar cell in the direct and concentrated light. The concentrator is adjusted by the method described above and the short circuit current is measured at the entrance and exit apertures. The concentration ratio was calculated by the expression

$$\text{Concentration ratio} = \frac{I_{sc}(C)}{I_{sc}(D)} \qquad (2.1)$$

where $I_{sc}(C)$ is the short circuit current in the concentrated light i.e., at the exit operative and $I_{sc}(D)$ is the short circuit current in the direct light i.e., at the entrance aperture. A few typical readings, spread over a few days, obtained for model W1 and model W2 (See Table 2.1) are given in Tables 2.2 and 2.3 respectively.

Table-2.2

Determination of the concentration ratio of model W1 by measuring the short circuit currents

S.No.	I_{sc}(D) (mA)	I_{sc}(C) (mA)	Concentration ratio
1.	0.86	2.68	3.1
2.	0.92	2.86	3.1
3.	0.83	2.58	3.1

Table - 2.3

Determination of the concentration ratio of model W2 by measuring the short circuit currents.

S.No.	I_{sc}(D) (mA)	I_{sc}(C) (mA)	Concentration ratio
1.	0.45	3.5	7.8
2.	0.50	4.0	8.0

(b) Thermal efficiency of the concentrator

The efficiency η, of the CPC solar concentrator is defined as

$$n = \frac{Q}{I_t} \quad (2.2)$$

where Q is the heat energy extracted and I_t is the total incident energy. The optical efficiency n_o. of the solar concentrator is defined as that fraction of I_t which reaches the absorber and is absorbed there. So the efficiency n of the concentrator can be written as

$$n = n_o - \frac{Q_{loss}}{I_t} \quad (2.3)$$

where Q_{loss} is the overall heat lost due to radiation, conduction and convection. It is clear from Eq. (2.3) that in order to have high efficiency n, of the solar concentrator, the losses should be very small. Here we have calculated the efficiency of model W1 and W2. The experiments performed on these models are described below:

(I) Model W1

In order to calculate the efficiency n, the concentrator is adjusted for parallel rays at 10.00 a.m. by the method described earlier. The circular blackened tube (aluminium circular pipe of outer diameter 2.7 cm, thickness 0.2 cm and blackened by black board paint) filled with water is kept at the exit aperture. Following readings are obtained:

(i) Amount of water filled in the circular tube

(M) = 180 Grams

(ii) Ambient Temperature = 22°C

(iii) Temperature rise (In one hour) $T = 34^{\circ}C$

(iv) Intensity of solar radiation = 85 mw/cm^2

(v) Area of the entrance aperture = $50 \times 20\ cm^2$

$\therefore$ Heat energy extracted (Q)

= MST

where S is the specific heat of the water

$\therefore$ Q = ($180 \times 1 \times 34$) Calories

= 2.57×10^4 Joules

Total incident energy (I)

$$= 50 \times 20 \times \frac{85}{1000} \times 3600 \times 0.92^{*} \text{ Joules}$$

$$= 2.81 \times 10^5 \text{ Joules}$$

$$\therefore\ n = \frac{2.57 \times 10^4}{2.81 \times 10^5} = .09$$

i.e. n = 9 %

---

*This factor(F) comes from the fact that for a fixed CPC concentrator tilted to the south, the normal incident solar flux will vary approximately as the cosine of the azimuth angle of the sun.[8] Hence integrating over the experimental time(the time for which the calculations are done i.e., from 10.00 a.m. to 11.00 a.m.) of approximately constant flux, a fixed CPC concentrator will be able to use roughly

$$\int_{-\pi/6}^{-\pi/12} \cos\theta\, d\theta \Big/ \int_{-\pi/6}^{-\pi/12} d\theta$$

$$= \frac{(\sin\theta)_{-\pi/6}^{-\pi/12}}{(\theta)_{-\pi/6}^{-\pi/12}} = 0.92$$

or 92 % of the incident energy.

(II) Model W2

For calculating the efficiency n, the concentrator is adjusted for parallel rays at 10.00 a.m. by the method described earlier. The circular blackened tube (Mild steel circular pipe of outer diameter 1.87 cm, width 0.18 cm and blackened by black board paint) filled with water is kept at the exit aperture. Following readings are obtained :

(i) Amount of water, filled in the circular tube,

(M) = 480 Grams

(ii) Ambient temperature = 20°C (i.e. temp. of water)

(iii) Temperature rise T = 80°C

(iv) Mass (m) of the water converted into steam in 4 hours

= 350 Grams

(v) Intensity of solar radiation = 90 mw/cm^2

(vi) Area of the entrance aperture = 200 x 20 cm^2

∴ Heat energy extracted (Q) = MST + mL

where S is the specific heat of water and L is the latent heat of steam.

i.e. Q = (480 x 1 x 80 + 350 x 536) Calories

$= 94.92 \times 10^4$ Joules

Total incident energy (I_t) = $\frac{200 \times 20 \times 90 \times 4 \times 3600 \times 0.95}{1000}$ + Joules

$= 49.25 \times 10^5$ Joules

$$\therefore n = \frac{94.92 \times 10^4}{49.25 \times 10^5} = 0.193$$

$\therefore$ n = 19.3 %

+ See footnote on page 62.

We have also performed an experiment to find the maximum temperature obtainable by this model (W2). The concentrator is adjusted at 10.00 a.m. for parallel rays. The circular blackened tube (the same used for calculating η of W 2) filled with transformer oil is kept at the exit aperture. The maximum temperature obtained is 170°C (stagnant temperature) in the month of December and 178°C in the month of April at 12.00 noon. The Table 2.4 shows the variation of oil temperature and ambient temperature from 10.00 a.m. to 2.00 p.m.

Table -2.4

Variation of oil temperature and ambient temperature

Time	Dec. 77		April 78	
	T_o (°C)	T_a(°C)	T_o(°C)	T_a(°C)
10.00 a.m.	20.0	20.0	27.0	27.0
10.30 a.m.	140.0	22.6	145.0	29.0
11.00 a.m.	156.0	26.0	160.0	30.0
11.30 a.m.	165.0	26.0	169.0	32.0
12.00 Noon	170.0	27.0	178.0	34.0
1.00 p.m.	140.0	26.0	146.0	33.0
2.00 p.m.	120.0	26.0	130.0	33.0

where T_o is the temperature of transformer oil and T_a is the ambient tempature.

(c) Intensity profile at the exit aperture

The lateral intensity profile at the exit aperture has been studied for models W1 and W3 (See Table 2.1). The experimental set up is same in both the cases and has been already described in section 2.3 . The experiment is conducted on various days from winter solstice to equinox. Now first we will describe the experiment performed on model W1.

(i) Experiment performed on model W1

As mentioned earlier in Sec. 2.3(a) that the concentration ratio of the concentrator can be expressed by the Eq.(2.1) as

$$\text{Concentration ratio} = \frac{I_{sc}(C)}{I_{sc}(D)} \qquad (2.4)$$

Therefore for testing the uniformity of illumination the concentration ratios are measured (using above Eq.(2.4)) at two different points (since the size of the exit aperture of model W1 is 2.8 cm, however in case of model W3 concentration has been measured at three different points because the size of exit aperture is 4.0 cm) along the width of the exit

---

* The factor F for this experiment is

$$\int_{-\pi/6}^{\pi/6} \cos\theta \, d\theta \Big/ \int_{-\pi/6}^{\pi/6} d\theta$$

(Since the calculations are done for the time from 10.00 a.m. to 2.00 p.m.)

$$= \frac{(\sin\theta)_{-\pi/6}^{\pi/6}}{(\theta)_{-\pi/6}^{\pi/6}} = \frac{0.5 + 0.5}{\pi/3} \quad \frac{3}{\pi}$$

$$= 0.95$$

or 95.0 % of the incident energy.

aperture by placing two solar cells. Table 2.5 shows the reading obtained on various dates. The nonuniformity of illumination for the model W1 comes out to 16 to 23 % . Thus, the intensity distribution at the exit aperture is nonuniform for the model W1.

It has been observed that uniformity of illumination is much better if we can provide scattering centres at the reflecting surface. The nonuniformity in the illumination can be smoothed by providing discontinuities on the reflecting surface. The discontinuities and scattering centres are also source of diffuse reflection and thus we lose a part of incoming radiation in this process and hence we gain in terms of uniformity but we lose in terms of concentration. These discontinuities on the reflecting surface can be obtained by granularly anodised aluminium sheet. The model W3 has been fabricated using granularly anodised aluminium sheet as reflecting material. Now we will describe the experiment performed on model W3.

(ii) Experiment performed on model W3

The experiment on the model W3 is conducted along the experiment of model W1 under identical conditions from winter solstice to equinox. As mentioned earlier, that for testing the uniformity of illumination the concentration ratios are measured at three different points along the width of the exit aperture by placing three solar cells at equal intervals. The reading obtained are given in Table 2.6. The nonuniformity

Table - 2.5

Diurnal and seasonal widthwise variation of concentration ratios of Winston's CPC(W1)

Date	TIME: 11.00 a.m.		12.00 Noon		1.00 p.m.		2.00 p.m.	
Concentration Ratio	Solar cells 1	Solar cells 2	Solar cells 1	Solar cells 2	Solar cells 1	Solar cells 2	Solar cells 1	Solar cells 2
20.12.78	2.6	3.7	2.1	3.2	2.5	3.45	2.4	3.5
21.12.78	2.85	4.0	2.3	3.4	2.15	3.2	2.6	3.65
10.1. 79	2.2	3.3	2.45	3.5	2.4	3.8	2.5	4.0
11.1. 79	2.75	3.95	2.46	3.46	2.4	3.6	2.7	3.8
2.2. 79	2.3	3.4	2.65	3.65	2.0	3.1	2.85	4.0
3.2. 79	2.5	3.7	2.8	3.85	2.7	3.7	2.9	4.0

Table -2.6

Diurnal and seasonal widthwise variation of concentration ratios of Winston's CPC(W3)

Date	Concentration Ratio	T I M E											
		11.00 a.m. Solar cells			12.00 Noon Solar cells			1.00 p.m. Solar cells			2.00 p.m. Solar cells		
		1	2	3	1	2	3	1	2	3	1	2	3
20.12.78		1.9	2.1	2.0	1.7	1.9	1.7	1.85	1.85	1.0	2.2	2.35	2.33
21.12.78		2.8	2.85	2.85	2.45	2.5	2.35	1.9	2.15	1.85	2.3	2.4	2.5
10.1. 79		2.8	2.6	2.6	2.4	2.5	2.2	2.0	2.15	2.0	2.15	2.3	2.15
11.1. 79		2.7	2.5	2.6	2.3	2.4	2.15	1.9	2.0	2.1	2.0	2.1	2.2
2.2. 79		2.7	2.7	2.5	2.35	2.5	2.35	2.1	2.3	2.15	2.2	2.3	2.3
3.2. 79		2.8	2.8	2.7	2.2	2.4	2.2	1.9	2.1	2.1	2.4	2.6	2.5

of illumination of model W3 comes out to 2 to 7 % .

2.4 Discussions and Conclusions

The experiments performed on the Winston's CPC models which we have fabricated are; (a) measurement of stagnant temperature, (b) thermal efficiency and (c) lateral intensity profile. In this section we have discussed the results obtained using these models with that of others work of similar type.

(a) Stagnant temperature

The stagnant temperature is measured for model W2 (Sec. 2.3) . The variation of stagnant temperature of oil and ambient temperature is given in Table 2.4. The highest stagnant temperatures of 170°C and 178°C were obtained in the month of December and April, respectively. Also the averaged out temperature of nearly 150°C is available contineously for four hours. The measurement of stagnant temperature has also been done by Pahoja and Nanda[3] who have fabricated a number of models of Winston's CPC with half-acceptance angle (ϕ) equal to 6° and exit aperture (d) equal to 1.0 c.m. These models were truncated at 38.0 c.m. height (actual height being 50.5 c.m.), so the corresponding geometrical concentration ratio comes out to be 9.4. The reflecting surfaces were made of aluminium sheets and four different types of absorber were used (i) copper pipe, (ii) aluminium pipe, (iii) flat metal strip inside a glass tube and (iv) black liquid in a glass tube. The highest stagnant temperature of 98°C was obtained for the 'flat metallic strip in glass tube' type of absorber. When a glass cover was used at the entrance aperture, the tempreture marginally increased to 101°C . It is also clear from their figure (drawn for the variation of stagnant temperature) that the averaged out temperature of 95°C is available contineously for four hours. Thus the averaged out temperature which we have obtained with model W2 is higher by 55°C compared to that obtained by Pohoja and Nanda[3] because the reflecting surface (mirror strips) used for model W2 .

(b) Thermal efficiency

The thermal efficiency i.e., the efficiency of solar energy extraction has been calculated for models W1 and W2.

(I) Model W1

The efficiency of solar energy extraction of this model comes out to be 9 % . The main reasons for this low collection efficiency are (i) Low reflectivity of the reflecting surface, since ordinary aluminium sheets have been used without any surface deposition and (ii) Absorber is also made of aluminium. The material of the absorber plays an important role in the efficiency of thermal conversion of solar energy. For example, it has been reported by Acharya and Misra[9] that the efficiencies of solar energy collection, using aluminium pipe and copper pipe as the absorber (keeping all other conditions of the experiments same), are 11.5 and 14.4 % respectively i.e. efficiency increases by 25 % using copper pipe as an absorber compared to aluminium pipe.

(II) Model W2

The efficiency of solar energy extraction of this model comes out to be 19.3 % . However, the maximum efficiency obtained by Collares - Pereira and et al[4] (with CPC of circular absorber) is 40 % using a CPC having half-acceptance angle equal to 8^{o} and absorber diameter 1.3 cm. The CPC was truncated to an effective concentration of 5.25 (actual concentration being 7.19). Aluminized mylar sheets were used for reflecting surface and a commercially available evacuated receiver was used as the absorber. The efficiency which we have obtained by model W2 is very less compared to that obtained by collares- Pereira and etal due to following reasons (i) G.I. pipe was used as the absorber and (ii) the absorber was not enclosed in a evacuated tube. Here we have not used the evacuated receivers since the cost of fabrication will be higher using these receivers.

It has been observed by Collares - Pereira and et al[6] that (i) the efficiency of CPC increases significantly using evacuated absorbers with selective surfaces compared to non-evacuated receivers which are useful only in the range of 50°C to 70°C and (ii) the CPC's having concentration higher than five (using these evacuated receivers) are not necessary because for the CPC of concentration ratio 5 the losses are already so small that a further increase in concentration ratio will corresponds to a negligible increase in operating efficiency.

The efficiency of extraction can also be increased by allowing the working fluid to flow through the absorber pipe. By adjusting the flow rate one can maintain the absorber temperature at any desired value and losses can be minimized. The experiment of this type has been performed by K.K. Rao et al[2]. Ten models of Winston's CPC were fabricated having half-acceptance angle equal to 14.5° and exit aperture of 1.25 cm. Aluminium sheets were used as reflecting material and G.I. pipes as the absorber. All the concentrators were placed parallel to each other and their absorbers were connected to one-another, in such a way that the output of one is the input of other. Water was allowed to flow at a constant rate and the flow rate was measured by rota-meter. The inlet and outlet temperatures were measured by copper constantan thermocouples. The experiments were performed for three different flow rates. It was observed that the efficiencies are 35 % , 50 % and 55 % at flow rates of 5 litres/hour, 10 litres/hour and 15 litres/hour, respectively.

It has also been observed that the degradation of reflecting surface was very fast in case of model W2. However, the reflecting material i.e. mirror strips used for this model are cheaper compared to other reflecting materials. At the same times, these strips provide mosaic structure which makes replacement easier.

(c) Intensity Profile

The variation of intensity at the exit aperture of model W1 is 16 to 23 % , however it is only 2 to 7 % for model W3. Thus, the lateral intensity profile at the exit aperture is more uniform in case of model W3 compared to model W1. The uniformity of illumination (desired for some purpose[10]) has been achieved by providing scattering centres (obtained using granularly anodized aluminium sheets) at the reflecting surfaces at the cost of decrease in concentration ratio.

To conclude it can be said that using mirror strips, the method by which we have fabricated the model W2 is not good from durability points of view, since by glueing the mirror strips on the plywood the coating of mirror strips vanishes within one and half years, also better conducting absorber can be used but it means additional cost of fabrication and finally the lateral intensity profile at the exit aperture becomes more uniform using granularly anodised aluminium sheets for reflecting surface. However, the uniformity of illumination is very important for photovoltaic applications and not for thermal applications.

R E F E R E N C E S

1. R. Winston, Principles of Solar Concentrators of A Novel Design, Solar Energy 16 (2) , 89-95(1974).

2. K.K. Rao, M.C. Gupta, S B Ahmed and R. Natarajan, An investigation of Experimental Performances of A Compound Parabolic Concentrator, Proc. National Solar Energy Convention 1978, Bhavnagar, pp.137-41.

3. M. H. Pahoja and S.K. Nanda, Comparative Performance of Tracking Type And Nontracking Type Solar Concentrators, SUN I, 2, Proc. International Solar Energy Society Congress, January 1978, New Delhi, pp. 1316-20.

4. M. Collares- Pereira, J.J. O'Gallagher, A. Rabl and R. Winston; A compound Parabolic Concentrator For A High Temperature Solar Collector Requiring Only Twelve Tilt Adjustments Per Year, SUN I, 2, Proc. International Solar Energy Society Congress, January 1978, New Delhi, pp. 1223 - 26.

5. M. Collares- Pereira, N.B. Goodman , P. Greenman, J. O'Gallagher, A. Rabl, H. Simmons, L. Wharton and R. Winston, Compound Parabolic Concentrators With Non-Evacuated Receivers; Prototype Performance And A Large Scale Demostration In A School Heating System, SUN I, 2

Proc. International Solar Energy Society Congress, January 1978, New Delhi, pp. 1227- 32.

6. M. Collares- Pereira, J.O'Gallagher, A Rabl, R. Winston , R. Cole, W. McIntire, K. Reed and W. Scherts Design And Performance Characterstics Of Compound Parabolic Concentrators With Evacuated And With Non-Evacuated Receivers, SUN II, 2 , Proc. of The International Solar Energy Society Silver Jubilee Congress, May 1979, Atlanta, Georgia, pp. 1295-99.

7. R. Winston, A. Rabl, N. Levitz, J. Allen, K. Reed and W. Schertz, Development of Compound Parabolic Concentrators For Solar Thermal Application, An ASME Publication 76-WA/SOL-11.

8. D.P. Grimmer and K.C. Herr, Solar Process Heat From Concentrating Flat Plate Collectors, Solar Collectors 2 Sharing The Sun, Solar Technology In The Seventies. pp. 351-74.

9. S.K. Acharya and L.N. Misra, Optimum Solar Energy Collection, Proc. National Solar Energy Convention 1976, Calcutta, pp. 181- 85.

10. S.R. Dhariwal, L.S. Kothari and S.C. Jain, Response of p-n Junction Solar Cells To Concentrated Sunlight And Partial Illumination, SUN I, 2, Proc. International Solar Energy Society Congress, January 1978, NewDelhi, pp. 714-18.

CHAPTER-3

MODIFIED WINSTON'S COMPOUND PARABOLIC CONCENTRATOR

CHAPTER-3

MODIFIED WINSTON'S COMPOUND PARABOLIC CONCENTRATOR

3.1 Logic And Methodology Of Second Stage Concentration

Upto now we have been discussing non-tracking concentrators which involve only the first stage of concentration of the solar radiation. It is for such a concentrator only that for an half-acceptance angle of 6° Tabor[1] got a concentration factor of about 3 and Winston[2] got a concentration factor of 9.6 etc. It is naturally tempting to ask whether it is possible to get higher concentrations by introducing more stages of concentrations so that the exit aperture for one stage of concentration becomes the entrance aperture for the next stage of concentration and so on. In answer to this question Tabor had proved that the second stage concentration makes only a marginal improvement and raises the concentration factor from 3 to 4 and that the third stage will not even do that much. For Winston's design a second or higher stage concentration will be of no advantage, in general, because the half-acceptance angle for the second stage itself will always be 90° irrespective of the starting $\emptyset$ value, and that implies no further concentration since $(1/\sin 90^{\circ})=1$. However, for thermal applications there can be a possibility of achieving effectively higher concentration factors. This follows from the fact that for the concentrators having a working fluid, the diameter of the pipe will be equal to the exit aperture and it will be heated only from the upper half portion and therefore we can think of a smaller pipe getting heat from bottom as well as from top. In this chapter we discuss this possibility in some detail and since the second stage of concentration is achieved by introducing some modifications at the bottom of Winston's CPC, this second stage concentrator is called as the modified Winston's CPC. It should be however, emphasized that since this modification effectively results in folding of the exit aperture of single stage Winston's CPC it cannot give any advantage, what soever in photovoltaic applications where the solar cells are to be illuminated only from one side.

The concentration ratio of Winston's CPC (Fig.1.4) is given by

$$C = \frac{1}{\sin \phi} = \frac{D}{d} \qquad (3.1)$$

where ϕ is the half acceptance angle

D is the size of the entrance aperture and

d is the size of the exit aperture.

If we want to use the Winston's CPC for thermal conversion, we will have to keep a flat absorber of width d or a circular pipe of diameter d at the exit aperture. The absorber will get heated from top only. If we use, a flat absorber of width AA' = d/2 as shown in Fig.(3.1 which only

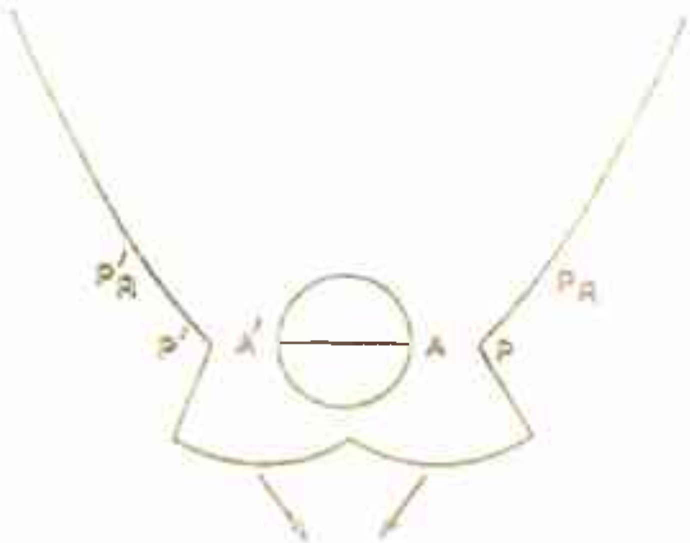

FIG. 3.1 TRANSVERSE VIEW OF THE BOTTOM PART OF TWO-STAGE NONTRACKING CONCENTRATOR

shows the bottom part of Winston's CPC shown earlier in Fig. 1.4)or a circular pipe of diameter AA' and reflectors below AA' in such a way that the light passing through P'A' and PA is reflected back to AA'. In this case the absorber will get light from top as well as from bottom and the heat concentration will be increased by a factor of 2. Here we have developed various types of heat concentrators (collector modified Winston's CPC), the heat concentration ratios in the range of 20 to 30 [3] have been achieved by combining the focussing properties of a pair of ellipses/circles and that of Winston's CPC. In Sec. 3.2 we have discussed the advantages and disadvantages of these models and the theory of modification of these models have been discussed in Sec. 3.3.

3.2 Advantages And Disadvantages of Second Stage Concentrators

The advantage of these models is that we can get the higher temperatures and hence the Carnot efficiency (given by Eq. 1.4) will be higher. The disadvantage of these models are;

(i) Due to more number of reflections(because of second reflectors) the optical losses will be more.

(ii) It can not be used for photovoltaic conversion.

3.3 Theory Of Modifications

Here we have studied four models of modified Winston's CPC. These concentrators are useful only for heat concentration.

In this section we would discuss the theory of modifications of these models. Since the second stage concentration arises from a modification of the bottom portion of the first stage concentrator, all diagrams in this section depict only the bottom part of the concentrators . In all the models discussed here first stage concentration is achieved by Winston's CPC and second stage concentration by a pair of ellipses in models I and II and by a pair of circles in models III and IV.

(a) Model I

The transverse cross-section of the model is shown in Fig. 3.2(a). The second stage concentration is obtained by using ellipses E and E' which are of equal size. P' and O are the focii of ellipse E', P and O are those of ellipse E. The circular absorber of diameter PP'/2 is placed at the centre of the exit apteture as shown in the figure. In case of flat absorber, the width of the absorber occupies the length PP'/2. The eccentricities 'e' of the ellipses have been chosen in such a way that the ellipses E and E' touch the absorber tangentially at two diametrically opposite points A' and A, respectively. This is achieved by taking 'e' to be equal to half for both the ellipses. Analysing the focussing properties of ellipse (Appendix 1), it has been observed that all the rays passing through P'A' and PA are not reaching to A' A

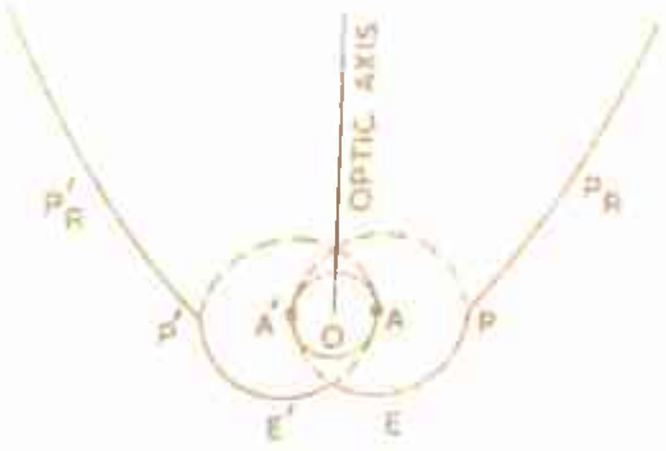

FIG. 3.2 TRANSVERSE VIEW OF THE BOTTOM PART OF THE MODIFIED WINSTON CPC
(a) MODEL I
(b) MODEL II

(a)

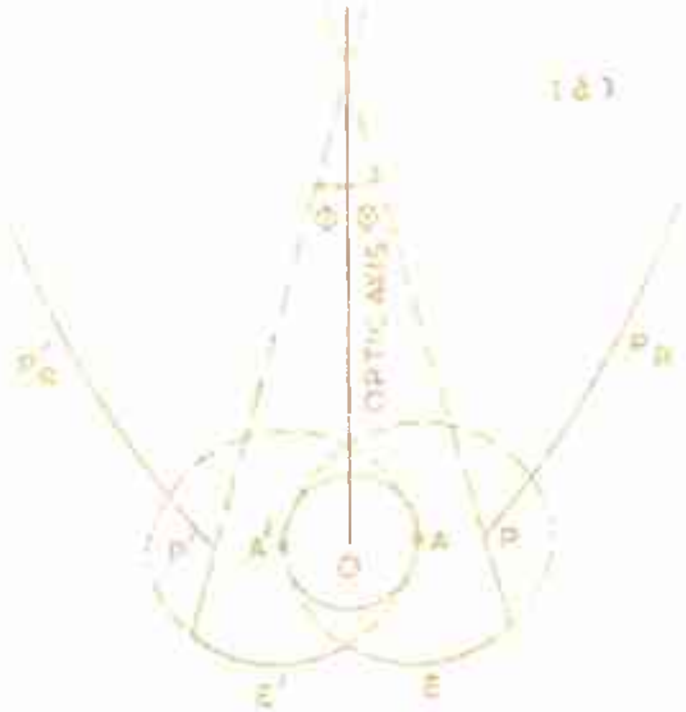

(b)

after reflection from the ellipses E' and E. So the second stage concentration is not two for this model. In Sec. 3.4 we have calculated the second stage concentration for this model which comes out to be 1.95.

(b) Model II

The transverse cross-section of the model is shown in Fig. 3.2(b). Both the ellipses E and E' are equal sized, having eccentricity equal to half and major axis equal to 2/3 of the exit aperture (PP') of the CPC. This results in an overlap (AA') equal to one third of the exit aperture. The absorber is placed in this overlap region and therefore occupies 1/3 of the exit aperture. The absorber can be circular in shape having diameter equal to AA' and flat in shape having width equal to AA'. In this model also, all the rays reaching the exit aperture (PP') of the Winston's CPC could not be made to reach the absorber after reflection from ellipses. Therefore, this design has the second stage concentration less than three.

(c) Model III

The transverse cross-section of the model is shown in Fig. 3.3(a). Both the circles C and C' having diameter equal to half of the exit aperture, touch each other at the centre of exit aperture as shown in the figure. Therefore, P'A' and PA are equal to 1/4 of the exit aperture. The

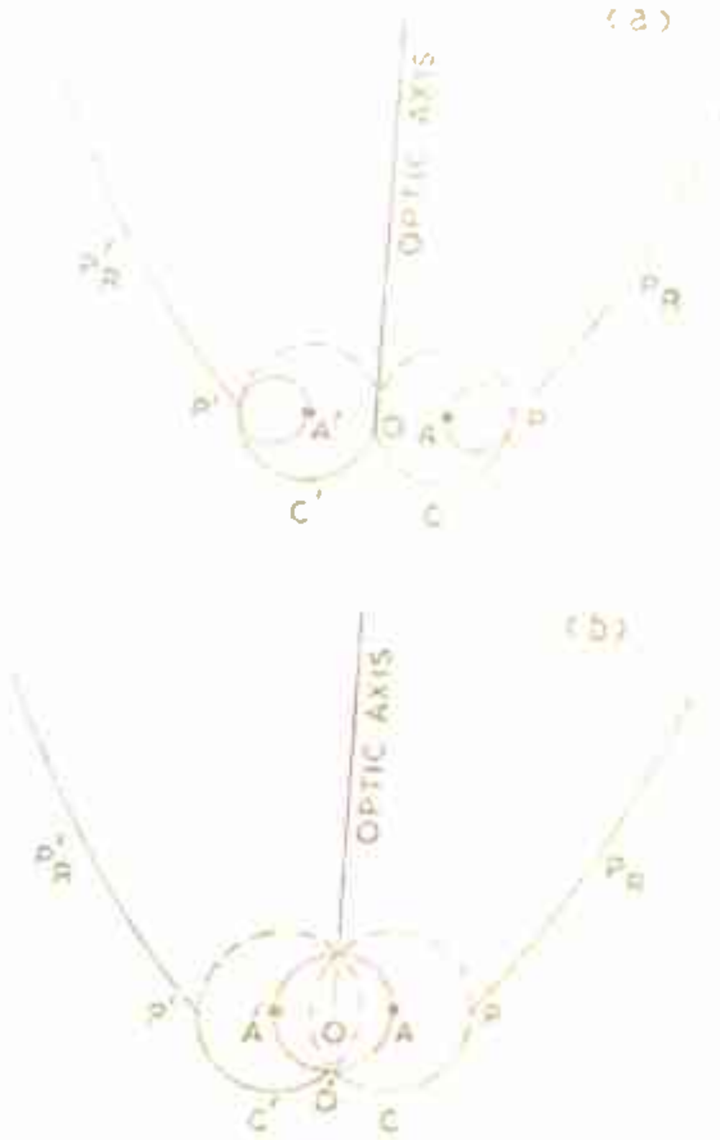

FIG.3.3 TRANSVERSE VIEW OF THE BOTTOM PART OF THE MODIFIED WINSTON CPC
(a) MODEL III
(b) MODEL IV

absorbers (which may be circular with diameter equal to 1/4 of the exit aperture or flat having width equal to 1/4 of the exit aperture) are placed at P'A' and PA. In this design all the rays passing through OA' and OA after reflection from respective circles C' and C reach the A'P' and AP respectively (Appendix 1). Hence the second stage concentration of this model is two.

(d) Model IV

The second stage concentration with a pair of circles at the bottom of CPC will be maximum if in the transverse section, the circles overlap at the bottom of CPC and the cirolular absorber passes through the centre of both the circles and also through the point of intersections of the circles C and C' as shown in Fig. 3.3(b). Under these conditions the radius r, of the absorber will be $R/\sqrt{2}$, where R is the radius of the circles (C or C'). Since from the figure it is clear that

$$(OA)^2 + (OO')^2 = (O'A)^2$$

i.e. $$r^2 + r^2 = R^2$$

$$\therefore\ r = R/\sqrt{2} \qquad (3.2)$$

In this design all the rays passing through P'A' and PA after reflection from C' and C respectively will reach the absorber. Now it is also clear from the Fig. 3.3(b) that

$$P'A' + A'O = d/2$$

$$R + r = d/2$$

$$2(R + r) = d$$

Putting the value of R from Eq . (3.2) we get

$$2(\sqrt{2} + 1)\, r = d$$

$$\therefore \quad d/2r = 1 + \sqrt{2}$$

$$= 1 + 1.414$$

$$\simeq 2.4$$

Thus the second stage concentration of this design is 2.4.

3.4 Calculation Of Second Stage Concentration

As mentioned earlier in Sec. 3.3(a), all the rays passing through entrance aperture, after reflection from the Winston's CPC and ellipses always do not reach the absorber in the second stage concentrator. In this section we have calculated the percentage of the total incident beam, reaching the absorber and the second stage concentration for model I (assuming reflection cofficient of the concentrator equal to one). The calculations are done for Winston's CPC having exit aperture (d) equal to 2 cm and geometrical concentration ratio equal to 10 (Fig. 3.4) or having half acceptance angle equal to 5.74°. So the entrance aperture RR' will be 20.0 cm. The entrance aperture is divided into 50 intervals of equal size i.e., into the intervals of 0.4 cm width. Therefore, we have $R' r^1 = 0.4$, $r^1 r^2 = 0.4$ and so on upto $r^{49} R = 0.4$ cm. The point P is connected to the points $R', r^1 \ldots r^{49}$ and R. Then all the angles these lines (e.g. P R', $Pr^1 \ldots$ P r^{49} and PR) make with the vertical are calculated. If the line is on the

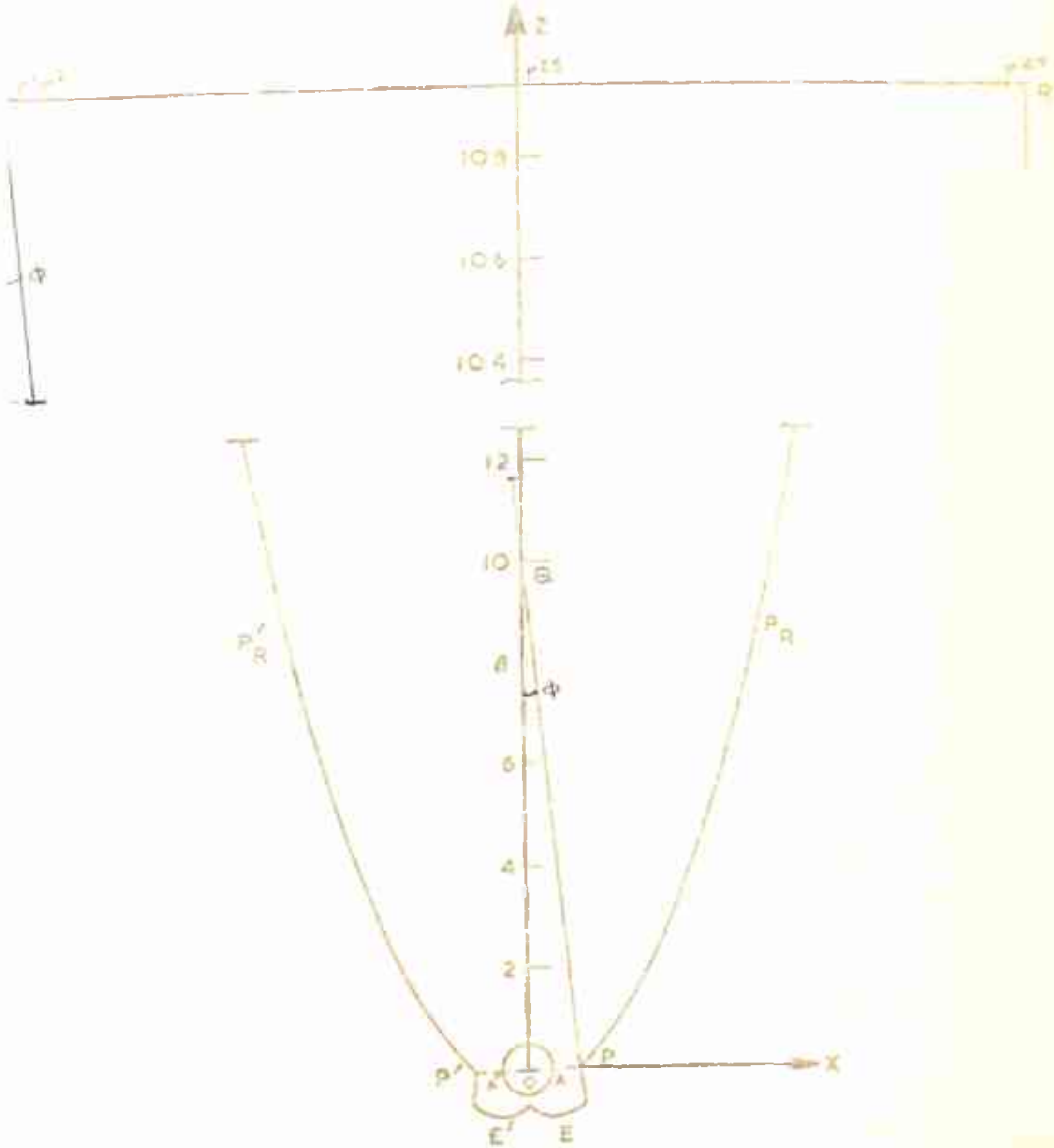

FIG. 3.4 TRANSVERSE CROSS-SECTION OF MODIFIED WINSTON'S CPC (MODEL I) FOR PARAMETERS C = 10 AND d = 2.0 C.M.

left side of the vertical, the angle is considered positive and if the line is on the right side, angle is considered negative. Now consider a parallel beam of light(making an angle R' Q r[25] with the vertical) incident at the entrance aperture. This beam after reflection (may be one or more number of reflections) from the concentrator will reach the exit aperture PP'. If the reflected rays are reaching within AA', these rays will strike the absorber and will be absorbed there. If the rays are reaching the exit aperture within AP, then these rays will be reflected by the ellipse E either towards the absorber or back through AP. If the rays are reaching the exit aperture within A'P', these rays will be reflected by the ellipse E' either towards the absorber or back through A'P', The contribution of the rays reflected back through AP or A'P' will be zero. Now we will discuss the method used in calculating the percentage of total incident beam (passing through the entrance aperture at a particular inclination θ), reaching to the absorber after reflection from Winston's CPC and ellipses E and E'. The equation of the surface P_R(Fig. 3.5) is given by

$$Z^2 \sin^2\phi + X^2 \cos^2\phi + 2XZ \sin\phi \cos\phi - 4a_1 Z \cos\phi$$
$$+ 4a_1 X \sin\phi - 4a_1^2 + 2ZL \sin\phi \cos\phi + L^2 \cos^2\phi$$
$$+ 2XL \cos^2\phi + 4a_1 L \sin\phi = 0 \qquad (3.3)$$

where ϕ is the half-acceptance angle of Winston's CPC, L is half of the exit aperture i.e. d/2 and

$a_1 = L (1 + \sin\phi)$

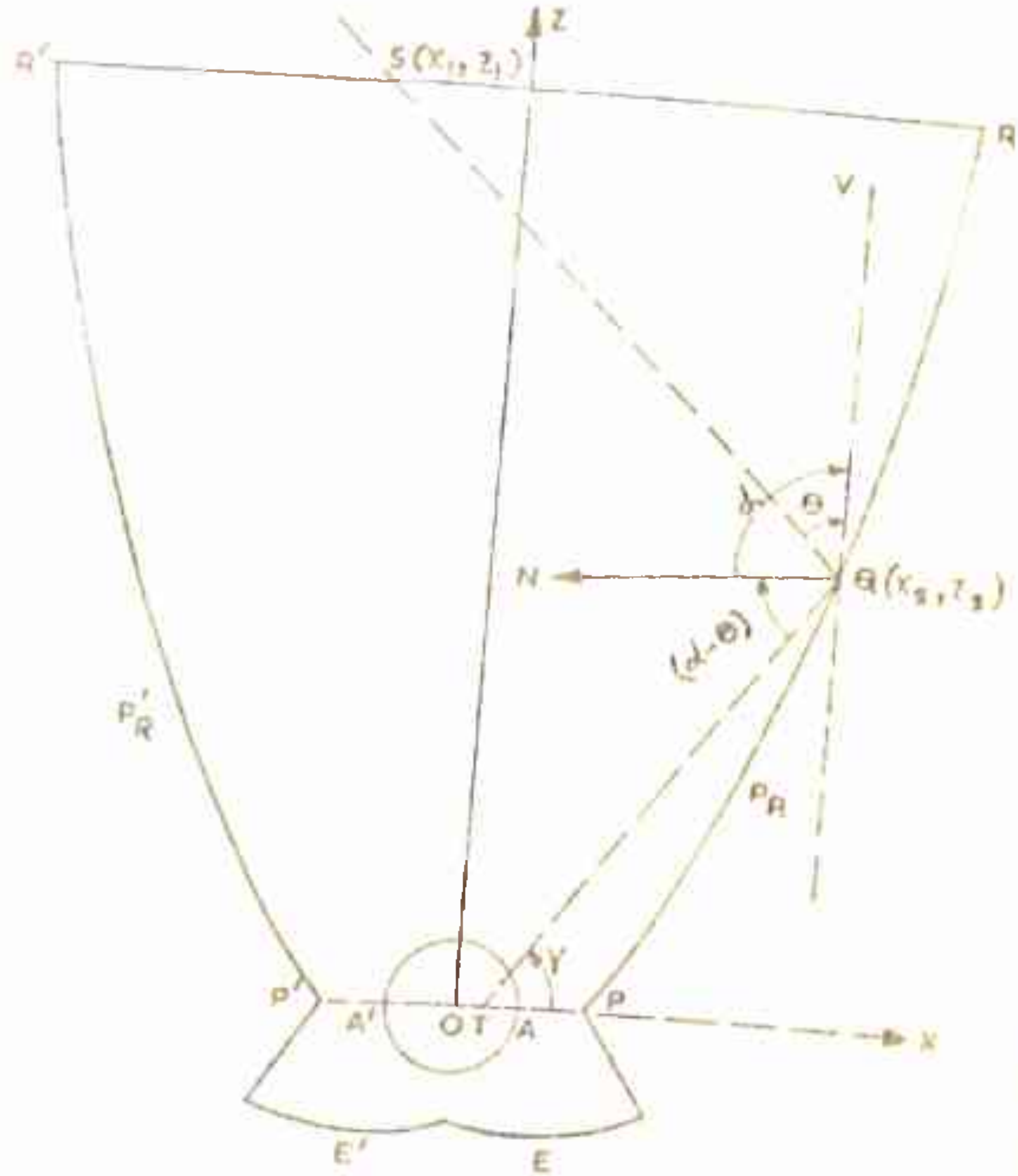

FIG. 3.5 TRANSVERSE CROSS-SECTION OF THE MODIFIED WINSTON'S CPC (MODEL I) SHOWING THE INCIDENT AND REFLECTED RAYS FOR A PARTICULAR INCLINATION

The angle α which the normal to the surface P_R at any point (X,Z) makes with the vertical is given by

$$\tan\alpha = \frac{dZ}{dx} = \frac{2L\cos^2\phi + 4a_1\sin\phi + 2X\cos^2\phi + 2Z\sin\phi\cos\phi}{4a_1\cos\phi - 2L\sin\phi\cos\phi - 2X\sin\phi\cos\phi - 2Z\sin^2\phi} \qquad (3.4)$$

Now consider a ray from S(a point on the RR' line) whose coordinates are (X_1, Z_1) where Z_1 will be $(L + \frac{L}{\sin\phi})\cot\phi$. Let the ray strike the reflector surface P_R at a point Q. The equation of SQ ray will be

$$Z - Z_1 = m(X - X_1)$$

or

$$Z = Z_1 + m(X - X_1) \qquad (3.5)$$

where $m = -\cot\theta$

The coordinate of the point $Q(X_s, Z_s)$ can be obtained as follows; Using Eq. (3.5) in Eq. (3.3) and simplifying we get

$$A X^2 + B X + C = 0 \qquad (3.6)$$

where $A = m^2\sin^2\phi + \cos^2\phi + 2m\sin\phi\cos\phi$

$$B = -2m^2X_1\sin^2\phi + 2mZ_1\sin^2\phi + 2Z_1\sin\phi\cos\phi - 2mX_1\sin\phi\cos\phi$$
$$-4a_1m\cos\phi + 4a_1\sin\phi + 2mL\sin\phi\cos\phi + 2L\cos^2\phi$$

and

$$C = (Z_1^2 + m^2X_1^2 - 2mX_1Z_1)\sin^2\phi - 4a_1Z_1\cos\phi + 4a_1mX_1\cos\phi$$
$$-4a_1^2 + L^2\cos^2\phi + 2Z_1L\sin\phi\cos\phi - 2mX_1L\sin\phi\cos\phi + 4a_1L\sin\phi$$

The X coordinate of the point Q, X_s can be obtained by solving Eq.(3.6) and the Z coordinate, Z_s will be (using Eq.3.5):

$$Z_s = Z_1 + m(X_s - X_1) \tag{3.7}$$

The angle γ which the reflected ray QT makes with the x-axis is given by

$$\gamma = 2\alpha - 90.0 - \theta \tag{3.8}$$

So the equation of the reflected ray QT will be

$$Z - Z_s = m_s(X - X_s) \tag{3.9}$$

where $m_s = \tan\gamma$

Putting $Z = 0$ in this equation we get

$$X = X_s - \frac{Z_s}{m_s} \tag{3.10}$$

This is the value of X-coordinate of the point T(i.e. OT) where the reflected ray meets the x-axis. If the magnitude of OT is less than d/2, the reflected ray QT is reaching the exit aperture after reflection from Q. If the magnitude of OT is greater than d/2, the reflected ray is not reaching the exit aperture. It will strike the surface P_R at any point Q_1 (not shown in the figure) between Q and P. The coordinates of Q_1 can be calculated by the same method used for calculating the coordinates of Q. Let the coordinates of Q_1 are (X_{s1}, Z_{s1}). The value of angle α_1 which the normal to the surface P_R at Q_1, makes with the vertical can be calculated from Eq.(3.4) and the values of θ_1 and γ_1 will be

$$\theta_1 = 2\alpha - 180.0 - \theta$$
$$\gamma_1 = 2\alpha_1 - 90.0 - \theta_1 \tag{3.11}$$

Now the equation of the reflected ray Q_1T will be

$$Z - Z_{s1} = m_{s1}(X - X_{s1}) \tag{3.12}$$

where $m_{s1} = \tan \gamma_1$

Putting $Z = 0$ in Eq. (3.12) we get

$$X = X_{s1} - \frac{Z_{s1}}{m_{s1}} \tag{3.13}$$

This is the value of X-coordinate where the reflected ray Q_1T meets the x-axis i.e., OT. If the magnitude of OT is less than d/2, the reflected ray Q_1T is reaching the exit aperture. If |OT| is greater than d/2 repeat the above discussed procedure until the reflected ray reaches the exit aperture. Now we check whether OT is positive and negative. The following two cases will be there.

(a) Case I

Let OT be positive. If OT is less than or equal to OA, the reflected ray will reach to the absorber. If OT is greater than OA i.e., point T is within AP, the reflected ray will strike the ellipse E. Then we have calculated that the ray after reflection from ellipse E(using the reflection property of ellipse discussed in Appendix 1) is reaching to the absorber or passing back through AP. If it is passing back through AP, this ray will not reach the absorber and its contributions will be zero.

(b) Case II

Let OT be negative. If OT is less than or equal to OA', the reflected ray will reach the absorber. If OT is greater OA' i.e., point T is within A'P', the reflected ray will strike the ellipse E'. Then calculate that this ray after reflection from ellipse is reaching to the absorber or passing back to A'P'.

For a particular inclination θ, of the incident beam the whole procedure is done for all the rays passing through all the 50 intervals (or 51 points on the entrance aperture) and for that value of θ, percentage contribution is calculated. In Table 3.1 we have given the percentage contribution for all angles varying from ∅ to 0. The symmetry of the concentrator design obviously implies that the percentage contribution for a particular -θ angle will be same as for θ angle. Hence the contributions for the range 0 to -∅ are not shown in this table.

It can be seen from Table 3.1 that 100 % of the incident beam reaches of the absorber except when θ angle lies between 3.5° and 5.5° approximately. Even when θ is within this range, 90 % or more of the beam still reaches the absorber. Therefore, a very small fraction of the incident beam is able to come out of AP or A'P' for a small duration of time. Hence for calculating the second stage

TABLE-3.1

The percentage of the total incident beam reaching the absorber after reflection from concentrator for various inclination of the incident beam

θ (Degree)	p %	θ (Degree)	p %	θ (Degree)	p %
5.74	100.0	3.66	94.60	1.57	100.0
5.53	100.0	3.45	100.0	1.36	100.0
5.32	90.25	3.24	100.0	1.15	100.0
5.11	90.80	3.03	100.0	0.94	100.0
4.90	90.67	2.82	100.0	0.73	100.0
4.70	90.95	2.61	100.0	0.52	100.0
4.49	89.67	2.40	100.0	0.31	100.0
4.28	92.32	2.19	100.0	0.10	100.0
4.07	92.77	1.99	100.0		
3.86	93.83	1.78	100.0		

concentration ratio, we have just taken the average of all the contributions given in Table 3.1, even though θ variation is not linear with time. This yields the resultant percentage con-tribution to be 97.35 and hence the second stage concen-tration factor as 1.95. If this nonlinearity is taken into account and an exact calculation is done, it will yield a result which is slightly higher than what we get by the simpler approach adopted here.

3.5 Experiment Performed

One model of modified Winston's CPC (MW1) of the type discussed in Sec. 3.3(a) has been fabricated. The specifications of which are given below;

(i) Size of the entrance aperture (D) = 18.7 cm.
(ii) Size of the exit aperture (d) = 2.6 cm.
(iii) Height of the concentrator (H) = 75.7 cm.
(iv) Length of the concentrator (l) = 75.0 cm.
(v) Half acceptance angle (ϕ) = 8^0
(vi) Material used- plain aluminium sheets.

This model is fabricated by the first method described in Sec. 2.2. The experiment performed on this model MW1 is discussed below;

The thermal efficiency of solar energy extraction, n of the model MW1 is calculated (using Eq.(2.2)) along with the model W1 (Sec. 2.2). The thermal efficiency n of the model W1 has already been calculated in Sec.2.3(b). To calculate the n, the concentrator is adjusted by the method described in Sec. 2.3. The circular blackened absorber (Aluminium circular pipe of outer diameter 1.26 cm, thickness .08 cm. and blackened by black board paint) filled with water is kept at the exit aperture (at a position described in Sec. 3.3(a)). The following readings have been obtained.

(i)	Amount of water filled in circular tube (M)	= 100 Grams
(ii)	Ambient Temperature	= $22^{o}C$
(iii)	Temperature rise(in one hour)T	= $75^{o}C$
(iv)	Intensity of solar radiation	= 85 mW/cm^2
(v)	Area of the entrance aperture	= 18.7x75 cm^2

∴ Heat Energy Extracted (Q) = MST

where S is the specific heat of water.

$$\therefore Q = (100 \times 1 \times 75) \text{ calories}$$

$$= 100 \times 75 \times 4.2 \text{ Joules}$$

$$= 3.15 \times 10^4 \text{ Joules}$$

Total Incident Energy (I_t)

$$= 18.7 \times 75 \times \frac{85}{1000} \times 3600 \times .92^{+} \text{ Joules}$$

$$= 39.48 \times 10^4 \text{ Joules}$$

$$\therefore \quad n = \frac{Q}{I_t} = \frac{3.15}{39.48} = 0.0798$$

i.e. n % = 7.98 %

≃ 8 %

+ The factor F for this model is same as for model W1 described in Sec. 2.3(b).

3.6 Results And Discussions

The efficiency of solar energy extraction η of model W1 is 9 % and that of model MW1 is 8 %. Thus in case of modified Winston's CPC the efficiency is less only by 1 % but the temperature obtained in one hour in model MW1 is 97°C where it is only 56°C in case of model W1. Thus the Carnot efficiency (Eq. 1.4) is a higher for model MW1.

R E F E R E N C E S

1. H. Tabor, Stationary Mirror Systems For Solar Collectors, Solar Enery 2 (3-4), 27-33 (1958).

2. R. Winston, Principles Of Solar Concentrator Of A Novel Design, Solar Energy 16 (2), 89-95 (1974).

3. Murlidhar, A. Gupta And V.K. Tewary, A Nontracking Heat Concentrator Capable Of Giving Concentration Factor Of The Order Of 20, Proc. National Solar Energy Convention 1976, Calcutta, pp. 62-63.

CHAPTER-4

UNIFORM CYLINDRICAL CONCENTRATORS

CHAPTER-4

UNIFORM CYLINDRICAL CONCENTRATORS

4.1 Introduction

We have already observed in chapter 2 that for Winston type nontracking concentrators the radiation reaching the absorber illuminates the same nonuniformly. Following two types of problems are usually faced when such concentrators are used for photovoltaic applications:

(i) Intensity distribution on the solar cells at the absorber is nonuniform,

(ii) Solar cells may be partially illuminated and some of the solar cells may be completely under shadow.

This results in the loss of power output from the solar cell panel.

If the solar cell is illuminated nonuniformly, the density of carriers generated by the incident light will also be nonuniform and a potential gradient will be developed along the junction. The voltage developed across the portion of the solar cell, which is under high illumination, will be more compared to the portion which is less illuminated and hence the latter will be forward biased, which will give rise to the hole current in a direction so as to reduce the voltage drop accross the highly illuminated portion.

In actual solar cell, this potential gradient gives rise to the internal circulatory currents[1]. These currents will reduce the voltage every where across the junction plane and the efficiency of the solar cell decresses.

While using solar cell panel along with the non-tracking concentrators, the panel may some times be partially illuminated. This also results in loss of power output from the panel. Let us consider the case when one of the cells is completely in shadow. If this shadowed cell is in series with some other illuminated cells, it will behave like a reverse biased diode and will block the current through the illuminated cells, allowing only the reverse saturation current to flow. On the other hand if the shadowed cell is in parallel with illuminated cells, it will become slightly forward biased and shunt a part of the current generated by the illuminated cells.

Thus the uniformity of illumination is quite important when solar cell panel is used along the absorber of nontracking concentrator. The ideal situation will obviously be to have a concentrator in which the whole of the absorber is completely and uniformly illuminated throughout the operating period. This, however, is not possible because of the complex nature of the apparent motion of the sun. Therefore, with an objective of achieving as much uniformity as possible we have developed a new type of nontracking concentrators[2-5] in which the absorber is uniformly illuminated at least sometimes during the operating period and no lateral shadowing throughout the period of operation. We have discussed the theoretical determination of the surface of such a nontracking concentrator in Sec. 4.2 and Sec. 4.3. In Sec. 4.4 we have discussed the theoretical intensity profile on the absorber for various angles of solar inclination. The details of models fabricated and the experiments performed on these models are discussed in Sec. 4.5 and Sec. 4.6.

4.2 Approach Used In Concentrator Designing

The problem of designing nontracking concentrators has been approached by various investigators in two different ways. In one approach the reflection pattern is specified first for a particular receiver shape and then the shape of the reflector is worked out. This method has been followed by Horton and McDermitt[6], Burkhard and Sheally[7] and Rabl[8]. In the other approach a particular reflector shape is considered and then its reflection pattern and concentration factor are worked out. Two important attempts of the latter type are by Tabor[9] and Winston[10]. In the present attempt we follow the first approach to determine the shape of the concentrator taking the absorber to be flat surface and reflection pattern to be uniform over the entire receiver surface for a particular inclination of the incident collimated beam.

The first part of the formulation is to obtain the ray trace equation which satisfies the laws of reflection on the reflector surface. The laws of reflections are that (i) The angle of incidence θ_i (Fig. 4.1) must be equal to the angle of reflection θ_r. This condition is satisfied provided,

$$(\vec{I} + \vec{R}) . \vec{N} = 0 \qquad (4.1)$$

where $\vec{I}$ and $\vec{R}$ are the unit vectors in the direction of incident and reflected rays respectively, and $\vec{N}$ is the unit vector normal to the surface.

(ii) The incident ray, reflected ray and surface normal must be coplaner i.e. all these three must lie in one plane. This condition requires that

$$(\vec{I} \times \vec{R}) . \vec{N} = 0 \qquad (4.2)$$

While formulating we must also ensure that energy must be conserved i.e., whatever energy is incident on the reflector must reach the receiver after reflection. These two conditions yield a differential equation of the reflector surface, which can be solved to get the required reflector surface.

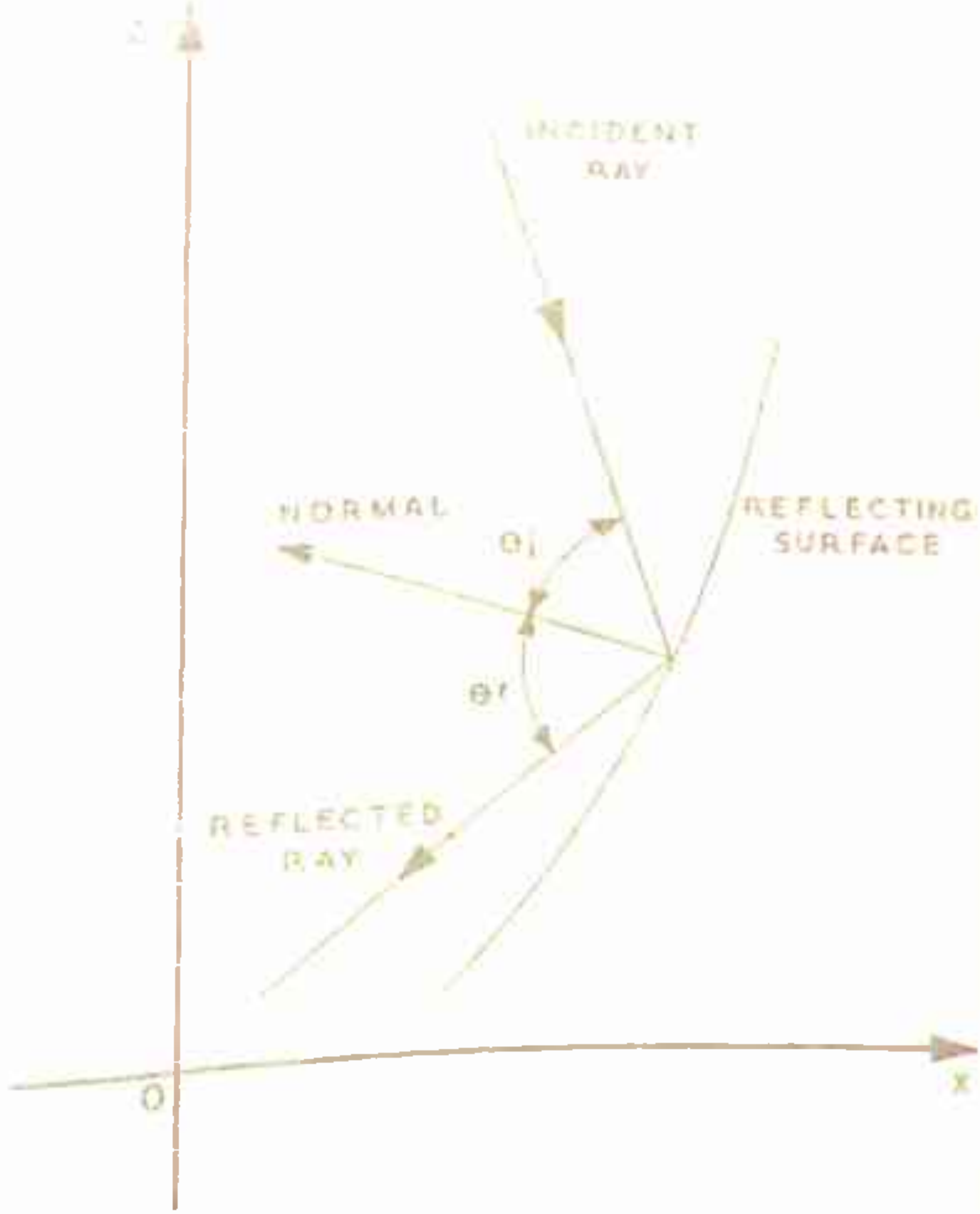

FIG. 4.1 CONSTRUCTION OF THE REFLECTING SURFACE OF THE CONCENTRATOR

4.3 Mathematical Formulation

Since every nontracking concentrator has to have an axis (length) in the east-west direction[9], we have only to determine the cross-section of the concentrator and take it to be cylindrical along the third direction. Thus the problem is only two-dimensional. A further simplification comes from the fact that during a day the EWV altitude α varies between α_1 and α_2 and therefore if we tilt the concentrator at an angle ($\alpha_1 + \alpha_2)/2$ to the horizontal, the cross-section of the concentrator can be taken to be symmetrical about the east-west plane inclined to the horizontal through the angle ($\alpha_1 + \alpha_2)/2$, this happens because EWV swing is through an angle ($\alpha_1 - \alpha_2)/2$ on either side. Thus we have to calculate the one side of the concentrator and other side is to be obtained by mirror symmetry about the optic axis.

Let the receiver be placed along X-axis from -L to L as shown in Fig. 4.2. The equation of one side (part) of the reflecting surface indicated by APR' can be written as

$$S = Z - F (x) = 0 \qquad (4.3)$$

where F(x) is the function to be calculated. The relationship between surface normal and gradient to the surface is given by

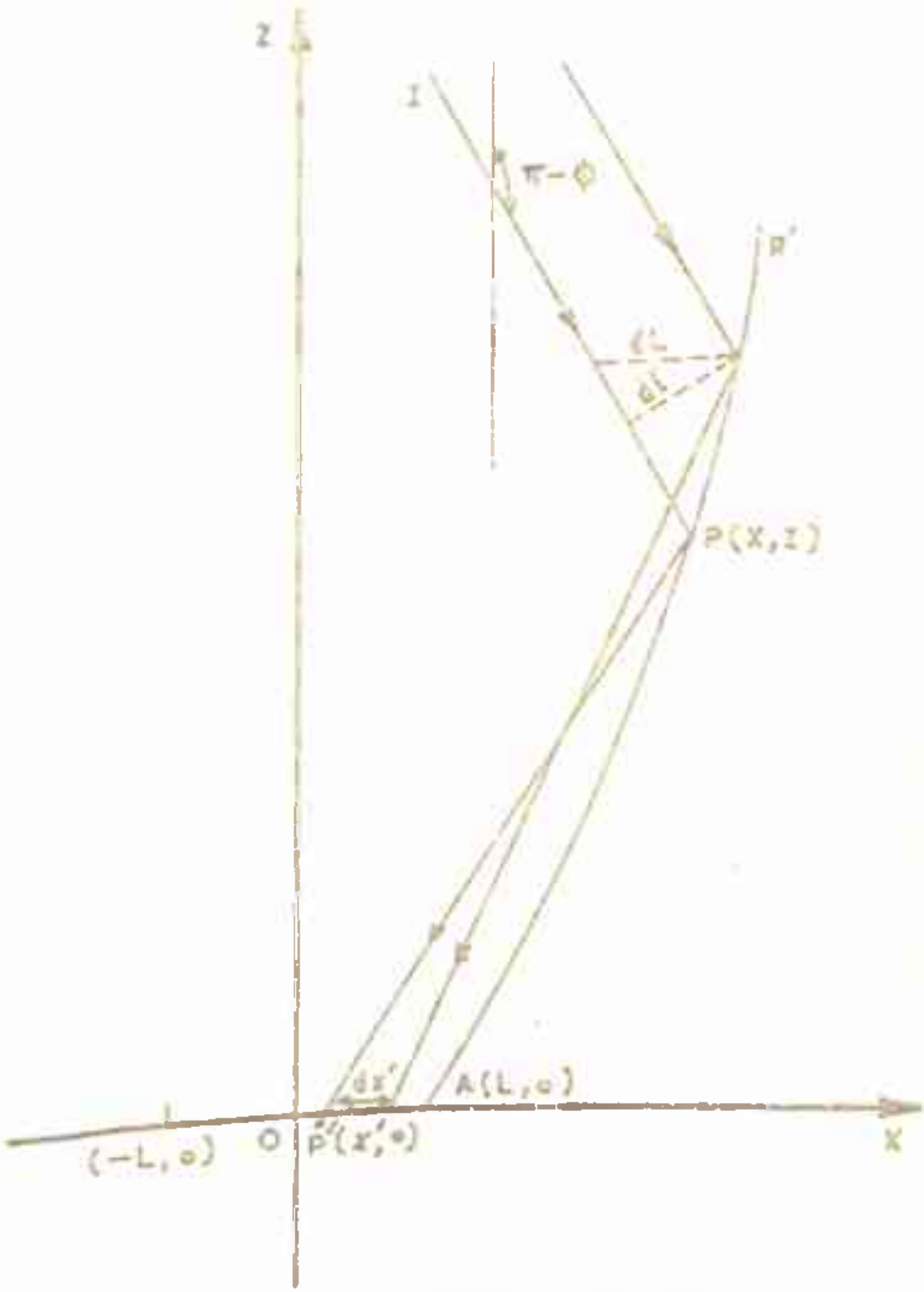

FIG. 4.2 ONE SIDE OF THE CROSS-SECTION OF THE REFLECTING SURFACE IN THE X-Z PLANE

$$\vec{N} = -\vec{\nabla S}$$

$$= (\hat{i}\, F'(x) - \hat{k}) \qquad (4.4)$$

where $\hat{i}$ and $\hat{k}$ are the unit vectors along X-axis and Z-axis, respectively.

Let the incident beam make an angle ($\pi - \phi$) with the Z-axis, as shown in Fig. 4.2, The direction cosines of the incident beam are ($\sin\phi$, $-\cos\phi$).

Now consider the incident ray IP which is incident on the reflector at the point P (X,Z) and is reflected to the point P'(X',0) on the receiver. The direction cosines of the reflected ray PP' will be $(X'-X)/R$, $-Z/R$ where

$$R^2 = (X'-X)^2 + Z^2 \qquad (4.5)$$

Now we can write the ray-trace equation (Eq. 4.1) for the configuration shown in Fig. 4.2 as,

$$\left[(\hat{i}\sin\phi - \hat{k}\cos\phi) + \hat{i}(X'-X)/R - \hat{k}\, Z/R\right] \cdot \left[\hat{i}\, F'(x) - \hat{k}\right] = 0 \qquad (4.6)$$

or $\sin\phi\, F'(x) + F'(x).(X'-X)/R + \cos\phi + Z/R = 0$

$$\therefore F'(x) = \frac{Z + R\cos\phi}{(X-X') - R\sin\phi} \qquad (4.7)$$

Let I be the intensity of incident solar beam and E be the intensity of solar radiation on the absorber. For the configuration shown in Fig. 4.2, the conservation of energy requires that

$$I\,dL = E\,dX'$$

or $$I\,dl \sec\phi = E\,dX'$$

or $$I(\cos\phi\, dX + \sin\phi\, dZ)\,.\sec\phi = E\,dX'$$

Now applying the energy boundary condition over the reflector and receiver surface we get

$$I\left[\int_{L}^{X} dX + \tan\phi \int_{0}^{Z} dZ\right] = E\int_{-L}^{X'} dX'$$

or $$I\left[(X-L) + Z\tan\phi\right] = E(X' + L)$$

or $$X' = -L + \left[(X-L) + Z\tan\phi\right] I/E$$

$$= -L + \left[(X-L) + Z\tan\phi\right]/M$$

where $M = E/I$

or $$X' = -L + m(X-L+ Z\tan\phi) \qquad (4.8)$$

where $m = 1/M$

Eq. (4.7) with X' given by Eq. (4.8) gives the desired differential equation for the reflecting surface. The appropriate boundary condition which satisfies the starting value of Z for X = L and which uniquely defines the solution is given by

$$Z_{X=L} = 0 \qquad (4.9)$$

i.e. starting point on the reflector is (L, 0).

To generate the surface of the reflector we have solved Eq. (4.7) using following two different methods:

(a) Taylor's series expansion method

In this method we start with Eq. (4.7) and then find the higher-order derivatives as follows;

$$F'(x) = \frac{F(x) + R\cos\phi}{(X - X') - R\sin\phi} \qquad \text{Since } Z = F(x)$$

or $$(X-X')F'(x) - F(x) = R\left[F'(x)\sin\phi + \cos\phi\right]$$

Squaring both the sides of this equation and putting the value of R^2 from Eq. (4.5) we get

$$F'(x)^2\left[(X-X')^2\cos^2\phi - F(x)^2\sin^2\phi\right] - 2F'(x)\left[(X-X')F(x) + (X-X')^2\sin\phi\cos\phi + F(x)^2\sin\phi\cos\phi\right] + F(x)^2\sin^2\phi - (X-X')^2\cos^2\phi = 0$$

Now differentiating this equation with respect to X and simplifying we get

$$F''(x) = \frac{T_1 + T_2 + T_3 + T_4}{T_5 - T_6}$$

where $T_1 = F'(x)^3\left[2(X-X')\sin\phi\cos\phi/M + 2F(x)\sin^2\phi\right]$,

$$T_2 = F'(x)^2\left[2(X-X')\sin^2\phi + 2(X-X')\cos^2\phi/M - 2F(x)\tan\phi/M - 4(X-X')\sin^2\phi/M + 4F(x)\sin\phi\cos\phi\right],$$

$$T_3 = F'(x)\left[2F(x)\cos^2\phi - 2F(x)/M + 4(X-X')\sin\phi\cos\phi - 6(X-X')\sin\phi\cos\phi/M\right]$$

$$T_4 = 2(X - X')\cos^2\phi\left(1 - \frac{1}{M}\right)$$

$$T_5 = 2F'(x)\left[(X - X')^2\cos^2\phi - F(x)^2\sin^2\phi\right] \text{ and}$$

$$T_6 = 2F(x)\left[(X - X') + F(x)\sin\phi\cos\phi\right] + 2(X - X')^2\sin\phi\cos\phi$$

In the same way higher-order derivatives can be obtained.

The initial slope of the surface is chosen in such a way that the extreme ray after reflection from (L,0) reaches to the point (-L,0). This implies that the coordinate of second point will be (h, h tan ψ) with $\psi = \pi/4 + \phi/2$ where ϕ is the angle which the extreme ray makes with the vertical. The value of X coordinate was increased in an interval of h and corresponding $Z = F(x)$ was obtained by Taylor series

$$F(x+h) = F(x) + hF'(x) + \frac{h^2}{2!}F''(x) + \ldots$$

The maximum value of X was taken upto the point at which dZ/dX becomes infinite i.e., upto the point at which tangent to the reflector is perpendicular to X-axis. A Computer program was made to obtain the various points of reflector surface for a given ϕ and M, for various values of h. It was found that the value of h = 0.05 gives good convergence. Using this method we have ...flecting surfaces, the details of which have been discussed

$$T_4 = 2(X - X')\cos^2\phi\left(1 - \frac{1}{M}\right)$$

$$T_5 = 2F'(x)\left[(X - X')^2\cos^2\phi - F(x)^2\sin^2\phi\right] \quad \text{and}$$

$$T_6 = 2F(x)\left[(X - X') + F(x)\sin\phi\cos\phi\right] + 2(X - X')^2\sin\phi\cos\phi$$

In the same way higher-order derivatives can be obtained.

The initial slope of the surface is chosen in such a way that the extreme ray after reflection from (L,0) reaches to the point (-L,0). This implies that the coordinate of second point will be (h, h tan ψ) with $\psi = \pi/4 + \phi/2$ where ϕ is the angle which the extreme ray makes with the vertical. The value of X coordinate was increased in an interval of h and corresponding $Z = F(x)$ was obtained by Taylor series

$$F(x+h) = F(x) + hF'(x) + \frac{h^2}{2!}F''(x) + \ldots$$

The maximum value of X was taken upto the point at which dZ/dX becomes infinite i.e., upto the point at which tangent to the reflector is perpendicular to X-axis. A Computer program was made to obtain the various points of reflector surface for a given ϕ and M, for various values of h*. It was found that the value of h = 0.05 gives good convergence of the reflecting surface. Using this method we have designed three models, the details of which have been discussed in Sec. 4.5.

---

* A listing of this computer program is given in Appendix-2.

(b) Displaced polar coordinate method

Eq.(4.7) can also be solved by transforming it to displaced polar coordinates R and θ with variable origin at X = X' as follows (Fig. 4.3):

$$X - X' = R \sin\theta \qquad (4.10)$$

and
$$Z = R \cos\theta \qquad (4.11)$$

where $R^2 = (X - X')^2 + Z^2$

Now differentiating Eqs. (4.10), (4.11) and (4.8) we get

$$dX - dX' = dR \sin\theta + R \cos\theta \, d\theta$$

i.e.
$$dX = dX' + dR \sin\theta + R \cos\theta \, d\theta, \qquad (4.12)$$

$$dZ = - R \sin\theta \, d\theta + \cos\theta \, dR \qquad (4.13)$$

and
$$dX' = m (dX + \tan\phi \, dZ) \qquad (4.14)$$

Substituting the value of dX' from Eq. (4.14) in Eq.(4.12) we have

$$dX = m (dX + \tan\phi \, dZ) + dR \sin\theta + R \cos\theta \, d\theta$$

or
$$dX(1-m) - m \tan\phi \, dZ = \sin\theta \, dR + R \cos\theta \, d\theta \qquad (4.15)$$

Now dividing Eq. (4.13) by Eq. (4.15) we get

$$\frac{dZ}{dX(1-m) - m \tan\phi \, dZ} = \frac{\cos\theta \, dR - R \sin\theta \, d\theta}{\sin\theta \, dR + R \cos\theta \, d\theta}$$

Dividing numerator and denominator of L.H.S. by dX and numerator and denominator of R.H.S. by dθ of this equation and solving we have

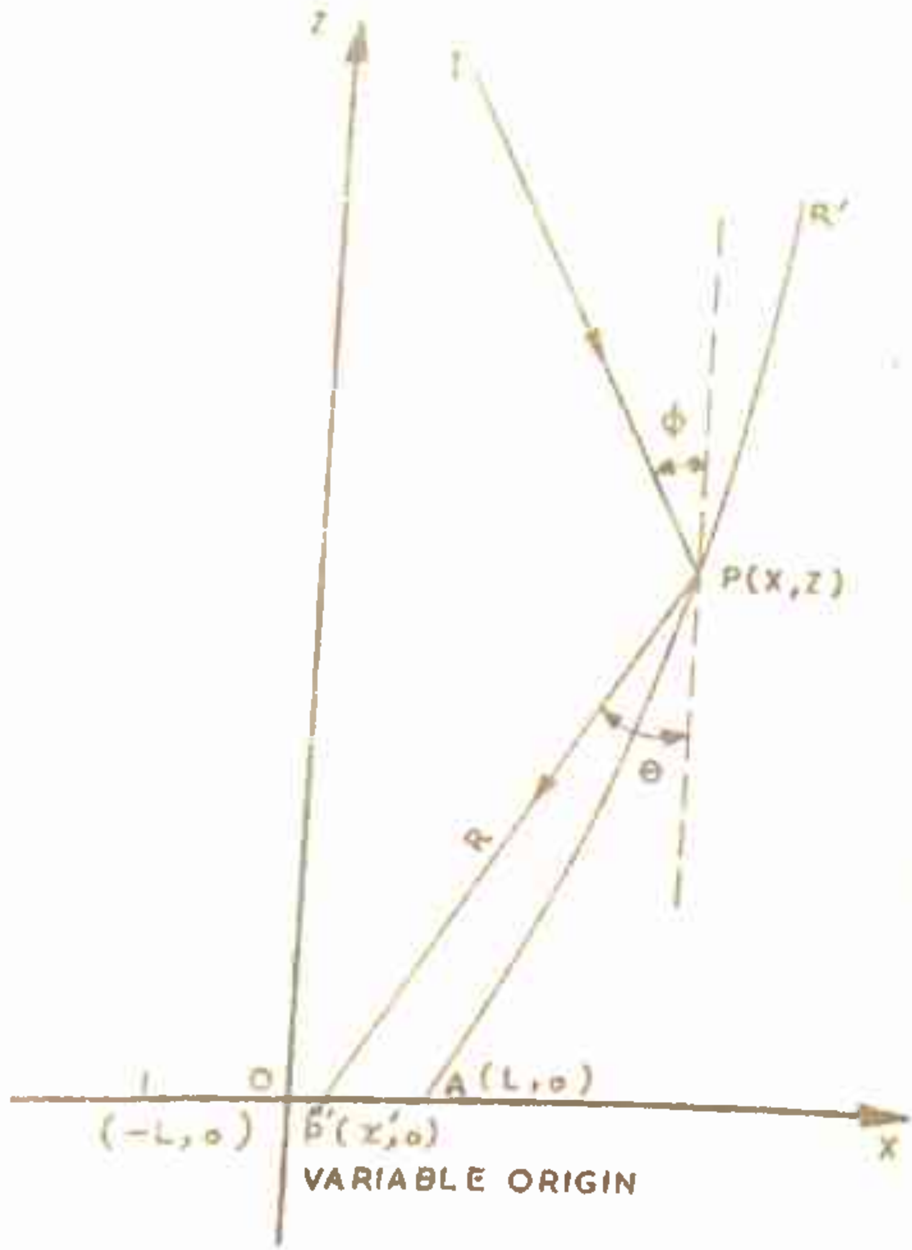

FIG. 4.3 DISPLACED POLAR CO-ORDINATES (R, Θ) CORRESPONDING TO THE POINT P(X,Z) ON THE REFLECTING SURFACE OF THE CONCENTRATOR

$$\frac{dZ}{dX} = \frac{(1-m)(\cos\theta . dR/d\theta - R\sin\theta)}{(\sin\theta + m\cos\theta\tan\phi)dR/d\theta + R\cos\theta - R\sin\theta\, m\tan\phi} \tag{4.16}$$

Now from Eq.(4.7) we have

$$\frac{dZ}{dX} = \frac{Z + R\cos\phi}{(X-X') - R\sin\phi}$$

Using Eqs. (4.10) and (4.11) we get from this equation that

$$\frac{dZ}{dX} = (\cos\theta + \cos\phi)/(\sin\theta - \sin\phi) \tag{4.17}$$

Comparing Eqs. (4.16) and (4.17) and solving for dR/dθ we have

$$\frac{1}{R}\frac{dR}{d\theta} = -\frac{\cos\phi . \cos[(\theta+\phi)/2] - m\sin\theta . \sin[(\theta+\phi)/2]}{\sin[(\theta+\phi)/2][\cos\phi + m\cos\theta]} \tag{4.18}$$

The transfomed boundary condition can be obtained from Eqs. (4.8), (4.9), (4.10) and (4.11) as follows;

Using Eq. (4.9) in Eqs. (4.8), (4.10) and (4.11) we get

$$R\sin\theta = 2L$$

$$R\cos\theta = 0$$

$\therefore$ $R = 2L$ and $\tan\theta = \infty$ i.e. $\theta = \pi/2$

Thus when $\theta = \pi/2$; $R = 2L$ (4.19)

The solution of Eq. (4.18) which satisfies the boundary condition (4.19) is given by (See Appendix-3)

$$\log\left[\frac{R(\theta)}{2L}\right] = \frac{1}{1+m}\log\left[\frac{1+\sin\phi}{[1-\cos(\theta+\phi)]}\right] - \frac{m}{1+m}\log\left[\frac{\cos\phi+m\cos\theta}{\cos\phi}\right]$$

$$+\frac{2m\sin\phi}{(1+m)\sqrt{(\cos^2\phi-m^2)}}\left[\tan^{-1}\left\{\frac{\sqrt{(\cos\phi-m)}}{\sqrt{(\cos\phi+m)}}\tan\theta/2\right\}\right.$$

$$\left.-\tan^{-1}\left\{\frac{\sqrt{(\cos\phi-m)}}{\sqrt{(\cos\phi+m)}}\right\}\right] \qquad (4.20)$$

or
$$\log\left[\frac{R(\theta)}{2L}\right] = \frac{M}{M+1}\log\left[\frac{1+\sin\phi}{1-\cos(\theta+\phi)}\right] - \frac{1}{1+M}\log\left[\frac{M\cos\phi+\cos\theta}{M\cos\phi}\right]$$

$$+\frac{2M\sin\phi}{(1+M)\sqrt{(M^2\cos^2\phi-1)}}\left[\tan^{-1}\left\{\frac{\sqrt{(M\cos\phi-1)}}{\sqrt{(M\cos\phi+1)}}\tan\frac{\theta}{2}\right\}\right.$$

$$\left.-\tan^{-1}\left\{\frac{\sqrt{(M\cos\phi-1)}}{\sqrt{(M\cos\phi+1)}}\right\}\right] \qquad (4.21)$$

where principal values of $\tan^{-1}$ has to be taken.

From Eq.(4.20) we have obtained the values of R for various values of θ. For actual fabrication purpose, from each pair of (R, θ) values, the corresponding values of (X, Z) was obtained by using Eqs. (4.8), (4.10) and (4.11). Now X_m, the maximum value of X and the corresponding value of Z_m can be obtained from the consideration that, the slope of Z(X) has to remain positive, since the negative slop would imply the folding of the reflecting surface on itself. Thus, X_m will be the value of X at which dZ/dX becomes infinite, beyond this dZ/dX will be negative. From Eqs.(4.7) and (4.10), this yields the minimum value of θ equal to

$$\theta_{min} = \phi$$

So from Eqs. (4.7),(4.10) and (4.11) we have

$$R \sin \phi = (X_m - X')$$

$$R \cos \phi = Z_m$$

$$\therefore \tan \phi = \frac{X_m - X'}{Z_m} \qquad (4.22)$$

Some important conclusions can be drawn from Eqs. (4.20), (4.8) and (4.7).

(i) (a) In case of extreme nonuniformity, characterised by M tending to infinity i.e. m tending to zero, Eq. (4.20) reduces to

$$\frac{R}{2L} = \frac{1 + \sin \phi}{1 - \cos (\theta + \phi)} \qquad (4.23)$$

Transforming Eq. (4.23) into cartesian (X,Z) co-ordinates, it can be shown that this is an equation of parabola with its axis inclined at an angle ϕ will the Z axis and its focus at X = -L i.e., the equation of Winston's parabolic surface.

(b) Substituting m = 0 in Eq. (4.8) we have X' = - L for all values of (X,Z) i.e., all the extreme rays after reflection from Winston's parabolic surface will reach to -L, which is true in Winston's C P C case.

(ii) The optimum value of M, M_o for which whole of the base will be illuminated can be obtained by putting X'= L, $X=X_m$ and Z = Z_m in Eq. (4.8), i.e., $L = -L + (X_m - L + Z_m \tan \phi)/M_o$

Substituting the value of $\tan \phi$ from Eq. (4.22) we have

$$L = - L + (X_m - L + Z_m \frac{X_m - L}{Z_m})/M_o$$

or $$2L = (X_m - L + X_m - L)/M_o$$

or $$2M_oL = 2 (X_m - L)$$

$$\therefore \quad M_o = \frac{2 X_m}{2L} - 1$$

$$= C_o - 1 \qquad (4.24)$$

where C_o is the ratio of entrance aperture to exit aperture, so the optimum concentration factor C_o will be equal to

$$C_o = M_o + 1 \qquad (4.25)$$

and the corresponding height of the concentrator can be obtained from equation (4.22) as

$$\tan \phi = \frac{(X_m - L)}{Z_m}$$

or $$Z_m = (X_m - L) \cot \phi$$

or $$\frac{Z_m}{L} = (\frac{X_m}{L} - 1) \cot \phi$$

$$= (C_o - 1) \cot \phi \qquad (4.26)$$

Now the maximum value of X' i.e. X'_m for the extreme point can be written as

$$X'_m = -L + (X_m - L + Z_m \tan \phi)/M$$

$$= -L + (X_m - L) 2/M \qquad (4.27)$$

Let the maximum values of X' at M_o and M be X'_{m_o} (= L) and X'_m then from Eq. (4.27) we have

$$X'_{m_o} - X'_m = 2\,(X_m - L)\left(\frac{1}{M_o} - \frac{1}{M}\right)$$

or $$L - X'_m = 2(X_m - L)\left(\frac{1}{M_o} - \frac{1}{M}\right) \qquad (4.28)$$

Now it is clear from Eq. (4.28) that if M is greater than M_o, X'_m will be less than L (since for a concentrator (X_m-L) will be positive) i.e., whole of the receiver will not be illuminated and for M less than M_o, X'_m will be greater than L, which implies that the rays reflected from the top portion of the reflecting surface will strike to its lower portions and will not reach the receiver directly.

The magnitude of M_o can be obtained by numbrically solving Eq. (4.20) for a specified value of ϕ. Putting $\theta = \phi$ in Eq. (4.20) we have

$$\log\left[\frac{R(\phi)}{2L}\right] = \frac{1}{(1+m)}\log\left[\frac{1+\sin\phi}{1-\cos 2\phi}\right] - \frac{m}{(1+m)}\log(1+m)$$

$$-\frac{2m\sin\phi}{(1+m)\sqrt{(\cos^2\phi-m^2)}}\left[\tan^{-1}\left(\frac{\sqrt{(\cos^2\phi-m^2)}}{m+(1+\sin\phi)}\right)\right]$$

or $$\log[R(\phi)] = \log(2L) + \frac{1}{(1+m)}\log\left(\frac{1+\sin\phi}{1-\cos 2\phi}\right) - \frac{m}{(1+m)}\log(1+m)$$

$$-\frac{2m\sin\phi}{(1+m)\sqrt{(\cos^2\phi-m^2)}}\left[\tan^{-1}\left(\frac{\sqrt{(\cos^2\phi-m^2)}}{m+(1+\sin\phi)}\right)\right] \qquad (4.29)$$

Now substituting $\theta = \phi$ and $X' = L$ in Eqs. (4.8),(4.10) and (4.11) we have

$$L = -L + m\,(R \sin\phi + R\cos\phi \tan\phi)$$
$$= -L + 2m\,R \sin\phi$$

i.e. $R\sin\phi = L/m$

Taking log of both the sides we get

$$\log R(\phi) = \log L - \log \sin\phi - \log m \qquad (4.30)$$

Equating Eqs. (4.29) and (4.30) we get

$$\log L - \log \sin\phi - \log m = \log L + \log 2 + \frac{1}{(1+m)}\log\left(\frac{1+\sin\phi}{1-\cos 2\phi}\right)$$
$$- \frac{m}{(1+m)}\log(1+m) - \frac{2m\sin\phi}{(1+m)\sqrt{(\cos^2\phi - m^2)}}\left[\tan^{-1}\left\{\frac{\sqrt{(\cos^2\phi - m^2)}}{m+(1+\sin\phi)}\right\}\right]$$

or $\quad F(\phi, m) = 0 \qquad (4.31)$

where

$$F(\phi,m) = \log m + \log\sin\phi + \log 2 + \frac{1}{(1+m)}\log\left(\frac{1+\sin\phi}{1-\cos 2\phi}\right)$$
$$- \frac{m}{(1+m)}\log(1+m) - \frac{2m\sin\phi}{(1+m)\sqrt{(\cos^2\phi - m^2)}}\left[\tan^{-1}\left\{\frac{\sqrt{(\cos^2\phi - m^2)}}{(1+\sin\phi)+m}\right\}\right]$$
$$(4.32)$$

Thus for a given value of ϕ (half-acceptance angle), the value of $M_o (M_o = \frac{1}{m_o})$ can be obtained by solving Eq. (4.31). For, this, function $F(\phi, m)$ given by Eq. (4.32) has been ploted against m for various values of ϕ ranging from $\phi = 4^o, 5^o, 6^o, 7^o, 8^o$ (Fig. 4.4) . The values of M_o for various ϕ values obtained from Fig. 4.4 are given in Table 4.1.

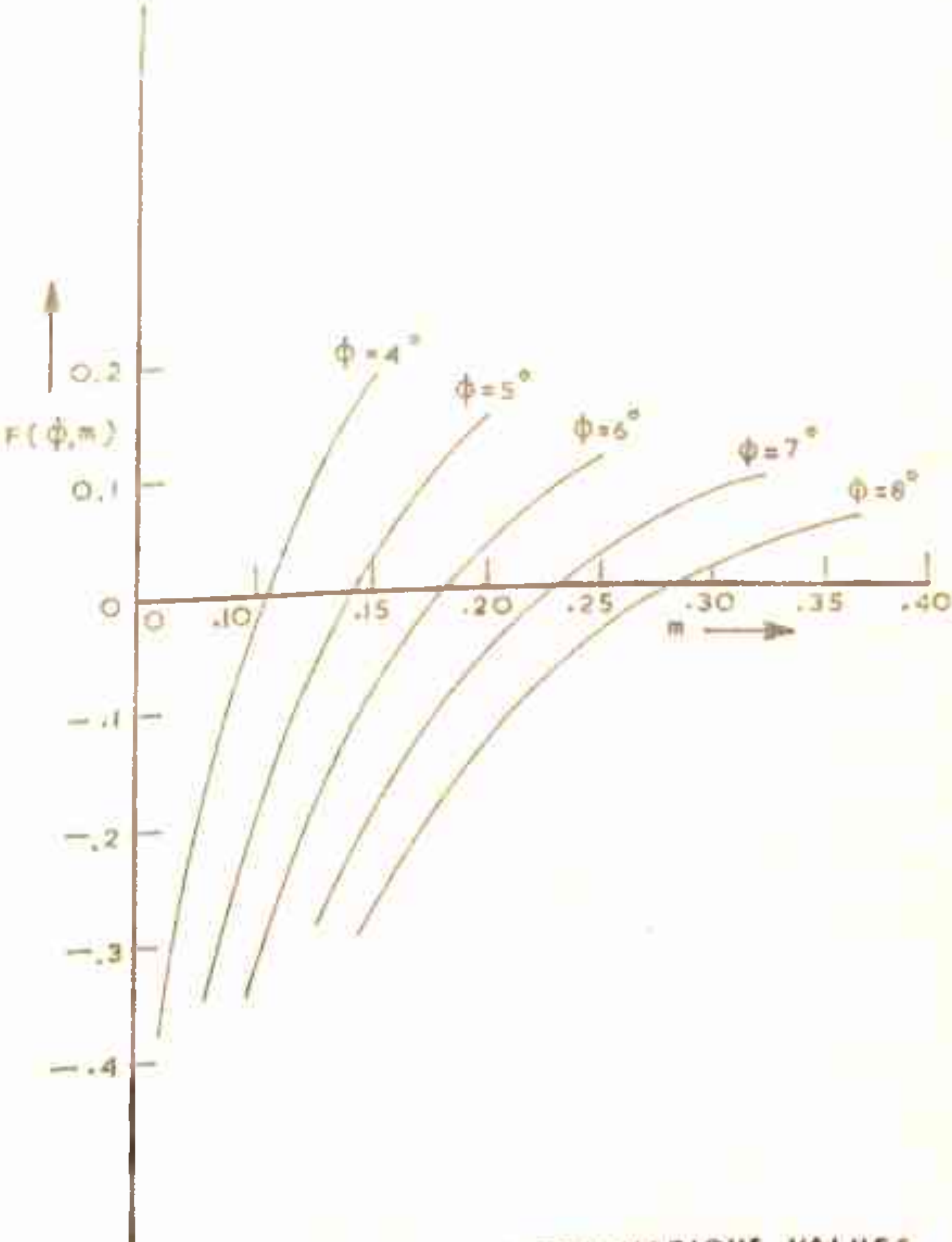

FIG. 4.4 F (φ, m) VERSUS m FOR VARIOUS VALUES OF φ, THE HALF-ACCEPTANCE ANGLE

Table- 4.1

Optimum concentration ratios for various values of ϕ (half-acceptance angle)

ϕ	8°	7°	6°	5°	4°
M_o	3.45	4.35	5.50	7.14	9.64

As can be seen from Table 4.1 that M_o for $\phi = 6^{\circ}$ comes out to be 5.5, which gives the concentration factor equal to 6.5 and the corresponding height in units of L will be 5.5 cot ϕ. The maximum concentration factor in Winston's design for $\phi = 6^{\circ}$ is about 9.6 and the corresponding height in units of L is 10.6 cot ϕ. Thus we see that for $\phi = 6^{\circ}$ and the same size of the receiver the present design as compared to the Winston's design has the advantage of uniform illumination and height reduction by about a factor of 2 but has the disadvantage of reduction in the concentration factor by about 32 % .

(c) Shape of the transverse cross-section of uniform cylindrical concentrator

The shape of the transverse cross-section of the uniform cylindrical concentrator for $\phi = 6^{\circ}$, $M_o = 5.5$ and L = 1 c.m. is shown in Fig. 4.5. One side of the concentrator (PR) was obtained by solving Eq.(4.21) for R for various values of θ from 90° to 6°. From each pair of (R,θ) values,

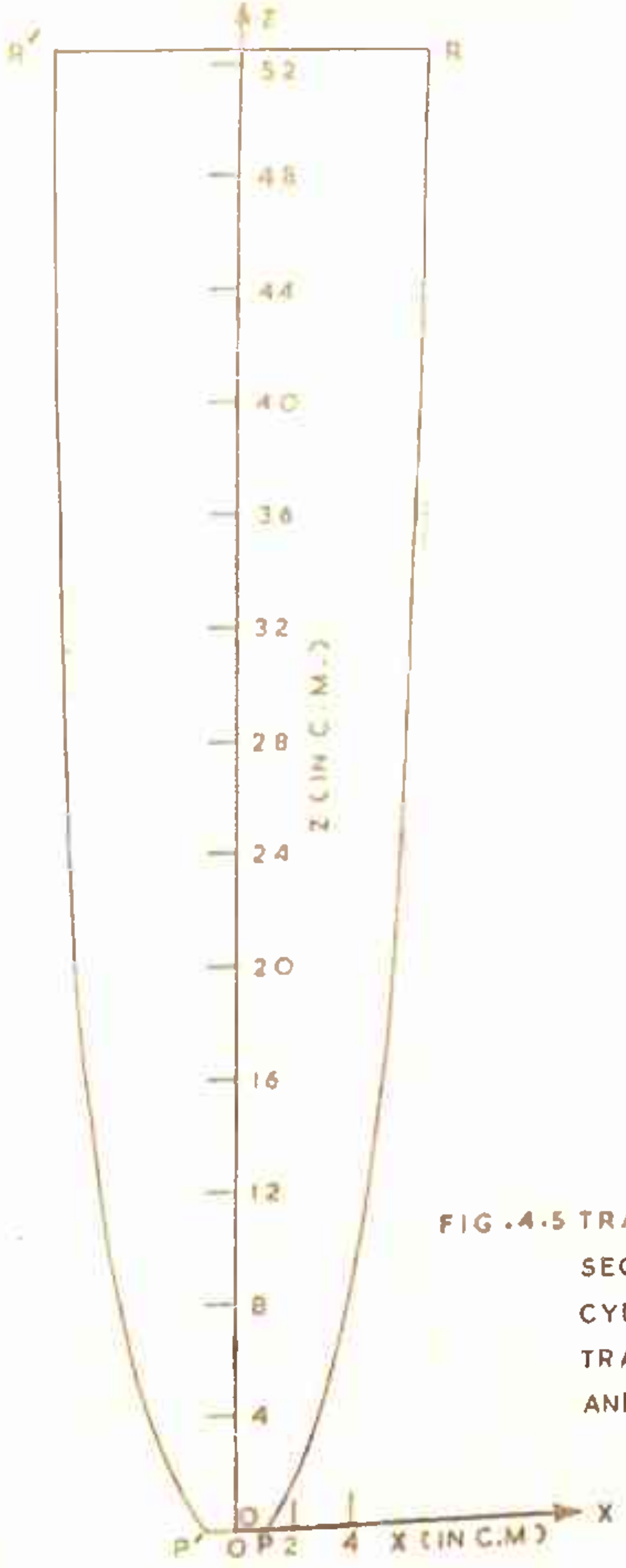

FIG.4.5 TRANSVERSE CROSS SECTION OF UNIFORM CYLINDRICAL CONCENTRATOR FOR $\phi = 6^\circ$ AND $M_o = 5.5$

the corresponding values of (X,Z) pair was obtained using Eqs.(4.8), (4.10) and (4.11). The values of (X,Z) which we have used for plotting the reflecting surface PR are given in Table 4.2. As mentioned earlier in Sec. 4.3, the other side of the concentrator can be obtained by mirror symmetry. Thus the surface P'R' was obtained by taking the mirror image of PR about Z-axis.

Table 4.2

Coordinates of the points used in plotting the transverse cross-section of the concentrator

X (c.m.)	Z (c.m.)	X (c.m.)	Z (c.m.)	X (c.m.)	Z (c.m.)
1.0	0.0	3.0	3.86	5.0	14.2
1.2	0.23	3.2	4.5	5.2	16.0
1.4	0.49	3.4	5.2	5.4	18.1
1.6	0.78	3.6	5.95	5.6	20.5
1.8	1.10	3.8	6.6	5.8	23.4
2.0	1.46	4.0	7.73	6.0	27.0
2.2	1.85	4.2	8.76	6.2	31.7
2.4	2.3	4.4	9.9	6.4	38.9
2.6	2.76	4.6	11.1	6.5	52.4
2.8	3.3	4.8	12.6		

4.4 Theoretical Calculation Of The Illumination Profile At The Absorber

In this section we present the theoretical intensity profile of uniform cylindrical concentrator having $\phi = 6^\circ$, $M_o = 5.5$ and of Winston's C P C having half-acceptance angle $\phi = 6^\circ$. The size of the absorber in both the cases has been taken to be 2 c.m. (i.e., the receiver is placed from (-1,0) to (1,0) as shown in Fig. 4.6).

Let the incident beam falling on the entrance aperature make an angle ϕ_1 with the optic axis of the concentrator, as shown in Fig. 4.6. This beam is divided into a number of portions of same width dX. Now consider one portion AB of this beam which after undergoing one or more reflections on surface PR reaches the absorber at points A'B'. The width of the beam reaching the absorber, compared to initial incident beam, is decreased by a factor, may be called as local concentration factor. So the local concentration factor for beam AB due to surface PR comes out to be C_1 where

$$C_1 = \frac{AB}{A'\ B'}$$

In the same fashion the local concentration factors were calculated for the total incident beam passing through the entrance aperture, taking into account the effect of both the reflected beams from PR, P'R' surfaces and that of the direct beam. The local concentration factor for the beam reaching directly

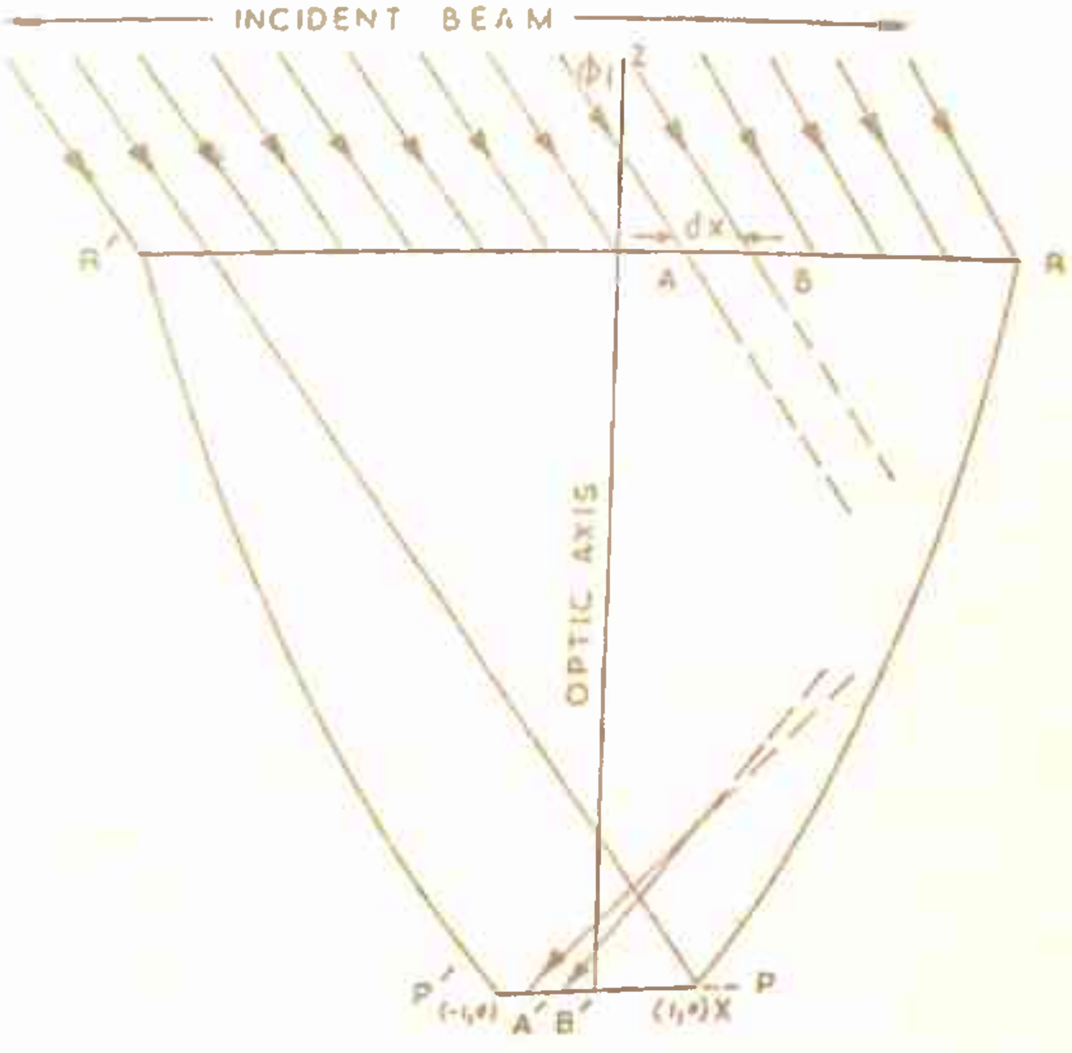

FIG. 4.6 THEORETICAL DETERMINATION OF INTENSITY PROFILE OF THE CONCENTRATORS

on the absorber is equal to one. In our calculation we have taken dX to be 0.5 c.m.

In case of Winston's C P C when $\phi_1 = 6^0$ the local concentration factors on the absorber are due to the reflecting surface PR only. For $\phi_1 = 5^0$, local concentration factors on the absorber will be due to the surface PR and direct beam, since for $\phi_1 = 5^0$ the 1.77 c.m. (from point P) of absorber width will get the direct beam. For $\phi_1 = 4^0, 3^0, 2^0, 1^0$ and 0^0 the local concentration factors on the absorber will be due to both the reflecting surface PR, P'R' and direct beam. However in case of uniform cylindrical concentrator, the local concentration factors on the absorber for all values of $\phi_1 = 6^0, 5^0, 4^0, 3^0, 2^0, 1^0, 0^0$ will be due to both the reflecting surfaces PR, P'R' and direct beam. For a given value of ϕ_1 the resultant of these local concentration factors is plotted along the width of the absorber. It was found that the resultant curve has various peaks. These peaks were smoothed out by dividing the absorber into the segments of 0.2 c.m. width (these segments are numbered from 1 to 10. The segment one is from (-1.0,0) to (-0.8,0), the second from (-.8, 0) to (-.6,0) and so on.) and then the relative intensities are calculated for these segments of the absorber.

The calculated values of relative intensities (segment wise) used in plotting are given in Tables 4.3 -4.5 for both the concentrators i.e., for uniform cylindrical concentrator and Winston's C P C. The Tables 4.3(a) and 4.3(b) give the comparision for relative intensities, considering the contribution only from surface PR for uniform cylindrical concentrator and Winston's C P C , respectively. The Tables 4.4(a) and 4.4(b) give the similar information from the surface P'R' for both the concentrators. Tables 4.5(a) and 4.5(b) give the comparision of resultant relative intensities, considering the contribution from both the surfaces PR, P'R' and that of direct light, for uniform cylindrical concentrator and Winston's C P C , respectively.

The relative intensity curves obtained for various values of ϕ_1 = 6^o – 0^o are shown in Figs. 4.7 – 4.13. It is clear from Fig. 4.7 that for ϕ_1 = 6^o, the intensity distribution along the absorber is almost uniform in case of uniform cylindrical concentrator and is extremely non-uniform in case of Winston's C P C, since intensity is ∞ at a particular point and zero else where. As the ϕ_1 changes from 6^o to 0^o, the intensity profile becomes less and less uniform in case of uniform cylindrical concentrator and becomes more and more uniform in case of Winston's C P C.

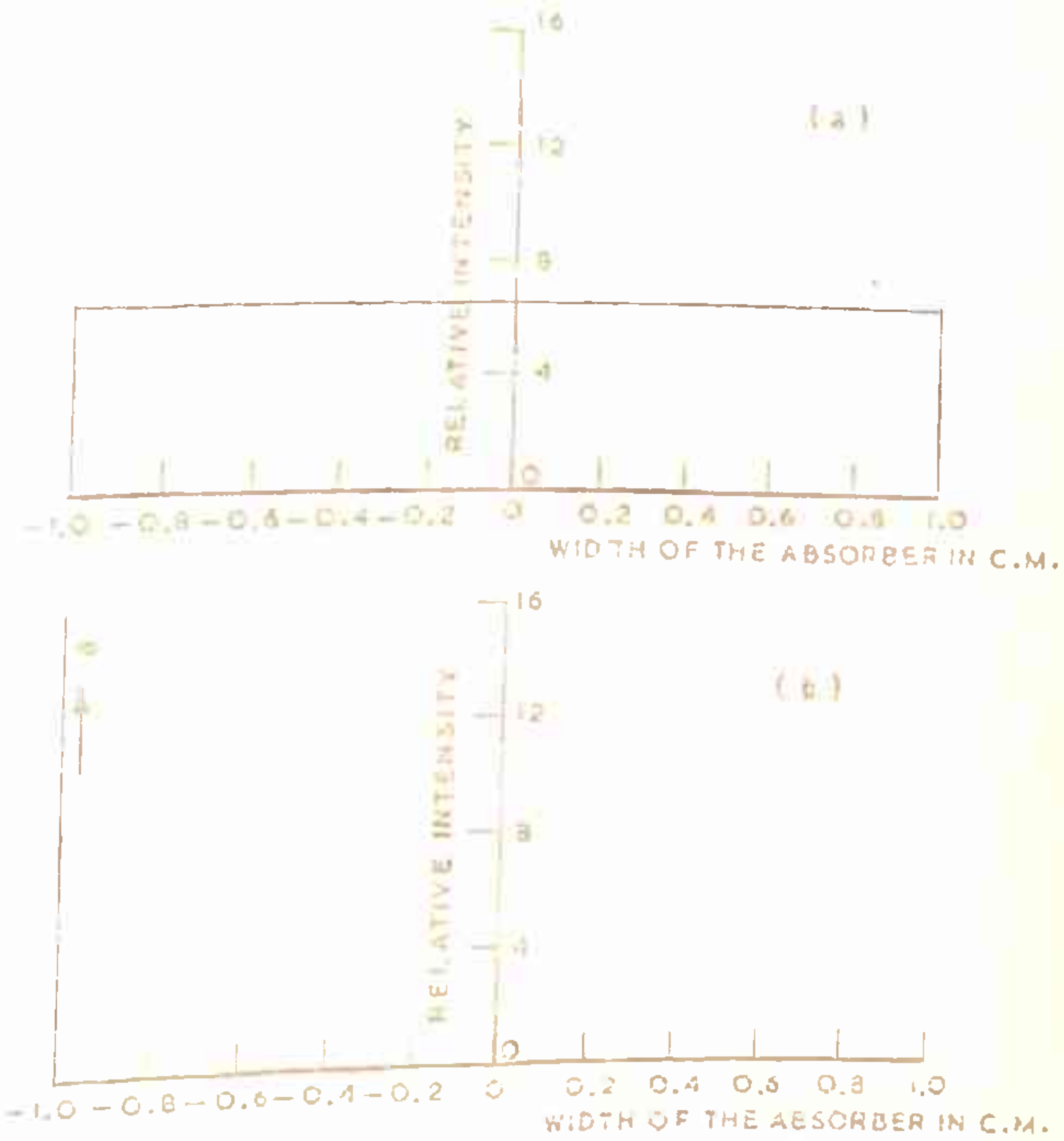

FIG.4.7 INTENSITY PROFILE ALONG THE WIDTH OF THE ABSORBER FOR $\psi = 0^{\circ}$

(a) UNIFORM CYLINDRICAL CONCENTRATOR.

(b) WINSTON'S CPC.

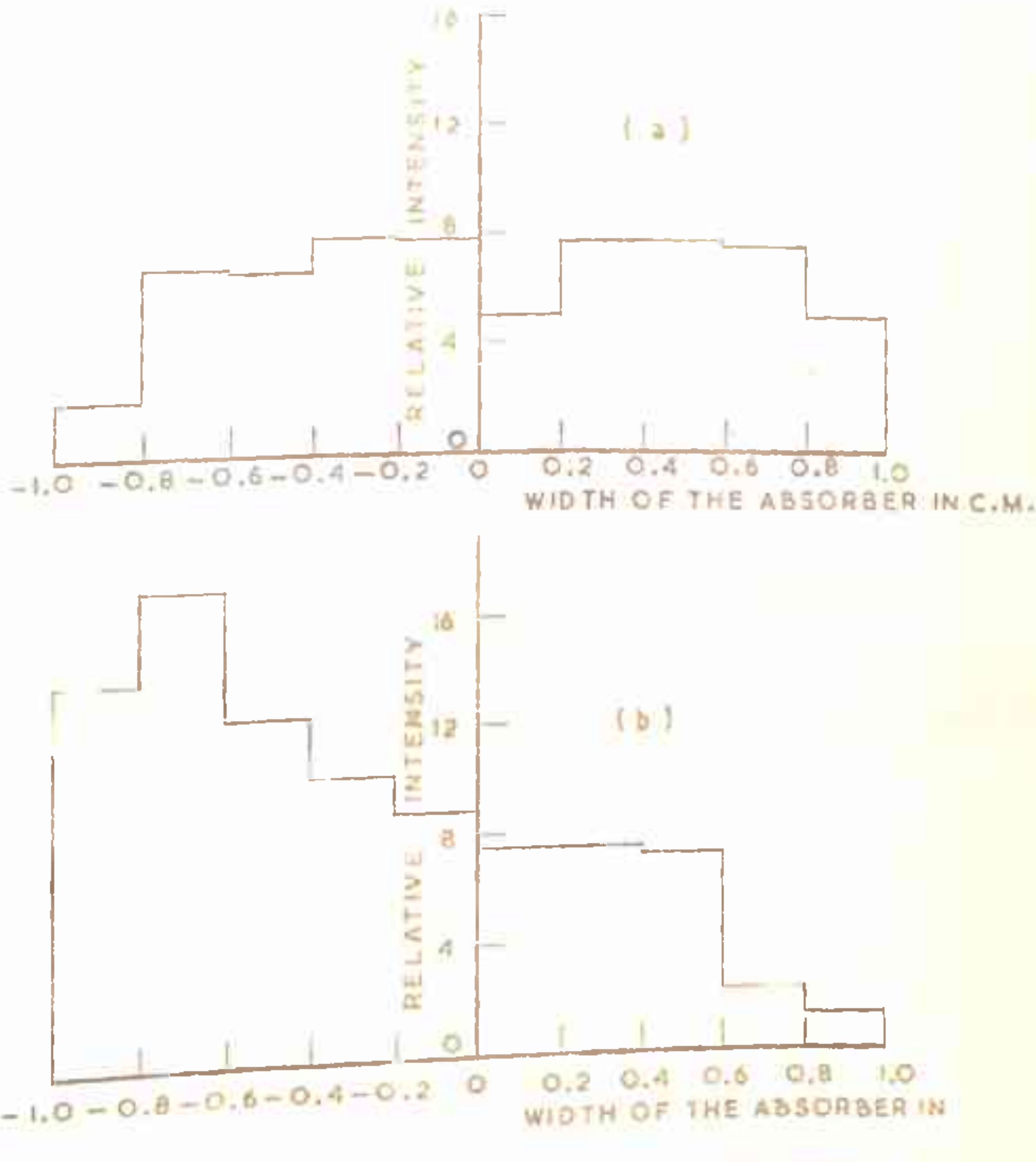

FIG.4.8 INTENSITY PROFILE ALONG THE WIDTH OF THE ABSORBER FOR $\phi = 5°$

(a) UNIFORM CYLINDRICAL CONCENTRATOR.

(b) WINSTON'S CPC.

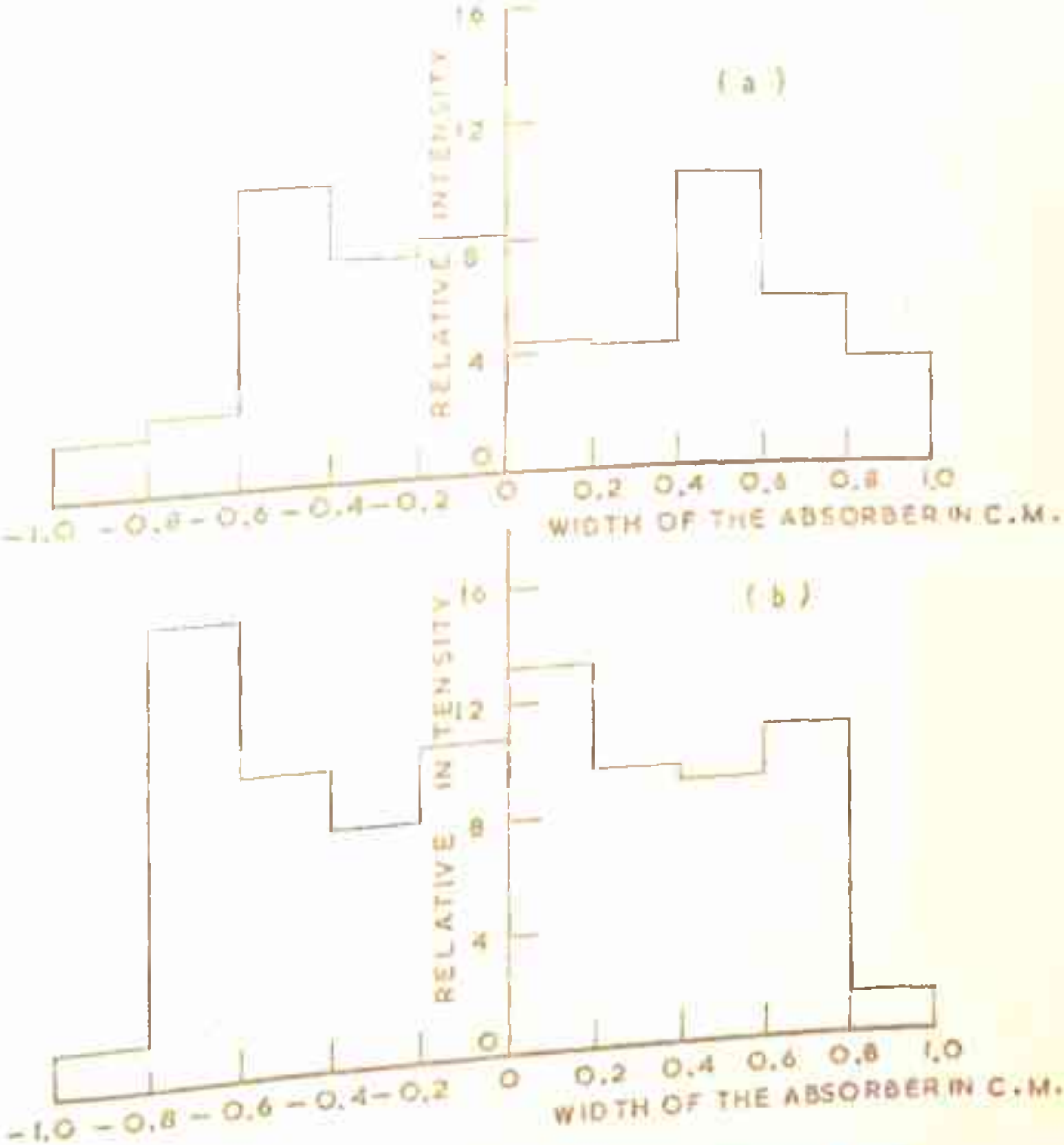

FIG.4.9 INTENSITY PROFILE ALONG THE WIDTH OF THE ABSORBER FOR $\Phi = 4°$
(a) UNIFORM CYLINDRICAL CONCENTRATOR.
(b) WINSTON'S CPC.

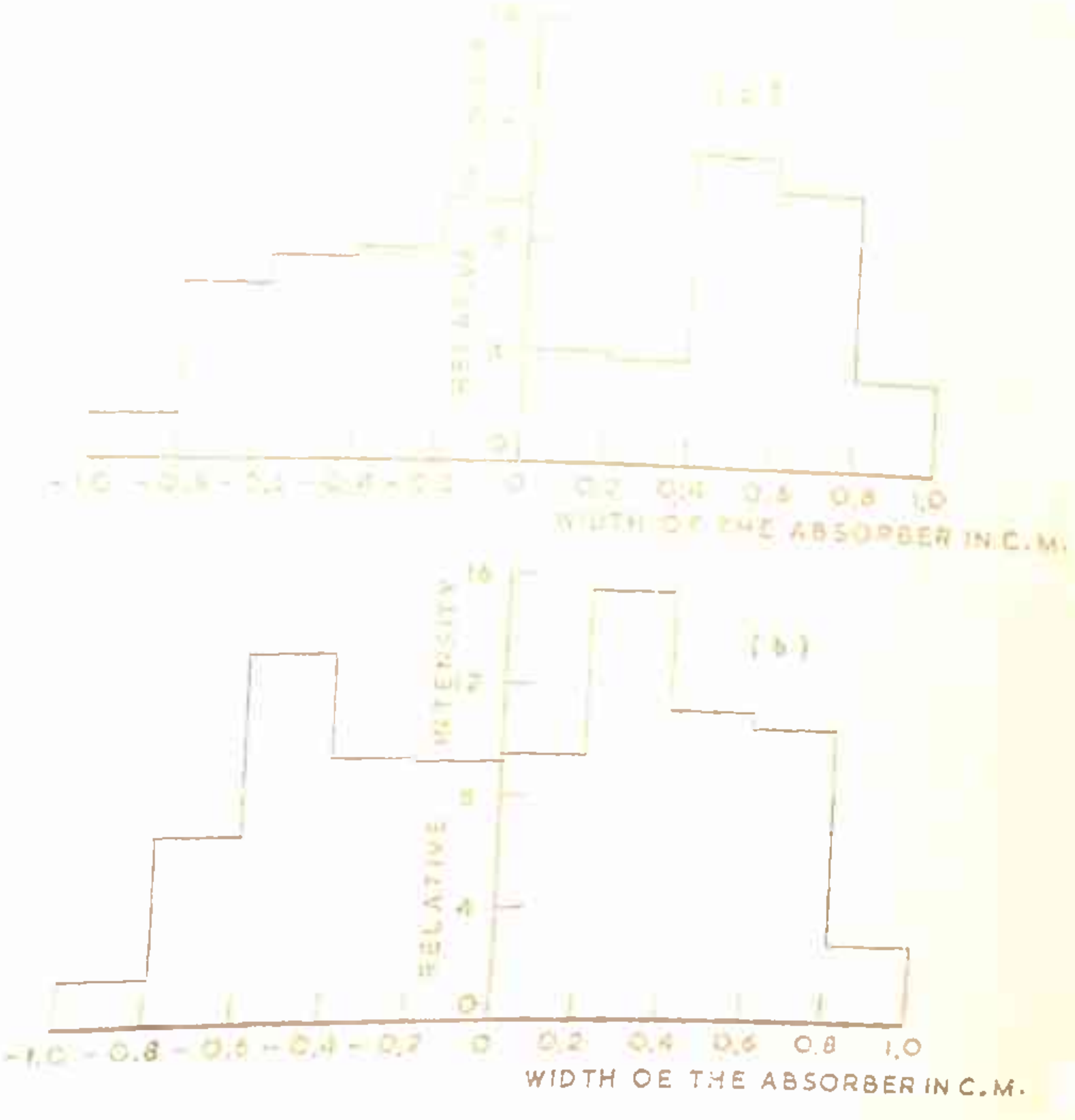

FIG.4.10 INTENSITY PROFILE ALONG THE WIDTH OF THE ABSORBER FOR $\phi = 3^{\circ}$

(a) UNIFORM CYLINDRICAL CONCENTRATOR.

(b) WINSTON'S CPC.

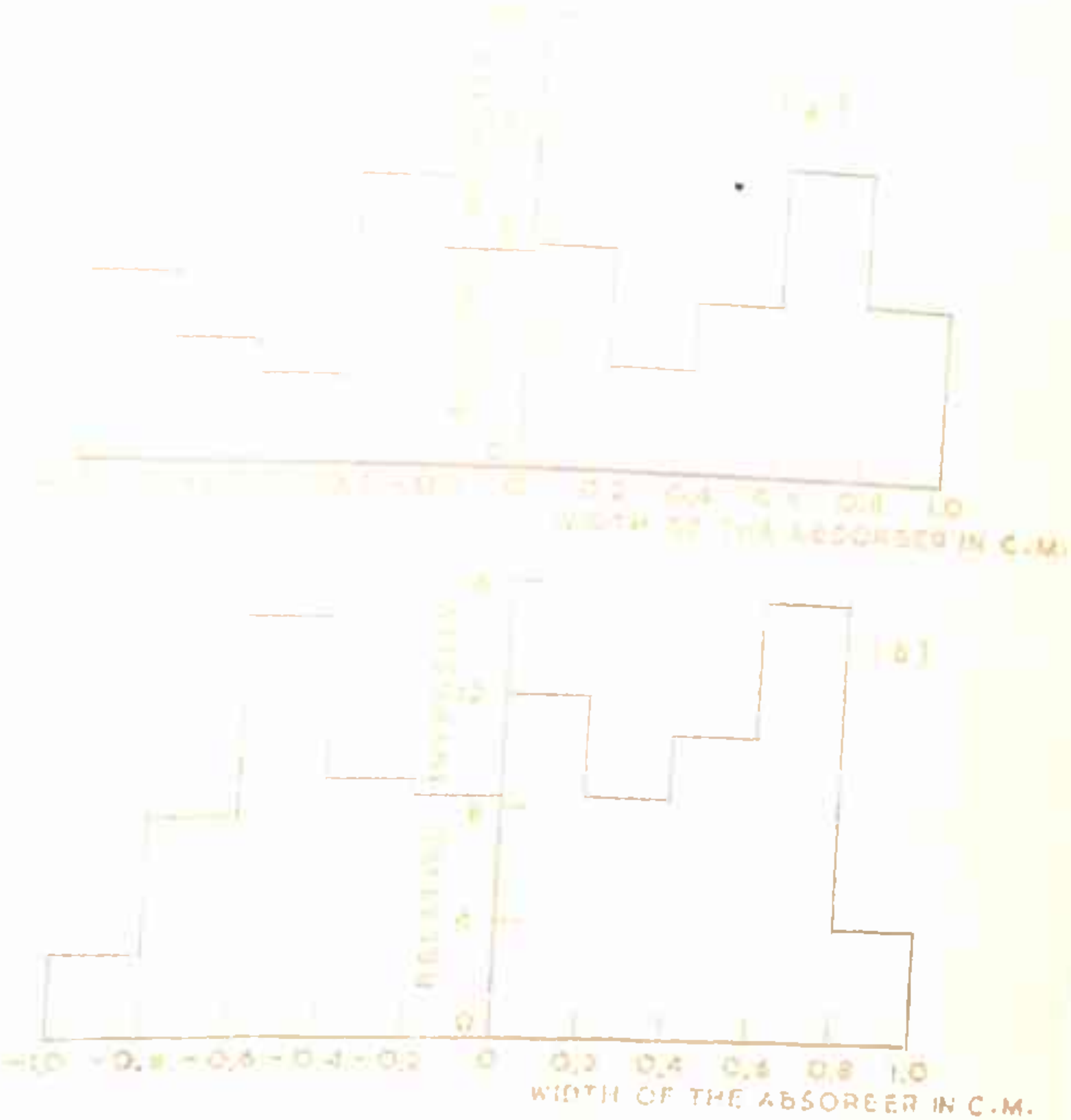

FIG. 4.11 INTENSITY PROFILE ALONG THE WIDTH OF THE ABSORBER FOR $\phi = 2^{\circ}$

(a) UNIFORM CYLINDRICAL CONCENTRATOR.

(b) WINSTON'S CPC.

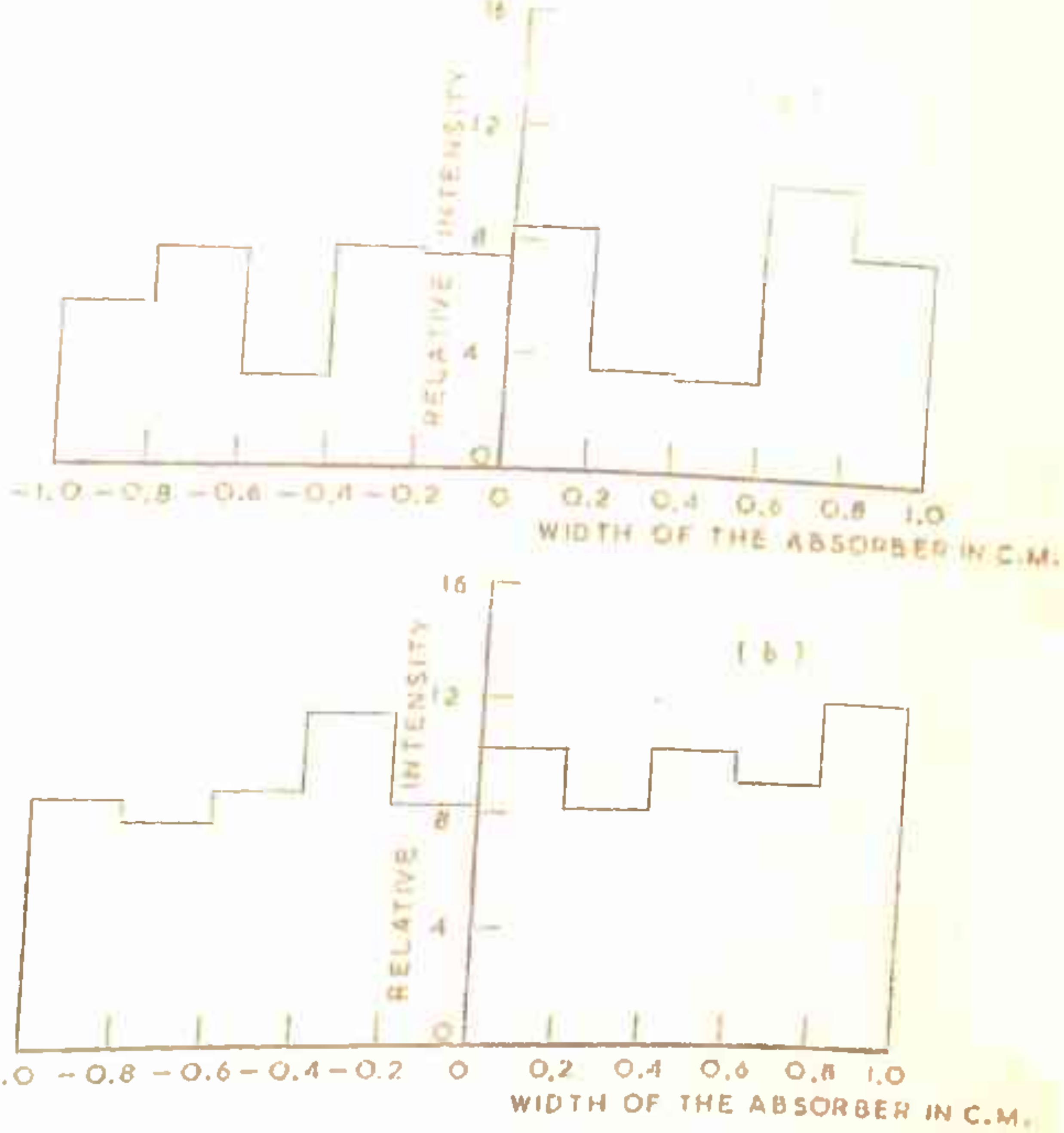

FIG. 4.12 INTENSITY PROFILE ALONG THE WIDTH OF THE ABSORBER FOR $\phi = 1^\circ$

(a) UNIFORM CYLINDRICAL CONCENTRATOR.

(b) WINSTON'S CPC.

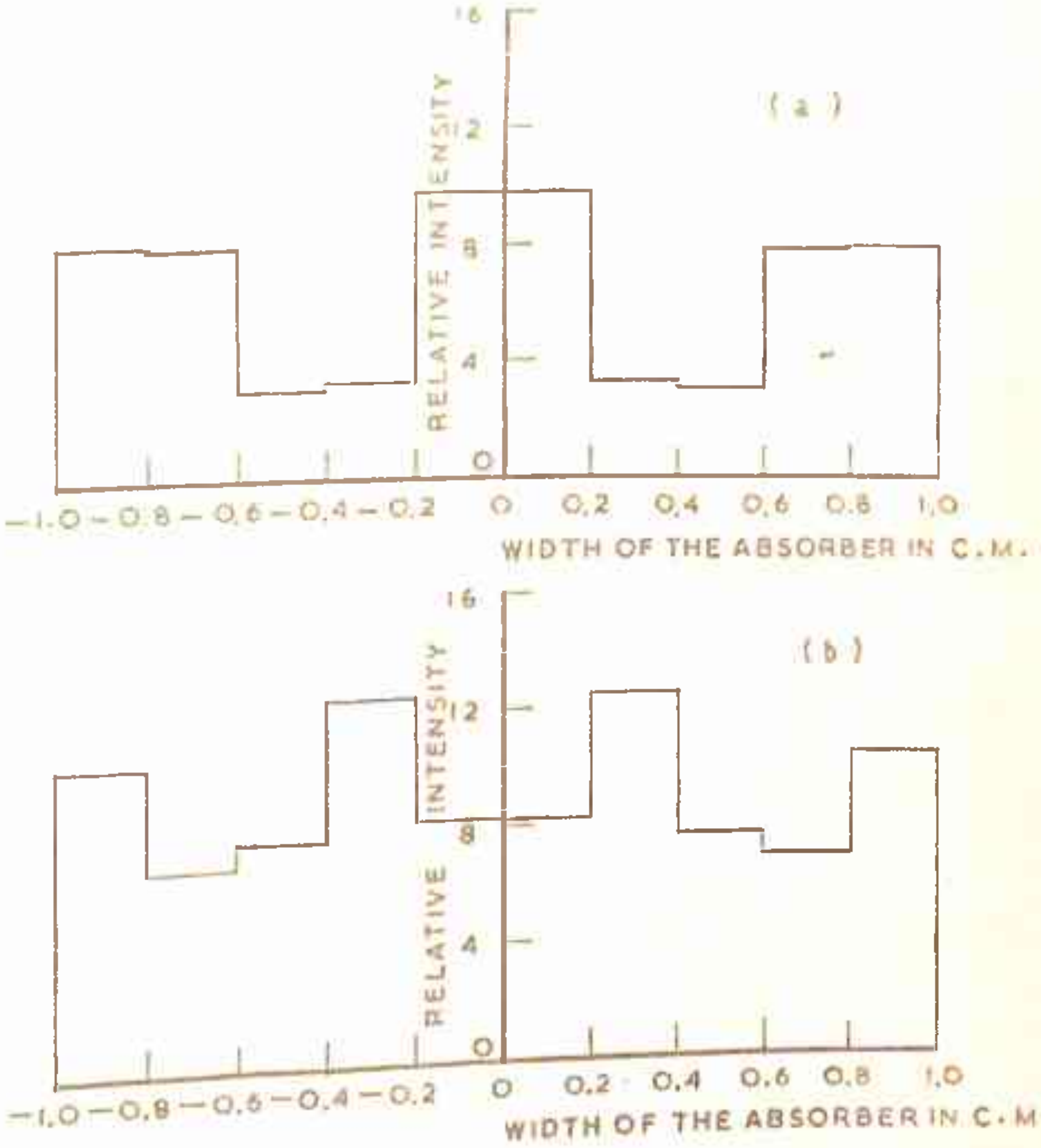

FIG.4.13 INTENSITY PROFILE ALONG THE WIDTH OF THE ABSORBER FOR $\phi = 0°$

(a) UNIFORM CYLINDRICAL CONCENTRATOR

(b) WINSTION'S CPC.

Table-4.3(a)

Segmentwise Relative Intensities from Surface PR for Uniform Cylindrical Concentrator

ϕ_1	Segments of the absorber width									
	1	2	3	4	5	6	7	8	9	10
6°	5.5	5.5	5.5	5.5	5.5	5.5	5.5	5.5	5.5	5.5
5°	0.5	5.25	5.15	4.7	4.3	4.0	6.7	6.7	6.5	3.9
4°	0.0	0.0	7.3	4.2	3.7	3.4	3.2	9.1	4.8	2.6
3°	0.0	0.0	4.4	4.3	3.4	3.0	2.7	10.2	9.0	2.2
2°	0.0	0.0	0.0	6.8	3.4	2.9	2.6	5.0	9.9	5.2
1°	0.0	0.0	0.0	4.4	3.6	2.7	2.4	2.2	9.2	6.8
0°	0.0	0.0	0.0	0.0	6.1	2.7	2.3	2.0	6.9	7.0

Table-4.3(b)

Segmentwise Relative Intensities from Surface PR for Winston's C P C

ϕ_1	Segments of the absorber width									
	1	2	3	4	5	6	7	8	9	10
6°	∞*	0.0	0.0	0.0	0.0	0.0	0.0	0.0	0.0	0.0
5°	13.8	16.25	11.4	9.2	7.9	6.5	6.5	6.2	1.2	0.3
4°	0.0	14.0	8.7	6.7	5.7	12.2	8.5	8.0	9.8	0.3
3°	0.0	3.9	10.0	5.8	4.8	4.1	14.4	10.1	9.6	1.7
2°	0.0	0.0	11.4	5.5	4.3	3.6	7.4	5.7	14.5	3.0
1°	0.0	0.0	3.9	7.8	4.2	3.3	2.9	9.3	8.2	11.1
0°	0.0	0.0	0.0	8.85	4.15	3.15	2.65	6.7	5.9	9.4

*Light reaches at the point (-1.0,0), so the ∞ concentration is only at that point.

Table-4.4(a)

Segmentwise Relative Intensities from Surface P'R' for Uniform Cylindrical Concentrator

β_1	Segments of the absorber width									
	1	2	3	4	5	6	7	8	9	10
6°	0.0	0.0	0.0	0.0	0.0	0.0	0.0	0.0	0.0	0.0
5°	0.55	0.55	0.55	2.2	2.5	0.0	0.0	0.0	0.0	0.0
4°	0.9	1.6	1.9	2.4	3.5	0.0	0.0	0.0	0.0	0.0
3°	0.5	5.2	1.8	2.3	4.9	0.0	0.0	0.0	0.0	0.0
2°	5.5	3.2	2.0	2.3	3.2	3.9	0.0	0.0	0.0	0.0
1°	4.5	6.4	2.0	2.2	2.8	4.8	0.0	0.0	0.0	0.0
0°	7.0	6.9	2.0	2.3	2.7	6.1	0.0	0.0	0.0	0.0

Table-4.4(b)

Segmentwise Relative Intensities from Surface P' R' for Winston's C P C

ϕ_i	Segments of the absorber width									
	1	2	3	4	5	6	7	8	9	10
6°	0.0	0.0	0.0	0.0	0.0	0.0	0.0	0.0	0.0	0.0
5°	0.0	0.0	0.0	0.0	0.0	0.0	0.0	0.0	0.0	0.0
4°	0.5	0.5	0.5	0.5	4.1	0.0	0.0	0.0	0.0	0.0
3°	0.5	1.6	2.0	2.5	3.4	4.4	0.0	0.0	0.0	0.0
2°	1.8	6.6	2.2	2.5	3.1	7.4	0.0	0.0	0.0	0.0
1°	7.4	6.36	3.8	2.6	3.0	5.9	4.2	0.0	0.0	0.0
0°	9.3	5.9	6.7	2.65	3.15	4.15	8.85	0.0	0.0	0.0

Table-4.5(a)

Resultant Segmentwise Relative Intensities for Uniform Cylindrical Concentrator

ϕ_1	Segments of the absorber width									
	1	2	3	4	5	6	7	8	9	10
6°	6.5	6.5	6.5	6.5	6.5	6.5	6.5	6.5	6.5	6.5
5°	2.05	6.8	6.7	7.9	7.8	5.0	7.7	7.7	7.5	4.9
4°	1.9	2.6	10.2	7.6	8.2	4.4	4.2	10.1	5.8	3.6
3°	1.5	6.2	7.2	7.6	9.3	4.0	3.7	11.2	10.0	3.2
2°	6.5	4.2	3.0	10.1	7.6	7.8	3.6	6.0	10.9	6.2
1°	5.5	7.4	3.0	7.6	7.4	8.5	3.4	3.2	10.2	7.8
0°	8.0	7.9	3.0	3.3	9.8	9.8	3.3	3.0	7.9	8.0

Table- 4.5(b)

Resultant Segmentwise Relative Intensities for Winston's C P C

ϕ_1	Segments of the absorber width									
	1	2	3	4	5	6	7	8	9	10
6°	∞^*	0.0	0.0	0.0	0.0	0.0	0.0	0.0	0.0	0.0
5°	13.8	17.1	12.4	10.2	8.9	7.5	7.5	7.2	2.2	1.3
4°	1.5	15.5	10.2	8.2	10.8	13.2	9.5	9.0	10.8	1.3
3°	1.5	6.5	13.0	9.3	9.2	9.5	15.4	11.1	10.6	2.7
2°	2.8	7.6	14.6	9.0	8.4	12.0	8.4	10.7	15.5	4.0
1°	8.4	7.6	8.7	11.4	8.2	10.2	8.1	10.3	9.2	12.1
0°	10.4	6.9	7.7	12.5	8.3	8.3	12.5	7.7	6.9	10.4

*Light reaches only at the point (-1.0,0), so the ∞ concentration ratio is only at that point.

4.5 Specifications of The Models Fabricated

Three models of uniform cylindrical concentrators have been fabricated. The specifications of these models are given in Table 4.6.

Table -4.6

Specifications of the uniform cylindrical concentrators fabricated

Model No.	D	d	H	l	ø	C	Material used
U1	15.2	2.0	60.2	100.0	6.0	7.6	Aluminium sheets
U2	15.4	4.0	33.8	150.0	11.5	3.8	Granularly anodised Aluminium sheet
U3	30.4	4.0	123.5	300.0	6.0	7.6	Plain anodised Aluminium shee

Notation used;

D - size of the entrance aperture (in cm)

d - size of the exit aperture, 2L (in cm)

H - Height of the concentrator (in cm)

l - Length of the concentrator (in cm)

ø - Half acceptance angle (in Deg.)

C - Geometrical concentration ratio

Model U1 was fabricated by the first method described in Sec. 2.2 and models U2 and U3 were fabricated by the second method described in the same section.

4.6 Experiments Performed

Two types of experiments were performed for (a) The determination of lateral intensity profile at the exit aperture of uniform cylindrical concentrators and (b) Comparision of intensity distribution along the length of uniform cylindrical concentrator and Winston's C P C. The experimental set up is same in both the cases and has been already described in Sec.2.3.

(a) Lateral intensity profile at the exit aperture

This experiment is performed for models U1,U2 and U3 (See Table 4.6).

(i) Experiment performed on model U1

For low values of concentration ratio, the photo diode current is directly proportional to the intensity. Hence the concentration ratio of the concentrator can be expressed as

$$\text{concentration ratio} = \frac{I\ (C)}{I\ (D)} \qquad (4.33)$$

where I(C) is the diode current in the concentrated light i.e., at the exit aperture and I(D) is the diode current in the direct light i.e., at the entrance aperture. The Eq.(4.33) can be written as

$$\text{concentration ratio} = \frac{I(C)xR}{I(D)xR} = \frac{V_C}{V_D} \qquad (4.34)$$

where V_C is the voltage drop across the load resistance R when diode is in the concentrated light and V_D is the voltage drop across R when diode is in direct light.

For testing the uniformity of illumination we have measured the concentration ratio at three different points along the width of the exit aperture by placing three germanium photo transistors (ACP 132 PNP) used as diode, along the width of the receiver (exit aperture) at equal intervals. The circuit shown in Fig. 4.14(a) is used and the voltage drops across load resistance R are measured at the entrance and exit aperture, the values of load resistance R and supply voltage V_s are chosen in such a way that the value of collector current remains within 10 mA to 20 mA (Property of ACP 132 PNP). The experiments are performed on various days from winter solstice to summer solstice. The Table 4.7 shows the readings obtained after an interval of 2 months. The nonuniformity of illumination for the model U1 comes to 1 to 5 %

(ii) Experiment performed on model U2 and U3

As mentioned earlier in Sec. 2.3(a) that the concentration ratio of the concentrator can be expressed by Eq. (2.1) as

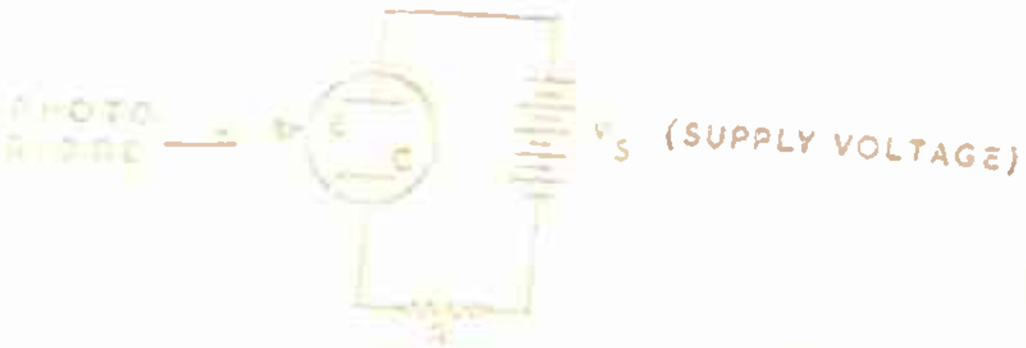

FIG. 4.14 (a) CIRCUIT FOR MEASURING THE VOLTAGE DROP ACROSS THE LOAD RESISTANCE (R)

FIG. 4.14 (b) ARRANGEMENT OF SOLAR CELLS USED FOR DETERMINING THE INTENSITY PROFILE AT THE EXIT APERTURE OF THE CONCENTRATORS

Table-4.7

Diurnal and seasonal widthwise variation of concentration ratios of uniform cylindrical concentrator(model U1)

Date	Concentration Ratio	10.00 A.M. Phototransistors 1	2	3	11.00 A.M. Phototransistors 1	2	3	12.00 Noon Phototransistors 1	2	3	1.00 P.M. Phototransistors 1	2	3	2.00 P.M. Phototransistors 1	2	3	V_s and R
22.12.77		1.6	1.5	1.6	1.4	1.45	1.4	1.3	1.4	1.35	1.3	1.4	1.3	1.5	1.5	1.6	4.2V,300 ohms
11.2. 78		1.94	1.8	1.9	1.66	1.62	1.6	1.61	1.55	1.62	1.85	1.70	1.78	2.0	1.85	1.92	4.9V.,400 ohms
20.4. 78		1.77	1.6	1.77	1.66	1.5	1.66	1.66	1.60	1.66	1.66	1.62	1.66	1.6	1.5	1.6	4.2V.,300 ohms
23.6. 78		2.2	2.2	2.1	1.94	1.94	1.9	1.8	1.8	1.75	1.4	1.4	1.5	1.6	1.6	1.7	3.9V.,300 ohms

$$\text{concentration ratio} = \frac{I_{sc}(C)}{I_{sc}(D)}$$

For testing the uniformity of illumination the concentrations are measured (using above equation) at three different points along the width of the exit aperture by placing three solar cells at equal intervals as shown in Fig. 4.14(b). The experiments are conducted on both the models U2 and U3 simultaneously on various days from winter solstice to equinox. The intensity profile curves (for few days after an interval of 20 days) obtained are shown in Figs 4.15-4.17. The percentage nonuniformity of illumination for model U2 is 1 to 5 and for model U3 is 3.0 to 8.0.

(b) Intensity distribution along the length of the uniform cylindrical concentrator and Winston's CPC

This experiment has been performed on models U2 and W3 to test the distribution of intensity along the length of the concentrators. The concentration ratio is measured (using Eq. 2.1) along the length of the concentrators by putting solar cells at 0, 30, 60, 90, 120 and 150 c.m. In case of model U2 (Fig. 4.18) at 10.00 a.m. the concentration ratio was measured at 0, 30, 60, 90 and 120 c.m. and then the curve was extended upto 131 c.m., since the length of the concentrator from 131 c.m. to 150 c.m. was in shadow. However in case of model W3 (Fig.4.18) at 10.00 a.m. the concentration was measured at 0, 30, 60, and

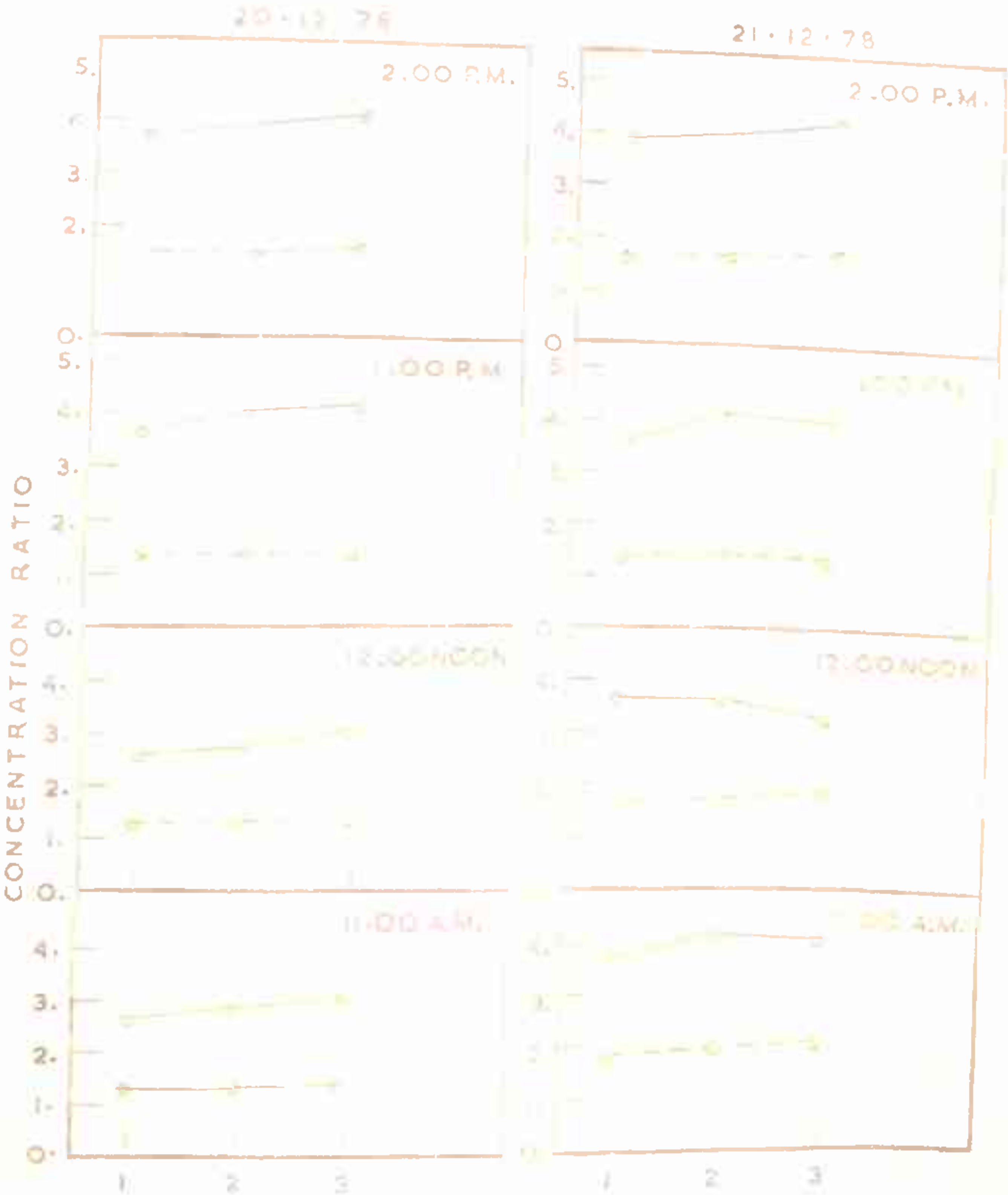

SOLAR CELLS (1,2,3) PLACED WIDTHWISE AT THE BASE

FIG.4.15 INTENSITY PROFILE AT THE EXIT APERTURE OF UNIFORM CYLINDRICAL CONCENTRATORS

MODEL U2 ---- MODEL U3 ———

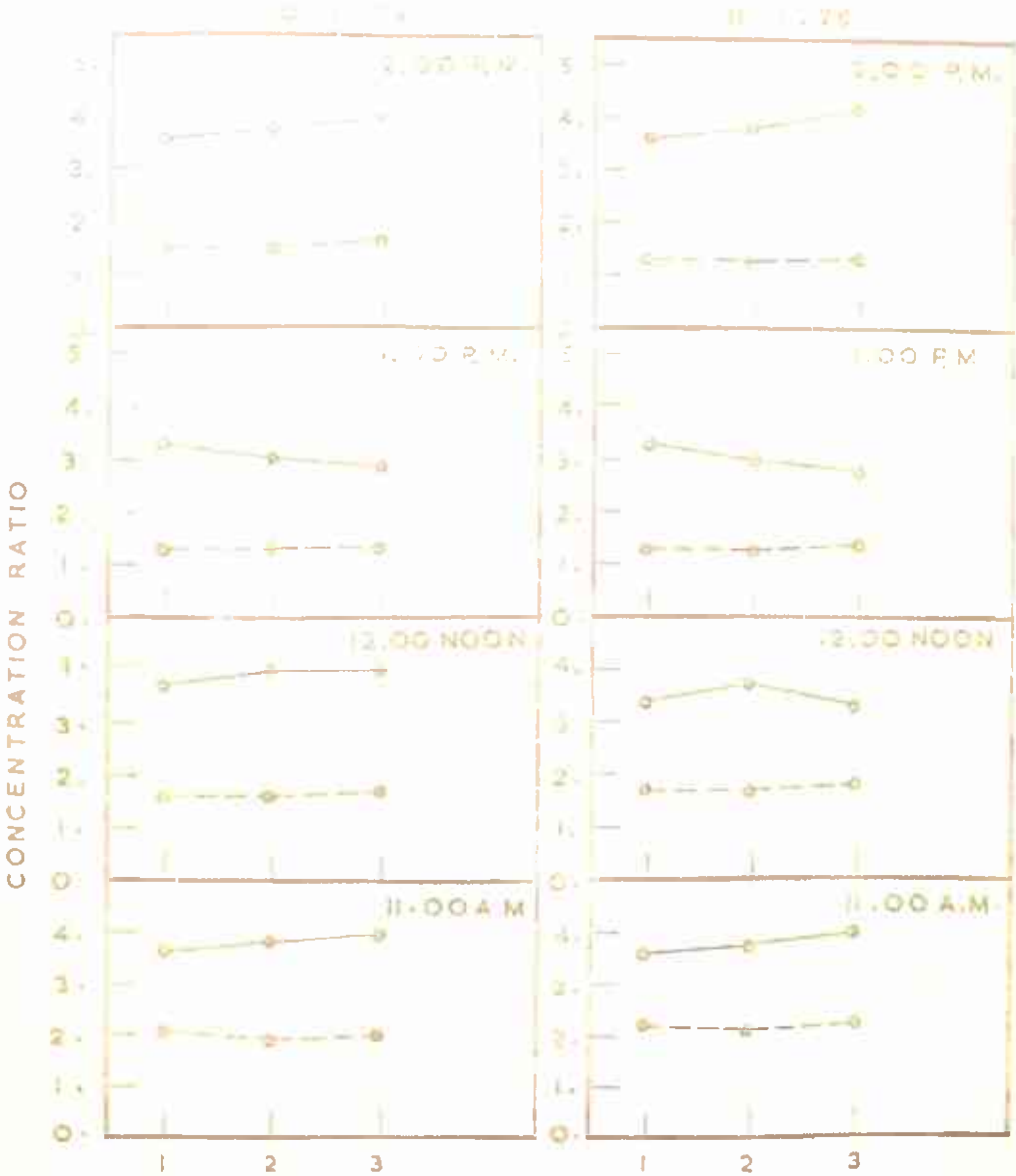

SOLAR CELLS (1, 2, 3) PLACED WIDTHWISE AT THE BASE

FIG.4.16 INTENSITY PROFILE AT THE EXIT APERTURE OF UNIFORM CYLINDRICAL CONCENTRATORS

MODEL U2 — — — — MODEL U3 ————

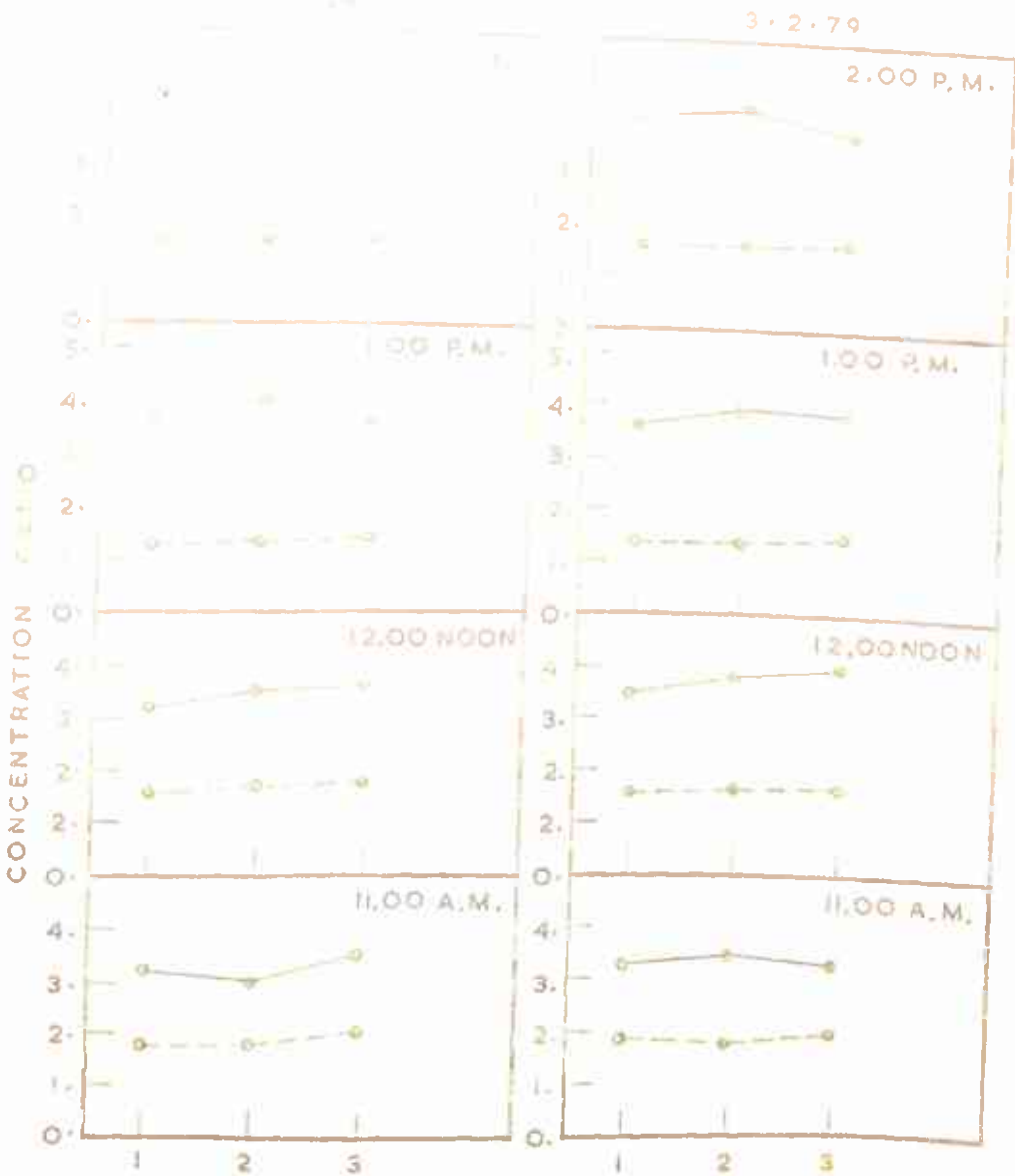

SOLAR CELLS (1, 2, 3) PLACED WIDTHWISE AT THE BASE

FIG. 4.17 INTENSITY PROFILE AT THE EXIT APERTURE OF UNIFORM CYLINDRICAL CONCENTRATORS

MODEL U2 – – – – – – MODEL U3 ————

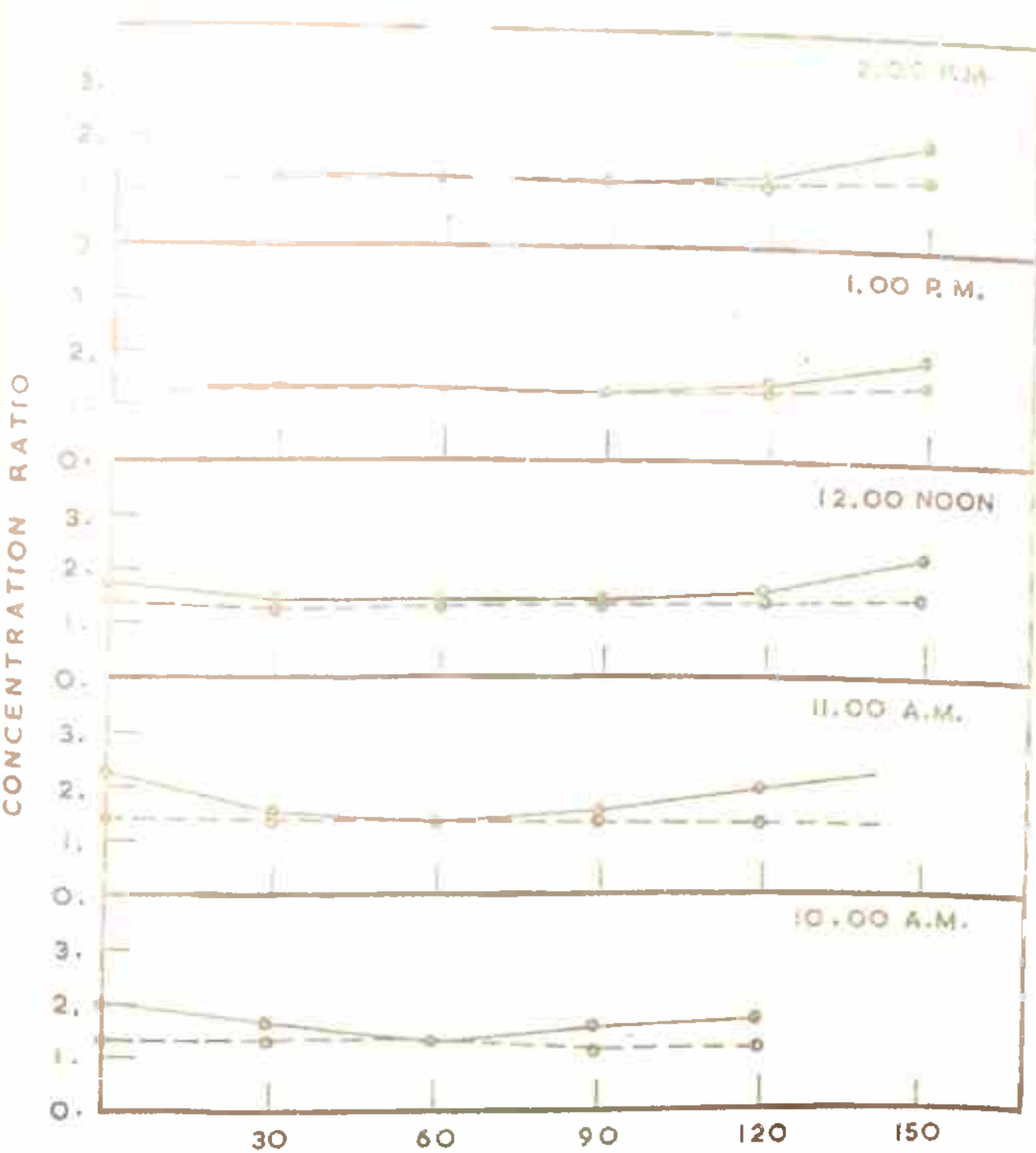

FIG. 4.18 INTENSITY DISTRIBUTION ALONG THE LENGTH OF THE CONCENTRATORS

MODEL U2 — — —   MODEL W3 ———

90 cm and then the curve was extended upto 117 cm, since rest of the length was in shadow. In this way we have plotted the curve for these two models from 10.00 a.m. to 2.00 p.m. This experiment was performed in the month of April after an interval of 4 days. It is clear from Fig. 4.18 that the 110 cm. of the length of U2 (i.e. from 21 cm to 131 cm) is getting concentrated light from 10.00 a.m. to 2.00 p.m., however in case of W3 only 80 cm of the length of W3 (i.e. from 37 cm to 117 cm) is getting concentrated light from 10.00 a.m. to 2.00 p.m.

4.7 Results and Discussions

The experiments performed on the uniform cylindrical concentrator models, which we have fabricated here are; (a) measurement of lateral intensity profile and (b) measurement of intensity distribution along the length. In this section we have discussed the results obtained using these models with that of Winston's CPC models (Chapter 2).

(a) Lateral intensity profile

The lateral intensity profile at the exit aperture is measured for models U1, U2 and U3. The nonuniformity of illumination of these models comes to 1 to 5 % , 1 to 5 % and 3 to 8 % respectively. The lateral intensity profile of model U1 is measured using photodiode and for models U2 and U3 we have used solar cells (Sec. 4.6). The non-uniformity of illumination of model W1 is 16 to 23 % (Sec.2.3). Thus the intensity profile at the exit aperture of uniform cylindrical concentrators is more uniform compared to Winston's CPC. Though using granularly anodised aluminium sheets (instead of plain aluminium sheets) for reflecting surface the uniformity of illumination at the exit aperture can be increased e.g. for model W3 nonuniformity of illumination is 2 to 7 % (Sec. 2.4), but at the same time intensity of illumination decreases. Therefore, for photovoltaic applications, where uniformity of illumination is very important, it would be more advantageous to use uniform cylindrical concentrators.

(b) Intensity distribution along the length

The intensity distribution along the length of the concentrator has been measured for model U2 and model W3. The variation of intensity comes 6 to 8 % and 20 to 27 % respectively. Thus the intensity distribution along the length of model U2 is more uniform compared to model W3. Also in case of model U2, 110 cm. of the length of the concentrator gets light (contineously) from 10.00 a.m. to 2.00 p.m., while in case of model W3 only 80 cm. of the length of the concentrator gets light (continuously) from 10.00 a.m. to 2.00 p.m. The intensity distribution along the length of the concentrator can be made more uniform by modifying the end walls. This is done by extending the procedure outlined in Sec. 4.3 in such a way as to avoid partial shadowing over the entire absorber area. The resulting concentrator is a combination of 2 two-dimensional uniform cylindrical concentrators, one along the north-south and the other along the east-west directions. Also the length to width ratio of the absorber in such a concentrator cannot be arbitrarily chosen but is determined by the operating period itself[11] so that the 2 two-dimensional concentrators, mentioned above, have the same height.

REFERENCES

1. S.R. Dhariwal, L.S. Kothari and S.C. Jain, Response Of p-n Junction Solar Cells To Concentrated Sunlight And Partial Illumination, SUN I, 2, Proc. International Solar Energy Society Congress, Jan. 1978, New Delhi. pp.714-18.

2. A. Gupta, S. Kumar and V.K. Tewary, Design of A Nontracking Concentrator Which Will Distribute Sunlight In A Uniform Manner Over A Flat Receiving Surface, Proc. National Solar Energy Convention 1976, Calcutta, pp. 66-67.

3. A Gupta, Murlidhar, S. Kumar and V.K. Tewary, Performance Studies on Uniform Illumination Type Nontracking Concentrators, Proc. National Solar Energy Convention 1978, Bhavnagar, pp. 462-66.

4. A. Gupta, S. Kumar, Murlidhar and V.K. Tewary, Design And Testing Of A New Type Of Nontracking Concentrator, Accepted For Presentation In 'International Solar Energy Symposium' To Be Held At Baghdad In Feb. 81.

5. A. Gupta, S. Kumar, Murlidhar and V.K.Tewary, Design And Testing Of A Uniform Illuminating Nontracking Concentrator, Communicated To Solar Energy.

6. J.H. McDermit and T.E. Horton, Reflective Optics For Obtaining Prescribed Irradiative Distribution From Collimated Sources, Applied Optics 13 (6), 1445-50 (1974).

7. D.G. Burkhard and D.L. Shealy, Design Of Reflectors Which Will Distribute Sunlight In A Specified Manner, Solar Energy 17 (4), 221-27 (1975).

8. A Rabl, Solar Concentrator With Maximal Concentration For Cylindrical Absorber, Applied Optics 15 (7), 1871-73 (1976).

9. H. Tabor, Stationary Mirror Systems For Solar Collecors, Solar Energy 2 (3-4), 27-33 (1958).

10. R. Winston, Principles Of Solar Concentrators Of A Novel Design, Solar Energy 16 (2), 89-95(1974).

11. A. Gupta and S. Kumar, Design Of Nontracking Concentrator Capable Of Avoiding Shadow On The Absorber Plate, Proc. National Solar Energy Convention 1978, Bhavnagar, pp. 127-30.

APPENDIX-1

(a) Reflection Properties of Ellipse

Now we will discuss the reflection properties of the ellipse, used in Sec.3.4. The equation of the ellipse [Fig. A1.1(a)] is

$$\frac{x^2}{a^2} + \frac{z^2}{b^2} = 1 \qquad (A1.1)$$

where a is the semimajor axis and b is semi-minor axis. The normal to the ellipse at any point $P(X_p, Z_p)$ makes an angle α_n with the x-axis. So we have

$$\tan \alpha_n = \frac{a^2 Z_p}{b^2 X_p} = \frac{Z_p}{(1-e^2) X_p} \qquad (A1.2)$$

Since $b^2 = a^2(1-e^2)$ where e is the eccentricity of the ellipse. Now consider an incident ray P'P on the ellipse as shown in Fig. A1.1(a). The inclination θ of this ray with the x-axis will be given by

$$\tan \theta = \frac{Z_p}{(X_p - X')} \qquad (A1.3)$$

and the angle of incidence θ_i of the ray at the point P can be expressed by the equation [using Eqs.(A1.2) and (A1.3)],

$$\tan \theta_i = \left[\frac{Z_p}{(1-e^2)X_p} - \frac{Z_p}{(X_p - X')} \right] / \left[1 + \frac{Z_p^2}{(1-e^2)X_p(X_p - X')} \right]$$

$$= \frac{Z_p (X_p e^2 - X')}{(1-e^2)(a^2 - X_p X')} \qquad (A1.4)$$

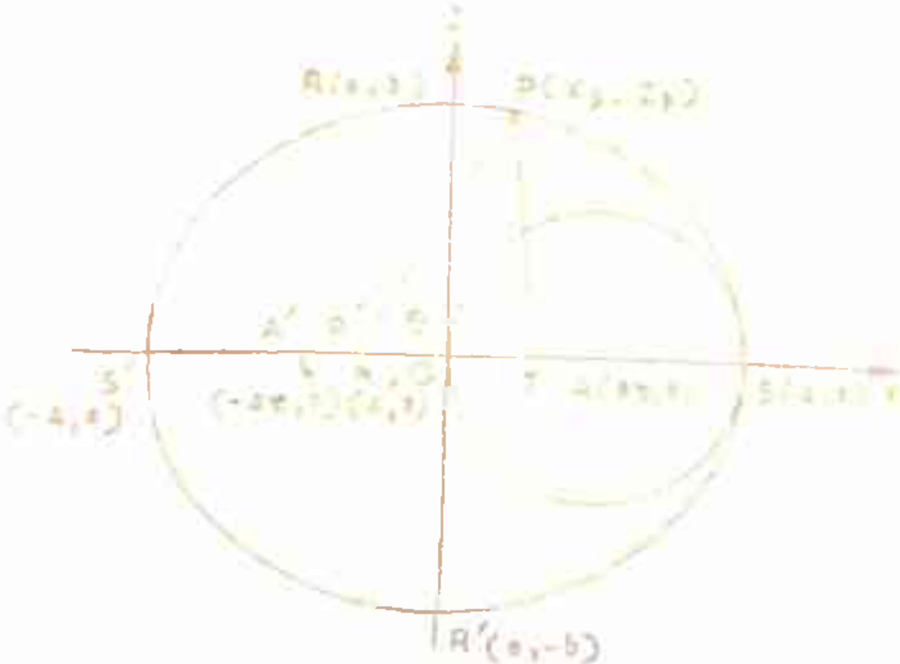

FIG. A1.1(a) REFLECTION PROPERTY OF ELLIPSE

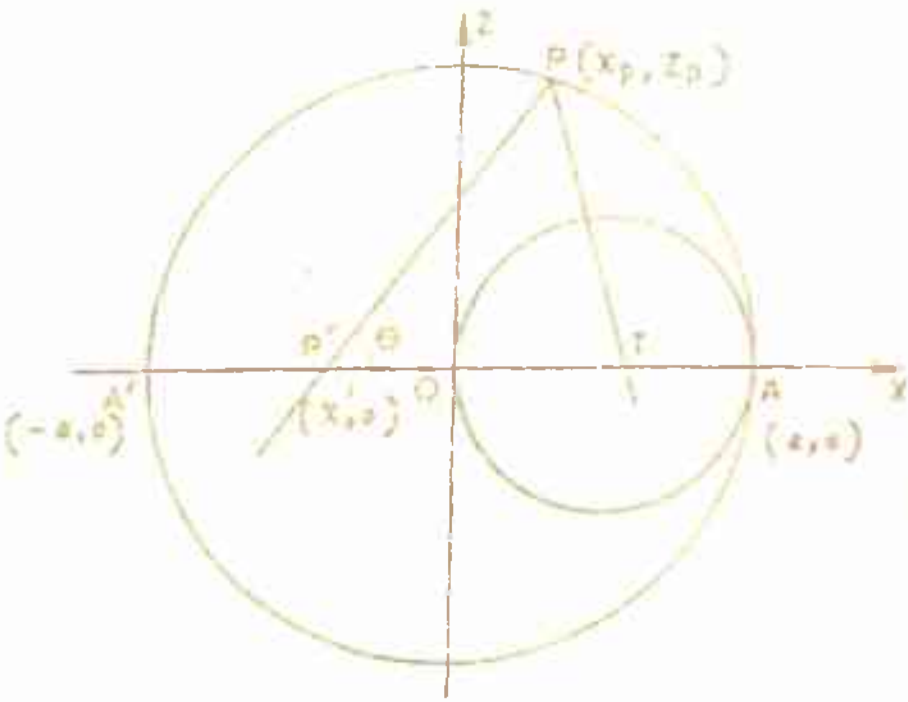

FIG. A1.1(b) REFLECTION PROPERTY OF CIRCLE

Therefore the equation of the reflected ray PT will be

$$Z-Z_p = \left[\frac{\dfrac{Z_p}{(1-e^2)X_p} + \dfrac{Z_p(X_p e^2 - X')}{(1-e^2)(a^2 - X_p X')}}{1 - \dfrac{Z_p^2(X_p e^2 - X')}{(1-e^2)^2 X_p (a^2 - X_p X')}} \right] [X - X_p]$$

or

$$Z-Z_p = \left[\frac{Z_p(a^2 - X_p X') + Z_p X_p (X_p e^2 - X')}{X_p (1-e^2)^2 (a^2 - X_p X') - Z_p^2 (X_p e^2 - X')} \right] (1-e^2)(X-X_p)$$

(A1.5)

The X-coordinate of the point T (X_T) where it will meet x-axis i.e., OT can be obtained by putting Z=0 in Eq.(A1.5)

$$X_T = \frac{2X_p e^2 a^2 - X'(a^2 + e^2 X_p^2)}{a^2 + X_p^2 e^2 - 2X_p X'} \qquad \text{(A1.6)}$$

Now consider $X' = a\,e\,(f - 1)$ with $0 \leq f \leq 1$ (i.e. the point P' is confined between origin O and focus A' and $X_p = qa$ with $-1 \leq q \leq 1$ (or $180^\circ \geq \theta \geq 0^\circ$) which means that the point P is confined to first and second quadrant. Putting the values of X_p and X' in Eq. (A1.6) we get

$$X_T = ae \left[\frac{(1 + eq)^2 - f(1 + e^2 q^2)}{(1 + eq)^2 - 2q\,e\,f} \right] \qquad \text{(A1.7)}$$

or

$$X_T = ae \left[\frac{(1 + e^2 q^2)(1 - f) + 2eq}{(1 + e^2 q^2) + 2eq(1 - f)} \right] \qquad \text{(A1.8)}$$

Now consider the following two cases

(i) Case I

Let q be positive i.e., point P is in first quadrant. From the R.H.S. of Eq.(A1.8) it is clear that X_T will be positive we known that

$$(1 - eq)^2 > 0$$

$$1 + e^2 q^2 > 2 eq$$

or

$$(1 + e^2 q^2) f > 2f eq$$

Since f is always positive. Therefore, the numerator of R.H.S. of Eq. (A1.7) is less than the denominator and hence $X_T < ae$ i.e. the reflected ray will pass through OA. Thus we can say that if the incident ray passes between A' and O (i.e. between one focus and origin) and the point P is in first quardrent, the reflected ray will always pass through OA(i.e., between origin and other focus) where the absorber (circular or flate) has to be kept as shown in Fig. A1.1(a).

(ii) Case II

Let q be negative i.e., point P is in second quadrant. Now consider the Eq. (A1.8) i.e.,

$$X_T = ae \left[\frac{(1+ e^2 q^2) (1-f) + 2 eq}{(1+ e^2 q^2) + 2 eq (1-f)} \right]$$

The values of X_T are calculated (for model I discussed in Sec. 3.4) for different values of f from 0 to 1 for various values of q ranging from 0 to -1. If X_T is positive the reflected ray will reach the absorber and if X_T is negative, the reflected ray will not reach the absorber.

For $0 \leqslant f \leqslant 0.62$, X_T is positive for all values of q(i.e.$-1 \leqslant q \leqslant 0$), hence the reflected ray is reaching the absorber. For other values of f ranging from $0.63 \leqslant f \leqslant 1$, the values of q(i.e., from q = 0 to that value of q, X_T is positive and beyond that X_T is negative) are listed in Table A1.1

Table-A1.1

The maximum value of q(upto which X_T is positive) for various f values

f	q	f	q	f	q	f	q
1.0	0.0	0.90	-0.10	0.80	-0.23	0.70	-0.39
0.99	-0.01	0.89	-0.11	0.79	-0.24	0.69	-0.40
0.98	-0.02	0.88	-0.13	0.78	-0.25	0.68	-0.42
0.97	-0.03	0.87	-0.14	0.77	-0.27	0.67	-0.45
0.96	-0.04	0.86	-0.15	0.76	-0.28	0.66	-0.48
0.95	-0.05	0.85	-0.16	0.75	-0.30	0.65	-0.50
0.94	-0.06	0.84	-0.17	0.74	-0.32	0.64	-0.53
0.93	-0.07	0.83	-0.19	0.73	-0.33	0.63	-0.56
0.92	-0.08	0.82	-0.20	0.72	-0.35		
0.91	-0.09	0.81	-0.21	0.71	-0.37		

It is obvious from Table -A1.1 that for $f = 0.75$ if the value of q is from 0 to -0.30 the reflected ray will reach the absorber and if q is between -0.30 to -1.0 , the reflected ray will not reach the absorber i.e., contribution by that ray will be zero. Using the reflection properties of ellipse discussed above we have calculated (Sec. 3.4) the percentage of total incident beam (entering the entrance aperture), reaching the absorber and the second stage concentration of Model I (Sec. 3.3(a)).

(b) Reflection Properties of Circle

Now we will discuss the reflection properties of the circle used in Sec. 3.3(c) and Sec. 3.3(d). The equation of the circle shown in Fig. A1.1(b) is

$$X^2 + Z^2 = a^2 \qquad (A1.9)$$

Now consider an incident ray P'P on the circle as shown in the figure. The inclination of this ray with the x-axis will be

$$\tan \theta = \frac{Z_p}{(X_p - X')} \qquad (A1.10)$$

Consider the situation that point P' lies between O and A' and point P varies in the first and second quadrant (i.e., $0^\circ < \theta < 180^\circ$). Then the reflected ray PT after reflection (one or more number of reflections) from the circle will always reach within OA where the absorber is to be kept.

LOG DRIV [illegible] PHY DRIV [illegible] 0002

V2 MO[illegible]

```
// FOR
*EXTENDED PRECISION
*IOCS(2[illegible] PRINTER)
*ONE WORD INTEGERS
*LIST SOURCE PROGRAM
      REAL LR,[illegible]
      DIMENSION FX([illegible]),PX([illegible]),FPX([illegible]),FDPX([illegible]),XR
     1([illegible]),TITL(40[illegible]),[illegible]([illegible]),FALF(100)
      HFL=[illegible]
      PI=3.1415[illegible]9
      CONV=PI/180.
      XP=HFL
      XL=-XP
      LT=300
      IN=[illegible]
      FI=IN*CONV
      F[illegible]=[illegible]
      CM=-[illegible]/F[illegible]
      WRITE([illegible])[illegible]
      DO [illegible]00 I[illegible]=[illegible]
      DX=0.0[illegible]*INT
      FINI=PI/[illegible]+FI/[illegible]
      PX([illegible])=[illegible]
      FX([illegible])=[illegible]
      FX(2)=DX*SIN(FINI)/COS(FINI)
      CM=CM/COS(FI)
      F[illegible]=SIN(FI)
      F[illegible]=F[illegible]*F[illegible]
      F[illegible]=COS(FI)
      FA4=FA3*FA3
      F[illegible]=F[illegible]*F[illegible]
      F[illegible]=F[illegible]2*FA[illegible]
      F[illegible]=F[illegible]1*FA3
      F[illegible]=F[illegible]4*FA3
      X=XP+DX
      DO 200 IQ=[illegible],L[illegible]
      I=I[illegible]
      XPR=XL-CM*((X-XP)*F[illegible]3+FX(I)*F[illegible])
      XR(I)=XPR
      DXXP=[illegible]-XP[illegible]
      [illegible]=SQRT((X-XPR)*(X-XPR)+FX(I)*FX(I))
      [illegible]([illegible]COS(FI)*LR+FX(I))/(DXXP-LR*F[illegible])
      FPX(I)=[illegible]
      F[illegible]LF(I)=[illegible]
      [illegible]FPX=[illegible](FPX(I))
      [illegible]F=[illegible]FPX/FPX(I)
      IF([illegible]F) 4[illegible],50,[illegible]
48    IT=I-1
      GO TO [illegible]
50    [illegible]=[illegible]*FPX(I)[illegible](FX(I)*F[illegible]-DXXP*CM*FA[illegible])
      T[illegible]=[illegible]*FPX(I)*FPX(I)*([illegible]XXP*F[illegible]+FX(I)*F[illegible]*CM+[illegible]
      TER2=2.0*FPX(I)[illegible]0*FX(I)*F[illegible]-DXXP*CM*F[illegible]9)
     1DXXP*F[illegible]CM+[illegible]*CM)+DXXP*([illegible]
      TER[illegible]=2.0*FPX(I)*(FX(I)*(F[illegible]+F[illegible]
     1[illegible]F[illegible]*CM))
      TER4=2.0*DXX[illegible]*(DXXP+DXXP*F[illegible]+-FX(I)*FX(I)*F[illegible])
      TER[illegible]=2.0*FPX(I)*DXXP+DXXP*DXXP*F[illegible]+FX(I)*FX(I)*F[illegible]
      [illegible]=[illegible]*(FX(I)[illegible]
      SUM=TER[illegible]+TER[illegible]
      DENO=TER[illegible]-TER[illegible]
      FDPX(I)=SUM/DENO
      PX(I)=X
      FX(I+1)=FX(I)+DX*FPX(I)+DX*DX*FDPX(I)/2.0
      X=X+DX
200   CONTINUE
      IT=LT
210   WRITE([illegible]) IT
```

```
      FALF(1)=FALF(2)
      FPX(1)=FPX(2)
      FDPX(1)=0.0
      XR(1)=-1.
      FTN=FX(IT)/(PX(IT)+1)
      FX=ATAN(FTN)
      THTU=(PI/2.0-FX)/CONV
      WRITE(5,500) THTU
500   FORMAT(2X,'THTM=',F[illegible])
      ITM=IT-1
      DO 220 IX=1,ITM
      TL=(FX(IT)-FX(IX))/(PX(IT)-PX(IX))
      TL=ATAN(TL)
      THTL(IX)=PI/2.0-TL
220   THT(IX)=THTL(IX)/CONV
      THTL(IT)=0.0
      THT(IT)=0.0
      WRITE(5,310)(PX(I),FX(I),XR(I),FPX(I),FDPX(I),THT(
     1I),FALF(I),I=1,IT)
400   CONTINUE
[illegible] FORMAT(5X,'IN=',F10.3,[illegible]X,'FM=',F[illegible])
310   FORMAT(2X,F[illegible].2,[illegible]E14.8)
300   FORMAT(2X,I4)
      CALL EXIT
      END

FEATURES SUPPORTED
 ONE WORD INTEGERS
 EXTENDED PRECISION
 IOCS

CORE REQUIREMENTS FOR
 COMMON          0  VARIABLES   [illegible]38   PROGRAM     904

END OF COMPILATION

// XEQ
```

APPENDIX-3.

Detailed Solution of Eq. (4.18)

Here we present the detailed solution of Eq.(4.18), given by

$$\frac{1}{R}\frac{dR}{d\theta} = -\frac{\cos\phi\cos[(\theta+\phi)/2] - m\sin\theta\sin[(\theta+\phi)/2]}{(\cos\phi + m\cos\theta)\sin[(\theta+\phi)/2]}$$

The R.H.S. of this equation can be written as

$$-\frac{\cos[(\theta+\phi)/2](\cos\phi + m\cos\theta)/2 - m\sin\theta\sin[(\theta+\phi)/2]}{(\cos\phi + m\cos\theta)\sin[(\theta+\phi)/2]}$$

$$+\frac{\cos[(\theta+\phi)/2](m\cos\theta - \cos\phi)}{2(\cos\phi + m\cos\theta)\sin[(\theta+\phi)/2]}$$

$$= T_1 + \frac{(m\cos\theta - \cos\phi)\cos[(\theta+\phi)/2]}{2(\cos\phi + m\cos\theta)\sin[(\theta+\phi)/2]} \qquad (A3.1)$$

where

$$T_1 = -\frac{\cos[(\theta+\phi)/2](\cos\phi + m\cos\theta)/2 - m\sin\theta\sin[(\theta+\phi)/2]}{(\cos\phi + m\cos\theta)\sin[(\theta+\phi)/2]}$$

So we have

$$\frac{1}{R}\frac{dR}{d\theta} = T_1 + \frac{\cos[(\theta+\phi)/2]}{2\sin[(\theta+\phi)/2]} - \frac{\cos\phi\cos[(\theta+\phi)/2]}{(m\cos\theta + \cos\phi)\sin[(\theta+\phi)/2]}$$

$$= T_1 + T_2 + T_3 \qquad (A3.2)$$

where $T_2 = \dfrac{\cos[(\theta+\phi)/2]}{2\sin[(\theta+\phi)/2]}$ and

$$T_3 = -\frac{\cos \phi \cos [(\theta + \phi)/2]}{(m \cos \theta + \cos \phi) \sin[(\theta+\phi)/2]}$$

$$\therefore \ dR/R = (T_1 + T_2 + T_3)\ d\theta \qquad (A3.3)$$

Now considering only $T_3 d\theta$ we have

$$T_3 d\theta = -\frac{\cos [(\theta + \phi)/2]}{\sin[(\theta + \phi)/2]} \times \frac{\cos \phi}{(m \cos \theta + \cos \phi)}\ d\theta$$

$$= -\frac{\cos(\theta/2)\cos(\phi/2) - \sin(\theta/2)\sin(\phi/2)}{\sin(\theta/2)\cos(\phi/2) - \cos(\theta/2)\sin(\phi/2)} \times \left[\frac{\cos \phi}{m \cos \theta + \cos \phi}\right] d\theta$$

Now dividing R.H.S. of this equation by $\cos(\theta/2)\cos(\phi/2)$

we get

$$T_3 d\theta = -\frac{1 - \tan(\theta/2)\tan(\phi/2)}{\tan(\theta/2) + \tan(\phi/2)} \times \left[\frac{\cos \phi}{m \cos \theta + \cos \phi}\right] d\theta$$

(A3.4)

Let $\tan(\theta/2) = t \quad \therefore \quad \sec^2(\theta/2) \times d\theta \ \frac{1}{2} = dt$

or $d\theta = 2dt/(1 + t^2)$

Now substituting the values of $d\theta$ and $\tan(\theta/2)$ in Eq.(A3.4)

we have

$$T_3 d\theta = -\frac{2 \cos \phi [1 - t.\tan(\phi/2)]\ dt}{[t + \tan(\phi/2)]\ [\cos \phi(1+t^2) + m(1-t^2)]}$$

$$= \frac{dt}{(1+m)} . \left[\frac{-2}{[t + \tan(\theta/2)]} + \frac{2(\cos \phi - m).t}{[(\cos \phi - m)t^2 + (\cos \phi + m)]} + \frac{2m \sin \phi}{[(\cos \phi - m)t^2 + (\cos \phi + m)]} \right] \qquad (A3.5)$$

Now substituting the values of T_1, T_2 and T_3 in Eq.(A3.3) and integrating we have

$$\log R = -\log[(\cos\phi + m\cos\theta)\sin\{(\theta+\phi)/2\}] - \log[\sin\{(\theta+\phi)/2\}]$$

$$-\frac{2}{(1+m)}\log[\tan(\phi/2)+t] + \frac{1}{(1+m)}\log[(\cos\phi - m)t^2$$

$$+(\cos\phi + m)] + \frac{2m\sin\phi}{(1+m)\sqrt{(\cos^2\phi - m^2)}}\tan^{-1}\{\frac{\sqrt{(\cos\phi - m)}}{\sqrt{(\cos\phi + m)}}t\}$$

$$+ K \qquad (A3.6)$$

where K is the constant of integration. Putting the value of $t = \tan(\theta/2)$ in Eq.(A3.6) we get.

$$\log R = -\log[(\cos\phi + m\cos\theta)\sin\{(\theta+\phi)/2\}] + \log[\sin\{(\theta+\phi)/2\}]$$

$$-\frac{2}{(1+m)}\log[\tan(\theta/2)+\tan(\phi/2)] + \frac{1}{(1+m)}\cdot$$

$$\log[\{\cos\phi - m\}\tan^2(\theta/2) + \{\cos\phi + m\}]$$

$$+\frac{2m\sin\phi}{(1+m)\sqrt{(\cos^2\phi - m^2)}}\tan^{-1}\{\frac{\sqrt{(\cos\phi - m)}}{\sqrt{(\cos\phi + m)}}\tan(\theta/2)\}$$

$$+ K \qquad (A3.7)$$

Now considering only first four terms of the Eq.(A3.7) we get

$$-\log[(\cos\phi + m\cos\theta)\sin\{(\theta+\phi)/2\}] + \log[\sin\{(\theta+\phi)/2\}]$$

$$-\frac{2}{(1+m)}\log[\tan(\theta/2)+\tan(\phi/2)] + \frac{1}{(1+m)}\log[\{\cos\phi - m\}\tan^2(\theta/2)$$

$$+(\cos\phi + m)]$$

$$= -\log(\cos\phi + m\cos\theta) - \log[\sin\{(\theta+\phi)/2\}] + \log[\sin\{(\theta+\phi)/2\}]$$

$$- \frac{2}{(1+m)}\log[\sin\{(\theta+\phi)/2\}] + \frac{2}{(1+m)}[\log\{\cos(\theta/2)\} + \log\{\cos(\theta/2)\}]$$

$$+ \frac{1}{(1+m)}\log[\cos\phi\{1+\tan^2(\theta/2)\} + m\{1-\tan^2(\theta/2)\}]$$

$$\text{Since } \tan(\theta/2) + \tan(\phi/2) = \frac{\sin\{(\theta+\phi)/2\}}{\cos(\theta/2)\cos(\phi/2)}$$

$$= -\log(\cos\phi + m\cos\theta) - \frac{1}{(1+m)}\log[1-\cos(\theta+\phi)]$$

$$+ \frac{1}{(1+m)}[\log\{\cos^2(\theta/2)\} + \log\{1+\cos\phi\}]$$

$$+ \frac{1}{(1+m)}\log(\cos\phi + m\cos\theta) - \frac{1}{(1+m)}\log\{\cos^2(\theta/2)\}$$

$$= \frac{-m}{(1+m)}\log(\cos\phi + m\cos\theta) + \frac{1}{(1+m)}\log\left[\frac{1+\cos\phi}{1-\cos(\theta+\phi)}\right]$$

$$\text{Since } 1 + \tan^2(\theta/2) = \sec^2(\theta/2)$$

$$\text{and } \frac{1-\tan^2(\theta/2)}{1+\tan^2(\theta/2)} = \cos\theta$$

Now from Eq. (A3.7) we have

$$\log R = \frac{-m}{(1+m)}\log(\cos\phi + m\cos\theta) + \frac{1}{(1+m)}\log\left[\frac{1+\cos\phi}{1-\cos(\theta+\phi)}\right]$$

$$+ \frac{2m\sin\phi}{(1+m)\sqrt{(\cos^2\phi - m^2)}}\tan^{-1}\left[\frac{\sqrt{(\cos\phi - m)}}{\sqrt{(\cos\phi + m)}}\tan(\theta/2)\right]$$

$$+ K \qquad (A3.8)$$

Now applying boundary conditions i.e., when $\theta=\pi/2$, $R = 2L$ in Eq. (A3.8) we get

$$K = \log(2L) + \frac{m}{(1+m)}\log(\cos\phi) - \frac{1}{(1+m)}\log\left[\frac{1+\cos\phi}{1+\sin\phi}\right]$$

$$-\frac{2m\sin\phi}{(1+m)\sqrt{(\cos^2\phi-m^2)}}\tan^{-1}\left[\frac{\sqrt{(\cos\phi-m)}}{\sqrt{(\cos\phi+m)}}\right]$$

Putting the value of K in Eq. (A3.8) we get

$$\log(R/2L) = -\frac{m}{(1+m)}\log\left[\frac{\cos\phi + m\cos\theta}{\cos\phi}\right] + \frac{1}{1+m}\log\left[\frac{1+\sin\phi}{1-\cos(\theta+\phi)}\right]$$

$$+\frac{2\,m\sin\phi}{(1+m)\sqrt{(\cos^2\phi-m^2)}}\left[\tan^{-1}\left\{\frac{\sqrt{(\cos\phi-m)}}{\sqrt{(\cos\phi+m)}}\tan(\theta/2)\right\}\right.$$

$$\left.-\tan^{-1}\left\{\frac{\sqrt{(\cos\phi-m)}}{\sqrt{(\cos\phi+m)}}\right\}\right] \qquad (A3.9)$$

Substituting $m = \frac{1}{M}$ in Eq. (A3.9) we get

$$\log(R/2L) = \frac{-1}{(1+M)}\log\left[\frac{M\cos\phi + \cos\theta}{M\cos\phi}\right] + \frac{M}{(1+M)}\cdot$$

$$\log\left[\frac{1+\sin\phi}{1-\cos(\theta+\phi)}\right] + \frac{2M\sin\phi}{(1+M)\sqrt{(M^2\cos^2\phi-1)}}\cdot$$

$$\left[\tan^{-1}\left\{\frac{\sqrt{(M\cos\phi-1)}}{\sqrt{(M\cos\phi+1)}}\tan(\theta/2)\right\} - \tan^{-1}\left\{\frac{\sqrt{(M\cos\phi-1)}}{\sqrt{(M\cos\phi+1)}}\right\}\right]$$

(A3.10)

LIST OF PUBLICATIONS

1. Murlidhar, A. Gupta And V.K. Tewary, A Nontracking Heat Concentrator Capable Of Giving Concentration Factor Of The Order Of 20, Proc. National Solar Energy Convention 1976, Calcutta, pp. 62-63.

2. A. Gupta, Murlidhar, S. Kumar and V.K. Tewary, Performance Studies on Uniform Illumination Type Nontracking Concentrators, Proc. National Solar Energy Convention 1978, Bhavanagar, pp. 462-66.

3. A. Gupta, S. Kumar, Murlidhar and V.K. Tewary, Design And Testing Of A New Type Of Nontracking Concentrator, Accepted For Presentation In 'International Solar Energy Symposium' To Be Held At Baghdad In Feb, 81.

4. A. Gupta, S. Kumar, Murlidhar and V.K. Tewary, Design And Testing Of A Uniform Illuminating Nontracking Concentrator, Communicated To Solar Energy.